The Innate Immune Receptors TLR2/4 Mediate Repeated Social Defeat Stress-Induced Social Avoidance through Prefrontal Microglial Activation

Nie, Xiang ; Kitaoka, Shiho ; Tanaka, Kohei ; Segi-Nishida, Eri ; Imoto, Yuki ; Ogawa, Atsubumi ; Nakano, Fumitake ; Tomohiro, Ayaka ;…

(Citation)
Neuron,99(3):464-479.e7

(Issue Date)
2018-08-08

(Resource Type)
journal article

(Version)
Accepted Manuscript

(URL)
https://hdl.handle.net/20.500.14094/90005129

Neuron | **Article**

Innate immune receptors TLR2/4 mediate repeated social defeat stress-induced social avoidance through prefrontal microglial activation

Xiang Nie[1-3,8,10], Shiho Kitaoka[1,8,10], Kohei Tanaka[2,10], Eri Segi-Nishida[4], Yuki Imoto[5], Atsubumi Ogawa[2], Fumitake Nakano[1], Ayaka Tomohiro[1,2], Kazuki Nakayama[1,2], Masayuki Taniguchi[1,8], Yuko Mimori-Kiyosue[6], Akira Kakizuka[3], Shuh Narumiya[2,7*] & Tomoyuki Furuyashiki[1,8,9*]

[1]Division of Pharmacology, Kobe University Graduate School of Medicine, Kobe, Hyogo 650-0017, Japan.

[2]CREST Project, Medical Innovation Center, Kyoto University Graduate School of Medicine, Kyoto, Kyoto 606-8509, Japan.

[3]Laboratory of Functional Biology, Kyoto University Graduate School of Biostudies, Kyoto, Kyoto 606-8501, Japan.

[4]Department of Biological Science and Technology, Faculty of Industrial Science and Technology, Tokyo University of Science, Katsushika-ku, Tokyo 125-8585, Japan.

[5]Department of Physiological Chemistry, Kyoto University Graduate School of Pharmaceutical Sciences, Kyoto, Kyoto 606-8304, Japan.

[6]Laboratory for Molecular and Cellular Dynamics, RIKEN Center for Biosystems Dynamics Research, Kobe, Hyogo 650-0047, Japan.

[7]Department of Drug Discovery Medicine, Kyoto University Graduate School of Medicine, Kyoto, Kyoto 606-8507, Japan.

[8]AMED-CREST, Chiyoda-ku, Tokyo 100-0004, Japan.

[9]Lead Contact

[10]These authors contributed equally

*Correspondence: tfuruya@med.kobe-u.ac.jp (T.F.), snaru@mfour.med.kyoto-u.ac.jp (S.N.)

SUMMARY

Repeated environmental stress has been proposed to induce neural inflammation together with depression and anxiety. Innate immune receptors, such as Toll-like receptors (TLRs), are activated by exogenous or endogenous ligands to evoke inflammation. Here we show that the loss of TLR2 and TLR4 (TLR2/4) abolished repeated social defeat stress (R-SDS)-induced social avoidance and anxiety in mice. TLR2/4 deficiency mitigated R-SDS-induced neuronal response attenuation, dendritic atrophy and microglial activation in medial prefrontal cortex (mPFC). Furthermore, mPFC microglia-specific TLR2/4 knockdown blocked the social avoidance. Transcriptome analyses revealed that R-SDS induced IL-1α and TNFα in mPFC microglia in a TLR2/4-dependent manner, and antibody blockade of these cytokines in mPFC suppressed R-SDS-induced social avoidance. These results identify TLR2/4 as crucial mediators of R-SDS-induced microglial activation in mPFC, which leads to neuronal and behavioral changes through inflammation-related cytokines, thus highlighting unexpected pivotal roles of innate immunity in mPFC in repeated environmental stress-induced behavioral changes.

Keywords

depression, innate immune receptor, medial prefrontal cortex, microglia, stress, Toll-like receptor

INTRODUCTION

Repeated environmental stress induces maladaptive behavioral changes including depression and anxiety, and is a risk factor for various human psychiatric disorders (Duman and Aghajanian, 2012; Krishnan and Nestler, 2008; McEwen and Morrison, 2013). To elucidate these mechanisms, rodent models of repeated environmental stress, such as repeated social defeat stress (R-SDS), repeated restraint stress and chronic unpredictable stress, have been frequently used. In these models, repeated environmental stress alters morphologies and activities of neurons in multiple brain areas involved in emotional and cognitive functions (Duman and Aghajanian, 2012; McEwen and Morrison, 2013). Among these brain areas, certain areas, such as the medial prefrontal cortex (mPFC) and nucleus accumbens (NAc), play pivotal roles in regulating repeated environment stress-induced behavioral changes. Various kinds of repeated environmental stress reduce excitatory synaptic transmission and attenuate environmental stress-induced response of mPFC pyramidal neurons (Ota et al., 2014; Perrotti et al., 2004). Shortening and reduced branching of dendrites as well as the loss of dendritic spines are also induced (Dias-Ferreira et al., 2009; Duman and Aghajanian, 2012; McEwen and Morrison, 2013). These neuronal changes are thought to be responsible for repeated environmental stress-induced depression-like behaviors, such as anhedonia and social avoidance (Golden et al., 2013; Li et al., 2011). Histological and brain imaging studies have reported reduced gray matter volumes and abnormal metabolic activities in the mPFC of psychiatric patients (Drevets et al., 2008). However, the underlying mechanism whereby repeated environmental stress induces alterations in morphologies and activities of mPFC neurons as well as consequent behavioral changes remains unknown.

Whereas the majority of studies have examined neuronal plasticity that underlies

repeated environmental stress-induced behavioral changes, several laboratories including ours have focused on neural inflammation or microglial activation as potential mechanisms of repeated environmental stress (Frank et al., 2007; Giovanoli et al., 2013; Hinwood et al., 2012; Kreisel et al., 2013; Tanaka et al., 2012; Wohleb et al., 2011; Wohleb et al., 2013). Indeed, genetic deletion of inflammation-related molecules or administration of a drug (minocycline) that potentially affects microglial properties has been shown to attenuate behavioral changes that are concomitant with microglial activation and/or monocyte infiltration in the brain, and which are induced by repeated environmental stress. However, since none of these studies have selectively manipulated microglia or gene expression in microglia, the direct evidence demonstrating a role of microglia in repeated environmental stress-induced behavioral changes is lacking.

Microglia can be activated by various extracellular stimuli, many of which are mediated by Toll-like receptors (TLRs) (Rivest, 2009). TLRs have been identified as pattern recognition receptors for pathogen-associated molecular patterns, and mediate inflammation and immune responses upon infection. In addition, recent studies have pointed to crucial roles of TLRs in diseases of the brain and other organs without apparent infection (Iwasaki and Medzhitov, 2010; Rivest, 2009), and have proposed that endogenous molecules are released from the cells upon cellular damage or stress and act as endogenous ligands for TLRs for inflammation and tissue remodeling.

To identify R-SDS-induced changes in gene expression profiles in the mPFC, we performed transcriptome analysis and obtained results suggesting that R-SDS upregulates potential ligands for TLR2 and TLR4 in the mPFC. Based on this finding, we analyzed roles of TLR2 and TLR4 in R-SDS and found that genetic deletion of TLR2 and TLR4 (TLR2/4) in combination abolishes R-SDS-induced social avoidance in mice. R-SDS

induced microglial activation and altered neuronal c-Fos expression and morphologies in the mPFC, and the TLR2/4 deletion mitigated these changes. Furthermore, we developed a method to manipulate gene expression in microglia in a specific brain area and has provided sound evidence for the first time that TLR2/4 in mPFC microglia are crucial for R-SDS-induced social avoidance.

RESULTS

TLR2/4 are crucial for R-SDS-induced social avoidance

We first set up an R-SDS model, in which a single male C57BL/6 mouse or a knockout mouse of the same genetic background (C57BL/6) was subjected to aggressive encounters with a male ICR mouse for 10 min daily, typically for 10 consecutive days (Figure 1A). To identify R-SDS-induced changes in gene expression profiles in the mPFC, we performed transcriptome analysis in the mPFC without or with R-SDS. Since the level of social avoidance varies across individuals, we separately analyzed and compared the data from susceptible mice, which showed social avoidance after R-SDS, and resilient mice, which did not, in addition to those from naïve mice, as previously reported (Krishnan et al., 2007) (see the "Behavioral tests" section of the Experimental Procedures for the definitions for susceptible and resilient mice). This analysis revealed that R-SDS upregulates many inflammation-related genes in mPFC tissue, such as *S100a8*, *S100a9*, *Lipocalin2*, *Clec4d* and *Ch25h* (cholesterol 25-hydroxylase) (Figure S1A-E). Among these genes, *S100a8* and *S100a9*, which were upregulated in both susceptible and resilient mice, have been shown to form a heterodimer, and, as ligands, to be functionally related to TLR4 and possibly TLR2 (Coveney et al., 2015; Vogl et al., 2007).

We then examined whether TLR2 and TLR4 were expressed in microglia before and after R-SDS. We subjected CX3CR1-EGFP mice, in which EGFP is selectively expressed in microglia in the brain and monocytes in peripheral tissues (Jung et al., 2000), to R-SDS, and isolated EGFP-positive cells and EGFP-negative cells by FACS from the whole brain of each mouse. Enrichment of microglia and monocytes (a minor population) in the EGFP-positive population was confirmed by mRNA expression of *Cd11b* (Integrin αM), a marker for microglia (Figure S1F). The expression levels of *Tlr2* and *Tlr4* mRNAs were

significantly higher in EGFP-positive cells, which include microglia, as compared with those in EGFP-negative cells, and were not affected by R-SDS (Figure S1G and S1H). On the other hand, the expression of mRNA for *Il1r1* (IL-1 receptor type I), which has been shown to be involved in stress-induced microglial changes in rodents (Kreisel et al., 2013), was detected only in EGFP-negative cells, and it was significantly up-regulated by R-SDS (Figure S1I). These results demonstrate that microglia in the brain express TLR2 and TLR4 regardless of R-SDS.

We then examined whether TLR2/4 were involved in R-SDS-induced behavioral changes. In wild-type mice, R-SDS induced social avoidance in the social interaction test (i.e. decreased time for the social interaction zone and increased time for the social avoidance zone, Figure 1B and 1C) and increased anxiety-like behavior in the elevated plus maze test (i.e. decreased time spent in open arms, Figure 1E), as reported previously (Tanaka et al., 2012). Mice lacking either *Tlr2* (TLR2-KO) or *Tlr4* (TLR4-KO) also displayed R-SDS-induced social avoidance, as observed in wild-type mice (Figures 2A-2D, S1J and S1K). Since TLR2 and TLR4 partly share an intracellular signaling pathway, we examined mice lacking *Tlr2* and *Tlr4* in combination (TLR double knockout; TLR-DKO), and found that the social avoidance was abolished in TLR-DKO mice (Figure 1C and 1D). Wild-type mice were categorized as either susceptible or resilient in a similar ratio (12 susceptible mice and 12 resilient mice), but TLR-DKO mice were mostly resilient (1 susceptible mouse and 18 resilient mice). The proportions of susceptible and resilient mice were significantly different between wild-type mice and TLR-DKO mice (χ^2=10.062, P=0.0015). In addition, TLR-DKO mice did not show elevated anxiety (Figure 1E). These results demonstrate that TLR2/4 are crucial for R-SDS-induced social avoidance and elevated anxiety. By contrast, wild-type mice and TLR-DKO mice

similarly showed a submissive posture, a defensive posture induced by SDS (Tornatzky and Miczek, 1993), and its increase along the 10-day course of R-SDS (Figure 1F), suggesting that these mice are able to perceive R-SDS and to maintain its memory.

To exclude the potential effects of rearing conditions on the phenotypes or to confirm the relationship between the genotypes and the phenotypes, we examined TLR-DKO mice and their littermates. Among the littermates obtained by crossing among TLR2-KO, TLR4-heterozygous mice (*Tlr2*(-/-);*Tlr4*(+/-)), TLR2-KO mice (*Tlr2*(-/-);*Tlr4*(+/+)), but not TLR-DKO littermates (*Tlr2*(-/-); *Tlr4*(-/-)), showed R-SDS-induced social avoidance (Figures 2A and 2B). R-SDS-induced social avoidance was significantly suppressed in TLR-DKO littermates, compared with TLR2-KO mice. Consistently, TLR2-KO mice were categorized to susceptible and resilient mice in a similar ratio (3 susceptible mice and 4 resilient mice), but none of TLR-DKO littermates was susceptible (0 susceptible mice and 6 resilient mice). Likewise, the social avoidance was intact in TLR4-KO mice (*Tlr2*(+/+);*Tlr4*(-/-)), but not in TLR-DKO littermates obtained by crossing among TLR2 heterozygous, TLR4-KO mice (*Tlr2*(+/-);*Tlr4*(-/-)) (Figures 2C and 2D). R-SDS-induced social avoidance was significantly suppressed in TLR-DKO littermates, compared with TLR4-KO mice. Consistently, TLR4-KO mice were categorized to susceptible and resilient mice in a similar ratio (3 susceptible mice and 5 resilient mice), but none of TLR-DKO littermates was susceptible (0 susceptible mice and 9 resilient mice). These results clearly demonstrated that the behavioral abnormalities of TLR-DKO mice are due to genotypes, but not due to differences in rearing conditions. These abnormalities were not due to their locomotor deficits, either; TLR-DKO mice showed locomotor activities similar to those of TLR2-KO or TLR4-KO littermates (Figures 2E and 2F).

We also analyzed *Il1r1* knockout (IL-1RI-KO) mice, and found that R-SDS

significantly induces social avoidance in IL-1RI-KO mice (Figures S1L and S1M). However, R-SDS-induced elevated anxiety was not apparent in these mice (Figure S1N), as previously reported (Wohleb et al., 2011). These results suggest that IL-1RI plays different roles from TLR2/4 in R-SDS-induced behavioral changes.

TLR2/4 are crucial for R-SDS-induced activation of mPFC microglia in susceptible mice

Previous reports have shown the involvement of the mPFC and NAc in repeated environmental stress-induced behavioral changes (Duman and Aghajanian, 2012; Krishnan and Nestler, 2008; McEwen and Morrison, 2013). We examined whether R-SDS as well as single social defeat stress (S-SDS) induced microglial activation in the mPFC and NAc and whether TLR2 and TLR4 were involved in these microglial responses. We performed immunostaining for several markers for microglial activation, namely CD68, Iba-1 and CD11b (Hinwood et al., 2012). Among these markers, we first examined CD68, which showed the lowest signals in basal conditions without R-SDS. In wild-type mice, S-SDS appeared to increase the punctate area positive for CD68 signals in mPFC microglia at 4 h after S-SDS, whereas it did not change at 1.5 h after S-SDS (Figure 3A, 3B and S3A). By contrast, R-SDS increased the CD68-positive area in mPFC microglia at 1.5 h after the last session of R-SDS in susceptible wild-type mice (Figure 3A, 3B, 3F and 3G), and this increase returned to the baseline at 4 h after R-SDS (Figure 3A and 3B). Indeed, the proportion of mice with the CD68-positive area beyond its distribution in naïve mice was significantly larger in the total of defeated wild-type mice (including both susceptible and resilient mice) than in the total of TLR-DKO mice (14/19 and 4/13, respectively; χ^2=5.776, P=0.016; Note that wild-type and TLR-DKO mice used

for this χ^2 analysis include all the mice used for CD68 immunostaining in this study). We then examined Iba-1 signals in mPFC microglia. S-SDS appeared to decrease Iba-1 fluorescent intensity at 1.5 h, but increased it at 4 h, after S-SDS (Figure 3C and 3D). R-SDS appeared to increase Iba-1 fluorescent intensity at 1.5 h after the last exposure of R-SDS in susceptible wild-type mice, and this increase returned to the baseline at 4 h after R-SDS (Figure 3C and 3D). These findings demonstrated that R-SDS induces activation of mPFC microglia at 4 h after the last exposure to R-SDS, and that social defeat stress (SDS)-induced activation of mPFC microglia occurs more rapidly with R-SDS, suggesting R-SDS-induced priming of mPFC microglia. Notably, both Iba-1 fluorescent intensity and CD68-positive area in mPFC microglia after R-SDS were significantly higher in susceptible wild-type mice than in resilient wild-type mice (Figure 3F-3H), indicating that R-SDS-induced activation of mPFC microglia is correlated to the level of social avoidance.

We also found that R-SDS increases CD11b signals in mPFC microglia at 1.5 h after the last exposure of R-SDS, but not after S-SDS (Figure 3E, 3I and 3J) in both susceptible and resilient wild-type mice (Figure 3I and 3J). It is also noted that our statistical analysis indicated that CD68 signals in the mPFC after R-SDS are more strongly correlated to the level of social avoidance than Iba-1 signals (CD68; r^2=0.6977, P<0.0001, Iba-1; r^2=0.3387, P=0.0142 for the time in the avoidance zone) Thus, among the three conventional markers for microglial activation, R-SDS-induced increase in CD68 signals in mPFC microglia were the most strongly correlated to the level of social avoidance.

Since we previously showed that R-SDS for 4 days was sufficient to induce social avoidance (Tanaka et al., 2012), we also performed immunostaining for CD68 and Iba-1 at 1.5 h and 4 h after R-SDS for 4 days. R-SDS for 4 days increased CD68-positive areas

in mPFC microglia at both of these time points (Figure 3K). Although Iba-1 intensity did not appear to increase after R-SDS for 4 days (Figure 3L), Iba-1 decrease, which occurred at 1.5 h after S-SDS (see Figure 3D), was not observed at 1.5 h after R-SDS for 4 days (Figure 3L). These results indicated that R-SDS for 4 days induces an intermediate pattern of microglial activation between those induced by S-SDS and R-SDS for 10 days.

We then examined whether TLR2/4 deficiency affected R-SDS-induced activation of mPFC microglia. In TLR-DKO mice, S-SDS did not increase CD68-positive area in mPFC microglia (Figure 3A and 3B). The CD68-positive area at 4 h after S-SDS was significantly smaller in TLR-DKO mice than in susceptible wild-type mice. The S-SDS-induced increase in Iba-1 fluorescent intensity in the mPFC at 4 h after S-SDS was also abolished in TLR-DKO mice (Figure 3C and 3D). These results indicated that TLR2/4 are crucial for S-SDS-induced activation of mPFC microglia. By contrast, at 1.5 h after S-SDS, Iba-1 signals were decreased in TLR-DKO mice, as similarly observed in wild-type mice, indicating that this microglial response was not mediated by either TLR2 or TLR4. In addition, TLR-DKO mice did not show R-SDS-induced increase in CD68 signals in mPFC microglia at 1.5 h after the last exposure of R-SDS, which was observed in susceptible wild-type mice (Figure 3A and 3B). These results demonstrated that TLR2/4 are crucial for the activation of mPFC microglia induced by R-SDS as well as that induced by S-SDS. Note that neither the fluorescent intensity of Iba-1 signals nor that of CD11b was affected by R-SDS in TLR-DKO mice (Figure 3C-E). It was also noted that neither TLR2 nor TLR4 deficiency affected the signals of CD68, Iba-1 or CD11b at the basal condition without SDS (Figure 3A-E and S2A-F).

We also examined roles of TLR2/4 in R-SDS-induced microglial activation with TLR-DKO littermates obtained from the heterozygous crossing. The R-SDS-induced CD68

increase in mPFC microglia was abolished in TLR-DKO littermates, although it remained in susceptible mice with the TLR4-KO genotype (Figure S2A, S2B, S2D and S2E). Iba-1 fluorescent intensity was not significantly increased in any of these genotypes (Figure S2A, S2C, S2D and S2F). These results suggested that the respective markers for microglial activation may be differently regulated. Neither TLR2/4 deficiency nor R-SDS affected the number of Iba-1-positive microglia in the mPFC (data not shown). These results demonstrated that the lack of R-SDS-induced activation of mPFC microglia in TLR-DKO mice is due to the TLR2/4 deletion, but not due to differences in rearing conditions. By contrast, neither S-SDS nor R-SDS significantly increased Iba-1 or CD68 signals in NAc microglia of either wild-type mice or TLR-DKO mice (Figure S3B-S3G).

As previously reported (Wohleb et al., 2013), R-SDS promotes infiltration of CD45-positive monocytes to the anterior cingulate cortex (ACC), which is located dorsal to the mPFC, in susceptible wild-type mice (Figure 4A, 4C, 4E and 4G). However, this monocyte infiltration in the ACC was unaffected in TLR-DKO mice. Notably, monocyte infiltration did not occur in the mPFC, in which R-SDS induces microglial activation (see Figure 3), in either wild-type or TLR-DKO mice (Figures 4B, 4D and 4F). Thus, R-SDS induces microglial activation in the mPFC and monocyte infiltration in the ACC, and TLR2/4 are involved in the former, but not in the latter.

TLR2/4 are crucial for the attenuation of SDS-induced c-Fos expression and dendritic atrophy of mPFC neurons by R-SDS in susceptible mice

We next examined whether TLR2/4 are involved in SDS-induced neuronal responses in the mPFC using immunostaining for c-Fos, a marker for neuronal response (Figure 5A). S-SDS induced c-Fos expression in mPFC neurons of both wild-type and TLR-DKO

mice (Figure 5B and 5C). This c-Fos expression was abolished by R-SDS in susceptible wild-type mice, but was maintained in resilient wild-type mice (Figure 5D and 5E). In TLR-DKO mice, R-SDS attenuated SDS-induced c-Fos expression, but it was maintained at a level similar to resilient wild-type mice (approximately 25 neurons/mm^2 in both mice) (Figure 5B-E). Indeed, the proportion of mice with the number of c-Fos-positive cells beyond its distribution in naïve mice was significantly smaller in the total of defeated wild-type mice (including both susceptible and resilient mice) than in the total of defeated TLR-DKO mice (12/18 and 16/17, respectively; χ^2=4.118, P=0.042; Note that wild-type and TLR-DKO mice used for this χ^2 analysis include all the mice used for c-Fos immunostaining in this study). These findings were confirmed with littermates obtained by crossing among TLR2-heterozygous, TLR4-KO mice or TLR2-KO, TLR4-heterozygous mice. SDS-induced c-Fos expression was observed in resilient, but not susceptible, mice with the TLR2-KO or TLR4-KO genotype (Figure S4), as was observed in wild-type mice. In TLR-DKO littermates, this SDS-induced c-Fos expression was maintained, as observed in resilient TLR2-KO or TLR4-KO mice. These results indicate that TLR2/4 are involved in the attenuation of SDS-induced c-Fos expression in mPFC neurons by R-SDS in susceptible mice.

Repeated environmental stress induces dendritic atrophy of mPFC neurons, which is thought to underlie concomitant behavioral changes (Duman and Aghajanian, 2012; McEwen and Morrison, 2013). We performed Golgi-Cox staining and measured the lengths of apical dendrites of mPFC deep-layer pyramidal neurons. R-SDS induced shortening of apical dendrites of mPFC neurons in susceptible wild-type mice, whereas TLR-DKO mice did not show this dendritic shortening (Figures 5F-5H). These results indicate that TLR2/4 are crucial for dendritic atrophy of mPFC neurons induced by R-

SDS in susceptible mice.

TLR2/4 in mPFC microglia are crucial for R-SDS-induced social avoidance

Since TLR2/4 are highly expressed in microglia (Figure S1G and S1H) and are required for R-SDS-induced activation of mPFC microglia as described above, we examined whether mPFC microglia are important for R-SDS-induced social avoidance. Transplantation of cultured microglia-like cells derived from wild-type neonates to the spinal cord has been used to investigate roles of microglia in neuropathic pain (Tsuda et al., 2003). We examined whether transplantation of these cells into the mPFC of TLR-DKO mice could restore R-SDS-induced social avoidance (Figure S5A). One week after the transplantation, microglia-like cells labeled with CFSE, a semi-permanent fluorescent tracer, showed amoeboid morphology reminiscent of maximally activated microglia (data not shown). After a four-week recovery period, these cells remained around the injection site and appeared to show a ramified morphology, suggesting that the transplanted microglia had become inactive (Figure S5B). Transplantation of wild-type, but not TLR-DKO, microglia-like cells to the mPFC of TLR-DKO mice significantly restored social avoidance induced by R-SDS for 4 days (Figures S5D-S5G). Without R-SDS, the transplantation of these microglia-like cells did not induce social avoidance in TLR-DKO mice (Figures S5E and S5G). These findings indicate that the transplantation of wild-type microglia-like cells to the mPFC restores the induction of social avoidance in a TLR2/4-dependent manner. However, this restoration was not sustained after R-SDS for 10 days (Figures S5H-S5K), although the transplanted cells were maintained similarly among the comparison groups (Figure S5C).

To examine whether TLR2/4 in mPFC microglia are necessary for R-SDS-induced

behavioral changes, we developed a method to reduce TLR2/4 expression specifically in mPFC microglia. For this purpose, we generated a lentiviral vector expressing artificial microRNAs targeting *Tlr2* and *Tlr4* mRNAs only in cells expressing Cre recombinase driven by the microglial-specific CX3CR1 promoter (Figure 6A). The specificity and efficiency of *Tlr2* and *Tlr4* microRNAs were validated in Lenti-X 293T cells overexpressing the respective TLR isoforms together with *Tlr2* or *Tlr4* microRNA (Figure S6A). Expression of *Tlr2* or *Tlr4* microRNA efficiently reduced the mRNA level of the corresponding *Tlr* isoform by approximately 80%, but not those of the other TLR isoforms, confirming the specificity of the *Tlr2* or *Tlr4* microRNAs (Figure S6A). In addition, in the N9 microglial cell line, lentivirus-delivered tandemly connected *Tlr2* or *Tlr4* microRNAs (TLR2/4 microRNA) reduced endogenous expression of both *Tlr2* or *Tlr4* (reduction by ~40% and ~60%, respectively) (Figure S6B).

Each lentiviral vector, which is able to express TLR2/4 microRNA or control microRNA only in cells expressing Cre recombinase, was injected into the mPFC of CX3CR1-CreER mice, in which tamoxifen-inducible Cre recombinase and EYFP are selectively expressed in microglia (Parkhurst et al., 2013). Four weeks after the lentiviral injection and tamoxifen treatment (Figure 6B), many EYFP-positive cells, mostly microglia, showed mCherry signals that were designed to co-express TLR2/4 or control microRNAs (Figure 6C, 6D and 6F). Most mCherry signals were observed in EYFP-positive cells, but much less in CD45-positive monocytes, without or with R-SDS (Figure 6E-G), suggesting that the mice were specifically expressing TLR2/4 or control microRNAs in mPFC microglia. Expression of TLR2/4 microRNAs in mPFC microglia by this method abolished R-SDS-induced social avoidance, whereas this social avoidance was induced in mice that had received the lentiviral vector expressing control microRNA

(Figures 6H and 6I). To exclude off-target effects of these microRNAs, we generated microRNA-resistant synonymous mutant cDNAs of *Tlr2* or *Tlr4* (i.e., without changing their amino acid sequences), and confirmed that the protein expression levels of these mutants were resistant to the respective microRNAs in Lenti-X 293T cells (Figures S6C-H). We generated lentiviral vectors expressing either of these mutants along with TLR2/4 microRNA in the presence of Cre recombinase, and injected these lentiviral vectors into the mPFC of CX3CR1-CreER mice. Simultaneous expression of the microRNA-resistant *Tlr2* or *Tlr4* mutant restored R-SDS-induced social avoidance in the presence of TLR2/4 microRNA (Figure 6J and 6K). These results excluded off-target effects of TLR2/4 microRNA, and demonstrated that TLR2/4 in mPFC microglia are crucial for R-SDS-induced social avoidance. By contrast, mPFC microglia-specific expression of TLR2/4 microRNA did not appear to affect R-SDS-induced elevated anxiety (Figure 6L).

We also examined the effect of TLR2/4 microRNA in mPFC microglia on SDS-induced c-Fos expression in mPFC neurons. The number of c-Fos-positive mPFC neurons in mice expressing TLR2/4 microRNA in mPFC microglia was significantly larger, as compared to susceptible mice without TLR2/4 microRNA expression (Figure 6M). Consistent with the experiments using TLR-DKO mice, these results indicate that TLR2/4 in mPFC microglia are involved in the attenuation of SDS-induced c-Fos expression in mPFC neurons by R-SDS in susceptible mice.

In addition, we evaluated the effect of TLR2/4 microRNA on excitatory synapses in mPFC neurons using super-resolution structured illumination microscopy (SIM) (Figure S7A). Surprisingly, R-SDS significantly increased the number of punctate signals of PSD95, a postsynaptic marker, in the deep layer of the mPFC in susceptible wild-type mice with expression of control microRNA in mPFC microglia. This effect was abolished

by expression of TLR2/4 microRNA in mPFC microglia (Figure S7B). R-SDS appeared to increase the number of punctate signals of synaptophysin, a presynaptic marker, although this increase was milder and not statistically significant (Figure S7C). These results suggest that R-SDS increases the number of excitatory synapses in mPFC in a manner dependent on TLR2/4 expressed in mPFC microglia.

IL-1α and TNFα are up-regulated in mPFC microglia by R-SDS in a TLR2/4-dependent manner and are crucial for R-SDS-induced social avoidance

Based on our observations that R-SDS induces different microglial responses in the mPFC and NAc (Figure 3 and S3), we performed transcriptome analysis of microglia isolated from the mPFC or NAc without or with R-SDS (Figure 7A-C). We found that different sets of genes are significantly up- or down-regulated by R-SDS in microglia isolated from the two brain areas (Figure 7D and 7E). Among these genes, several cytokines, such as *Tnfa* and *Il1a*, were significantly upregulated in mPFC microglia, and marginally in NAc microglia, in a TLR2/4-dependent manner (Figure 7F-I). In contrast, *Ccl3* and *Ccl4* appeared to be upregulated in both mPFC and NAc microglia in a TLR2/4-dependent manner (Figure 7F and 7G). Whereas *Il1b* and *Il6* also appeared to be up-regulated in both mPFC and NAc microglia, the involvement of TLR2/4 was elusive (Figure 7F, 7G, 7J and 7K).

To examine whether IL-1α and TNFα in mPFC are involved in R-SDS-induced social avoidance, we infused neutralizing antibodies for these cytokines into the mPFC. To reduce the amounts of the antibodies to be used, we employed a shorter version of R-SDS, which is composed of three exposures to SDS within a single day (Figure 8A). This shorter version of R-SDS appeared to increase CD68 signals in microglia in the mPFC,

but not in the NAc, at 1.5 h and 4 h after R-SDS (Figure S2G-J). We administered a mixture of neutralizing antibodies for IL-1α and TNFα in to the mPFC at 2 h before R-SDS, and found that the normal R-SDS-induced CD68 increase in mPFC microglia was absent with these neutralizing antibodies in the mPFC. Notably, this shorter version of R-SDS significantly decreased the time in the interaction zone, indicating the induction of social avoidance, although it only moderately increased the time in the avoidance zone (Figure 8B and 8C), compared with the original longer version of R-SDS. The mPFC infusion of these neutralizing antibodies abolished these behavioral changes. Either of these antibodies also blocked the induction of social avoidance (Figure 8D and 8E). These results strongly indicate that IL-1α and TNFα associated with mPFC microglia activated by R-SDS are responsible for the induction of social avoidance.

DISCUSSION

In this study, we found that TLR-DKO mice show resilience to R-SDS-induced social avoidance and anxiety. TLR2/4 are also crucial for R-SDS-induced activation of mPFC microglia as well as response attenuation and dendritic atrophy of mPFC neurons. These microglial activation and neuronal changes occur in susceptible, but not resilient, mice. Knockdown of TLR2/4 in mPFC microglia abolishes R-SDS-induced social avoidance. *Il1a* and *Tnfa* are up-regulated in mPFC microglia by R-SDS in a manner dependent on TLR2/4, and are crucial for R-SDS-induced social avoidance. These findings link TLR2/4 function in mPFC microglia to neuronal and microglial changes in the mPFC, thereby leading to R-SDS-induced social avoidance. In our model, R-SDS activates mPFC microglia through TLR2/4, which attenuates the stress response of mPFC neurons and induces social avoidance through IL-1α and TNFα (Figure S8).

TLR2/4 in mPFC microglia mediate R-SDS-induced social avoidance

In this study, we showed that TLR2/4 mediate R-SDS-induced social avoidance and elevated anxiety as well as neuronal and microglial changes in the mPFC. Our transcriptome analysis demonstrated that R-SDS increases mRNA levels of *S100a8* and *S100a9*, potential ligands for TLR2/4, in the mPFC of susceptible and resilient mice. It remains to be examined whether the S100A8/S100A9 heterodimer is released into the extracellular space in response to R-SDS and acts as an endogenous TLR2/4 ligand for R-SDS-induced activation of mPFC microglia. Notably, our histological examinations showed that R-SDS induces microglial activation in susceptible, but not resilient, mice. Thus, *bona fide* TLR ligands other than S100A8/S100A9 could be upregulated and/or secreted specifically in the mPFC.

Previous studies have reported roles of several molecules in repeated environmental stress-induced microglial activation, but none of these studies has identified their sites of action. Although it is difficult to manipulate gene expression selectively in microglia in a given brain area, the transplantation of microglia-like cells obtained from neonates has been used to elucidate roles of microglia in the spinal cord in neuropathic pain (Tsuda et al., 2003). We used similar transplantation methods in the brain, and found that wild-type, but not TLR-DKO, microglia-like cells transplanted into the mPFC of TLR-DKO mice restored R-SDS-induced social avoidance. However, the effect of this transplantation was transient, and recent studies have revealed differences in gene expression profiles between microglia *in vitro* and *in vivo* and between neonatal and adult microglia (Butovsky et al., 2014). Therefore, we developed a lentivirus-based method to express TLR2/4 microRNA selectively in mPFC microglia. Using this method, most cells expressing TLR2/4 or control microRNA were microglia rather than infiltrated monocytes in the mPFC, and selective TLR2/4 knockdown in mPFC microglia abolished R-SDS-induced social avoidance. These results document for the first time the critical roles of innate immune receptors in microglia in repeated environmental stress-induced behavioral changes, and provide the first evidence for mPFC microglia as the site of action of molecules involved in repeated environmental stress-induced microglial activation.

However, we note that our findings did not exclude the possibility that TLR2/4 in non-microglial cells or in other brain areas may also be involved in the behavioral changes. Indeed, we found that systemic TLR2/4 deficiency, but not specific TLR2/4 knockdown in mPFC microglia, abolishes R-SDS-induced elevated anxiety. In addition, other brain areas, such as the ventral hippocampus and amygdala, have been shown to be involved in

R-SDS-induced behavioral changes (Bagot et al., 2015; Wohleb et al., 2011).

Many rodent studies have suggested a role of IL-1β in anhedonia after chronic unpredictable stress and elevated anxiety induced by R-SDS (Goshen et al., 2008; Koo and Duman, 2008; Wohleb et al., 2011). It has recently been reported that mice lacking NLRP3, a component of the inflammasome, which converts pro-IL-1β to its active form, show decreased anxiety without stress and the lack of anhedonia after chronic unpredictable stress (Iwata et al., 2015). However, we observed that the IL-1RI deletion did not abolish R-SDS-induced social avoidance and that *Tlr2* and *Tlr4*, but not *Il1r1*, are expressed in microglia. These different expressions may explain why TLR2/4 rather than IL-1RI are integral to the social avoidance. It has been reported that IL-1RI is critical for R-SDS-induced monocyte infiltration and elevated anxiety (Wohleb et al., 2013) and that splenectomy prevents an anxious tendency induced by R-SDS (McKim et al., 2016). Thus, IL-1RI-mediated monocyte infiltration has been proposed to be involved in R-SDS-induced elevated anxiety. By contrast, TLR2/4 deficiency did not affect monocyte infiltration from the periphery to the ACC, and IL-1RI deficiency did not affect R-SDS-induced social avoidance. These findings indicate that different inflammation-related mechanisms underlie R-SDS-induced social avoidance and elevated anxiety.

TLR2/4 in microglia mediate R-SDS-induced neuronal remodeling in the mPFC

Based on our observation that TLR2/4 in mPFC microglia are crucial for R-SDS-induced social avoidance, we speculated that R-SDS-activated mPFC microglia could locally affect mPFC neurons. Indeed, we showed that systemic TLR2/4 deletion mitigates R-SDS-induced c-Fos response attenuation and dendritic atrophy in mPFC neurons, and that mPFC microglia-specific TLR2/4 knockdown at least mitigates the former of these

R-SDS-induced changes. These findings indicate that TLR2/4 in mPFC microglia are involved in R-SDS-induced changes in mPFC neurons.

c-Fos expression has frequently been used as a marker for neuronal response to repeated environmental stress (Perrotti et al., 2004; Tanaka et al., 2012). We found that SDS-induced c-Fos expression in mPFC neurons is attenuated after R-SDS in susceptible, but not resilient, mice. In addition, repeated environmental stress-induced dendritic atrophy in mPFC pyramidal neurons is thought to underlie the concomitant behavioral changes (Dias-Ferreira et al., 2009; Duman and Aghajanian, 2012). Therefore, the TLR2/4-dependent changes in mPFC neurons described above could underlie R-SDS-induced social avoidance.

In addition to these changes, our histological analyses of the number of PSD-95 puncta suggested that R-SDS increases the number of excitatory synapses in the deep layer of the mPFC in susceptible wild-type mice in a manner dependent on TLR2/4 expressed in mPFC microglia. This result was unexpected, based on our observations that R-SDS induces dendritic atrophy of mPFC pyramidal neurons (Figure 5F-H) (Shinohara et al., 2017). However, since PSD-95 immunostaining cannot discriminate excitatory synapses on various types of neurons, R-SDS may increase the number of excitatory synapses on some types of neurons other than mPFC pyramidal neurons. Indeed, it has been reported that chronic restraint stress induces dendritic hypertrophy in a subpopulation of mPFC interneurons identified mainly as Martinotti cells (Gilabert-Juan et al., 2013). It remains to be elucidated whether R-SDS induces distinct types of morphological changes in different types of neurons in the mPFC and whether and how these morphological changes may impact the concomitant behavioral changes.

IL-1α and TNFα are responsible for the action of TLR2/4 in mPFC microglia for R-SDS

We showed that R-SDS significantly induces *Il1a* and *Tnfa* mRNAs in mPFC microglia, and marginally in NAc microglia, and that administration of their neutralizing antibodies into the mPFC abolishes R-SDS-induced social avoidance. These observations strongly imply that IL-1α and TNFα released from activated mPFC microglia are responsible for R-SDS-induced social avoidance. These neutralizing antibodies appeared to inhibit R-SDS-induced CD68 increase, indicative of microglial activation, in the mPFC. Thus, these cytokines could constitute an autocrine loop for R-SDS-induced microglial activation. It has also been reported that IL-1α and TNFα are sufficient to induce neurotoxic reactive astrocytes (Liddelow et al., 2017). TNF receptor type 1 (TNFR1) in astrocytes has been shown to be instrumental in hippocampal synaptic alteration and impaired contextual learning in an animal model of multiple sclerosis (Habbas et al., 2015). Therefore, microglia-derived TNFα could act on astrocytic TNFR1 to induce R-SDS-induced neuronal and behavioral changes. The mechanism of action of IL-1α remains elusive. Interestingly, it has been shown that IL-1α or IL-1β in combination with TNFα induces different types of astrocytes, neurotoxic or protective astrocytes, respectively (Liddelow et al., 2017), suggesting different mechanisms of action of IL-1α and IL-1β.

We also found that, among three conventional markers for microglial activation, the R-SDS-induced increase in CD68 signals in mPFC microglia was the most correlated with the level of social avoidance. CD68 is a scavenger receptor that is predominantly located at the late endosomal and lysosomal compartments, and is thought to be associated with phagocytic activity (Murphy et al., 2005). It has been suggested that

microglia engulf synaptic structures into CD68-positive phagosomal compartments for synaptic pruning during postnatal development (Paolicelli et al., 2011; Schafer et al., 2012) and in a mouse model of Alzheimer's disease (Hong et al., 2016). Similarly, R-SDS-activated microglia could also engulf synaptic and dendritic elements of mPFC neurons into CD68-positive phagosomal compartments. It has been shown that astrocyte-derived TGFβ induces C1q expression in retinal ganglion cells, which is crucial for complement- and microglia-dependent synaptic pruning (Bialas and Stevens, 2013). Since it has been reported that IL-1α and TNFα induce neurotoxic astrocytes (Liddelow et al., 2017), these cytokines derived from microglia upon R-SDS could alter astrocytic functions to promote synaptic and dendritic engulfment by mPFC microglia.

Conclusions

Collectively, our study demonstrates the unexpected pivotal role of TLR2/4 for R-SDS-induced behavioral changes as well as neuronal and microglial changes in the mPFC, and strongly indicates that TLR2/4 in mPFC microglia mediate R-SDS-induced neuronal and behavioral changes through IL-1α and TNFα. Therefore, we propose that targeting innate immunity may provide therapeutic benefits for stress-related pathophysiology in psychiatric disorders.

STAR★METHODS

Detailed methods are provided in the online version of this paper and include the following:

- KEY RESOURCES TABLE
- EXPERIMENTAL MODEL AND SUBJECT DETAILS
    - Mice
- METHOD DETAILS
    - Social defeat stress
    - Social interaction test
    - Elevated plus maze test
    - Immunostaining
    - Analyses of immunofluorescent images
    - Golgi-Cox staining
    - Isolation of microglia from the brain
    - Quantitative RT-PCR
    - Transplantation of cultured microglia-like cells into the mPFC
    - Lentiviral vectors
    - Knockdown of TLR2/4 in cultured cells
    - Injection of lentiviral vectors into the mPFC
    - Transcriptome analyses
    - Local infusion of neutralizing antibodies into the mPFC
- QUANTIFICATION AND STATISTICAL ANALYSIS

SUPPLEMENTAL INFORMATION

Supplemental Information includes eight figures and one table and can be found with this article online.

ACKNOWLEDGMENTS

We thank Dr. Hiroyuki Hioki for technical advice on generating lentiviral vectors, Dr. Ryota Shinohara for technical advice on designing microRNA and Dr. Hirotaka Nagai for technical advice on isolation of microglia by FACS. We also thank Atsushi Mizutani and Nodoka Asamoto for animal care, Tae Arai, Akiko Washimi and Misako Takizawa for secretarial helps, and Kimiko Nonomura for technical assistance, and Professor James Hejna (Kyoto University) for critical reading of the manuscript. This study was supported in part by a CREST grant from JST (JP15gm0410006 to S.N.), a CREST grant from AMED (JP17gm0910012 to T.F.), Grants-in-Aids for Scientific Research (24689015, 16H05132 and 17K19457 to T.F., 17K08593 to S.K.) and Grants-in-Aids for JSPS Research Fellow (15J07561 to X.N. and 17J09360 to M.T.) from the Japan Society for the Promotion of Science, Grants-in-Aids for Scientific Research from the Ministry of Education, Culture, Sports, Science and Technology in Japan (25116517, 25116715, 15H01289, 17H06057, 17H05572 to T.F.), research grants from the Uehara Memorial Foundation (T.F.), the Sumitomo Foundation (T.F.), the Naito Foundation (T.F.), the Astellas Foundation for Research on Metabolic Disorders (T.F.) and the Takeda Science Foundation (T.F.).

AUTHOR CONTRIBUTIONS

T.F., S.N. and S.K. designed the project. T.F., S.N., S.K. and A.K. wrote the manuscript.

X.N. and S.K. performed most experiments. X.N. and K.T. performed behavioral experiments using knockout mice. A.O. and S.K. performed transplantation of microglia-like cells. S.K. generated lentiviral vectors, and X.N, A.T., K.N. and F.N. analyzed knockdown efficiency. F.N. generated microRNA-resistant TLR2/4 mutant cDNAs and performed behavioral experiments with these mutants. S.K. and X.N. acquired mPFC microglia-specific transcriptome data, and S.K., E.S.-N. and Y.I. analyzed these transcriptome data. X.N. and Y.M.-K. acquired fluorescent images using SIM, and X.N. and M.T. analyzed these images. Project management was carried out by S.K. and T.F.

DECLARATION OF INTERESTS

The authors declare no competing intersests.

REFERENCES

Bagot, R.C., Parise, E.M., Peña, C.J., Zhang, H.X., Maze, I., Chaudhury, D., Persaud, B., Cachope, R., Bolaños-Guzmán, C.A., Cheer, J.F., *et al.* (2015). Ventral hippocampal afferents to the nucleus accumbens regulate susceptibility to depression. Nat Commun 6, 7062.

Bialas, A.R., and Stevens, B. (2013). TGF-β signaling regulates neuronal C1q expression and developmental synaptic refinement. Nat Neurosci 16, 1773-1782.

Butovsky, O., Jedrychowski, M.P., Moore, C.S., Cialic, R., Lanser, A.J., Gabriely, G., Koeglsperger, T., Dake, B., Wu, P.M., Doykan, C.E., *et al.* (2014). Identification of a unique TGF-β-dependent molecular and functional signature in microglia. Nat Neurosci 17, 131-143.

Coveney, A.P., Wang, W., Kelly, J., Liu, J.H., Blankson, S., Wu, Q.D., Redmond, H.P., and Wang, J.H. (2015). Myeloid-related protein 8 induces self-tolerance and cross-tolerance to bacterial infection via TLR4- and TLR2-mediated signal pathways. Sci Rep 5, 13694.

Dias-Ferreira, E., Sousa, J.C., Melo, I., Morgado, P., Mesquita, A.R., Cerqueira, J.J., Costa, R.M., and Sousa, N. (2009). Chronic stress causes frontostriatal reorganization and affects decision-making. Science 325, 621-625.

Drevets, W.C., Price, J.L., and Furey, M.L. (2008). Brain structural and functional abnormalities in mood disorders: implications for neurocircuitry models of depression. Brain Struct Funct 213, 93-118.

Duman, R.S., and Aghajanian, G.K. (2012). Synaptic dysfunction in depression: potential therapeutic targets. Science 338, 68-72.

Frank, M.G., Baratta, M.V., Sprunger, D.B., Watkins, L.R., and Maier, S.F. (2007). Microglia serve as a neuroimmune substrate for stress-induced potentiation of CNS pro-inflammatory cytokine responses. Brain Behav Immun 21, 47-59.

Gilabert-Juan, J., Castillo-Gomez, E., Guirado, R., Moltó, M.D., and Nacher, J. (2013). Chronic stress alters inhibitory networks in the medial prefrontal cortex of adult mice. Brain Struct Funct 218, 1591-1605.

Giovanoli, S., Engler, H., Engler, A., Richetto, J., Voget, M., Willi, R., Winter, C., Riva, M.A., Mortensen, P.B., Feldon, J., *et al.* (2013). Stress in puberty unmasks latent neuropathological consequences of prenatal immune activation in mice. Science 339, 1095-1099.

Glaccum, M.B., Stocking, K.L., Charrier, K., Smith, J.L., Willis, C.R., Maliszewski, C., Livingston, D.J., Peschon, J.J., and Morrissey, P.J. (1997). Phenotypic and functional characterization of mice that lack the type I receptor for IL-1. J Immunol 159, 3364-3371.

Golden, S.A., Christoffel, D.J., Heshmati, M., Hodes, G.E., Magida, J., Davis, K., Cahill, M.E., Dias, C., Ribeiro, E., Ables, J.L., *et al.* (2013). Epigenetic regulation of RAC1 induces synaptic remodeling in stress disorders and depression. Nat Med 19, 337-344.

Goshen, I., Kreisel, T., Ben-Menachem-Zidon, O., Licht, T., Weidenfeld, J., Ben-Hur, T., and Yirmiya, R. (2008). Brain interleukin-1 mediates chronic stress-induced depression in mice via adrenocortical activation and hippocampal neurogenesis suppression. Mol Psychiatry 13, 717-728.

Habbas, S., Santello, M., Becker, D., Stubbe, H., Zappia, G., Liaudet, N., Klaus, F.R., Kollias, G., Fontana, A., Pryce, C.R., *et al.* (2015). Neuroinflammatory TNFα Impairs Memory via Astrocyte Signaling. Cell 163, 1730-1741.

Hinwood, M., Morandini, J., Day, T.A., and Walker, F.R. (2012). Evidence that microglia mediate the neurobiological effects of chronic psychological stress on the medial prefrontal cortex. Cereb Cortex 22, 1442-1454.

Hioki, H., Kameda, H., Nakamura, H., Okunomiya, T., Ohira, K., Nakamura, K., Kuroda, M., Furuta, T., and Kaneko, T. (2007). Efficient gene transduction of neurons by lentivirus with enhanced neuron-specific promoters. Gene Ther 14, 872-882.

Hong, S., Beja-Glasser, V.F., Nfonoyim, B.M., Frouin, A., Li, S., Ramakrishnan, S., Merry, K.M., Shi, Q., Rosenthal, A., Barres, B.A., *et al.* (2016). Complement and

microglia mediate early synapse loss in Alzheimer mouse models. Science 352, 712-716.

Hoshino, K., Takeuchi, O., Kawai, T., Sanjo, H., Ogawa, T., Takeda, Y., Takeda, K., and Akira, S. (1999). Cutting edge: Toll-like receptor 4 (TLR4)-deficient mice are hyporesponsive to lipopolysaccharide: evidence for TLR4 as the Lps gene product. J Immunol 162, 3749-3752.

Iwasaki, A., and Medzhitov, R. (2010). Regulation of adaptive immunity by the innate immune system. Science 327, 291-295.

Iwata, M., Ota, K.T., Li, X.Y., Sakaue, F., Li, N., Dutheil, S., Banasr, M., Duric, V., Yamanashi, T., Kaneko, K., *et al.* (2015). Psychological Stress Activates the Inflammasome via Release of Adenosine Triphosphate and Stimulation of the Purinergic Type 2X7 Receptor. Biol Psychiatry.

Jung, S., Aliberti, J., Graemmel, P., Sunshine, M.J., Kreutzberg, G.W., Sher, A., and Littman, D.R. (2000). Analysis of fractalkine receptor CX(3)CR1 function by targeted deletion and green fluorescent protein reporter gene insertion. Mol Cell Biol 20, 4106-4114.

Koo, J.W., and Duman, R.S. (2008). IL-1beta is an essential mediator of the antineurogenic and anhedonic effects of stress. Proc Natl Acad Sci U S A 105, 751-756.

Kreisel, T., Frank, M.G., Licht, T., Reshef, R., Ben-Menachem-Zidon, O., Baratta, M.V.,

Maier, S.F., and Yirmiya, R. (2013). Dynamic microglial alterations underlie stress-induced depressive-like behavior and suppressed neurogenesis. Mol Psychiatry 19, 699-709.

Krishnan, V., Han, M.H., Graham, D.L., Berton, O., Renthal, W., Russo, S.J., Laplant, Q., Graham, A., Lutter, M., Lagace, D.C., *et al.* (2007). Molecular adaptations underlying susceptibility and resistance to social defeat in brain reward regions. Cell 131, 391-404.

Krishnan, V., and Nestler, E.J. (2008). The molecular neurobiology of depression. Nature 455, 894-902.

Li, N., Liu, R.J., Dwyer, J.M., Banasr, M., Lee, B., Son, H., Li, X.Y., Aghajanian, G., and Duman, R.S. (2011). Glutamate N-methyl-D-aspartate receptor antagonists rapidly reverse behavioral and synaptic deficits caused by chronic stress exposure. Biol Psychiatry 69, 754-761.

Liddelow, S.A., Guttenplan, K.A., Clarke, L.E., Bennett, F.C., Bohlen, C.J., Schirmer, L., Bennett, M.L., Münch, A.E., Chung, W.S., Peterson, T.C., *et al.* (2017). Neurotoxic reactive astrocytes are induced by activated microglia. Nature 541, 481-487.

McEwen, B.S., and Morrison, J.H. (2013). The brain on stress: vulnerability and plasticity of the prefrontal cortex over the life course. Neuron 79, 16-29.

McKim, D.B., Patterson, J.M., Wohleb, E.S., Jarrett, B.L., Reader, B.F., Godbout, J.P.,

and Sheridan, J.F. (2016). Sympathetic Release of Splenic Monocytes Promotes Recurring Anxiety Following Repeated Social Defeat. Biol Psychiatry 79, 803-813.

Murphy, J.E., Tedbury, P.R., Homer-Vanniasinkam, S., Walker, J.H., and Ponnambalam, S. (2005). Biochemistry and cell biology of mammalian scavenger receptors. Atherosclerosis 182, 1-15.

Ota, K.T., Liu, R.J., Voleti, B., Maldonado-Aviles, J.G., Duric, V., Iwata, M., Dutheil, S., Duman, C., Boikess, S., Lewis, D.A., *et al.* (2014). REDD1 is essential for stress-induced synaptic loss and depressive behavior. Nat Med 20, 531-535.

Paolicelli, R.C., Bolasco, G., Pagani, F., Maggi, L., Scianni, M., Panzanelli, P., Giustetto, M., Ferreira, T.A., Guiducci, E., Dumas, L., *et al.* (2011). Synaptic pruning by microglia is necessary for normal brain development. Science 333, 1456-1458.

Parkhurst, C.N., Yang, G., Ninan, I., Savas, J.N., Yates, J.R., Lafaille, J.J., Hempstead, B.L., Littman, D.R., and Gan, W.B. (2013). Microglia promote learning-dependent synapse formation through brain-derived neurotrophic factor. Cell 155, 1596-1609.

Paxinos, G., and Franklin, K.B. (2003). The mouse brain in stereotaxic coordinates: second edition. (Academic Press).

Perrotti, L.I., Hadeishi, Y., Ulery, P.G., Barrot, M., Monteggia, L., Duman, R.S., and Nestler, E.J. (2004). Induction of deltaFosB in reward-related brain structures after

chronic stress. J Neurosci 24, 10594-10602.

Rivest, S. (2009). Regulation of innate immune responses in the brain. Nat Rev Immunol 9, 429-439.

Schafer, D.P., Lehrman, E.K., Kautzman, A.G., Koyama, R., Mardinly, A.R., Yamasaki, R., Ransohoff, R.M., Greenberg, M.E., Barres, B.A., and Stevens, B. (2012). Microglia sculpt postnatal neural circuits in an activity and complement-dependent manner. Neuron 74, 691-705.

Shinohara, R., Taniguchi, M., Ehrlich, A.T., Yokogawa, K., Deguchi, Y., Cherasse, Y., Lazarus, M., Urade, Y., Ogawa, A., Kitaoka, S., *et al.* (2017). Dopamine D1 receptor subtype mediates acute stress-induced dendritic growth in excitatory neurons of the medial prefrontal cortex and contributes to suppression of stress susceptibility in mice. Mol Psychiatry, doi: 10.1038/mp.2017.177.

Takeuchi, O., Hoshino, K., Kawai, T., Sanjo, H., Takada, H., Ogawa, T., Takeda, K., and Akira, S. (1999). Differential roles of TLR2 and TLR4 in recognition of gram-negative and gram-positive bacterial cell wall components. Immunity 11, 443-451.

Tanaka, K., Furuyashiki, T., Kitaoka, S., Senzai, Y., Imoto, Y., Segi-Nishida, E., Deguchi, Y., Breyer, R.M., Breyer, M.D., and Narumiya, S. (2012). Prostaglandin E2-mediated attenuation of mesocortical dopaminergic pathway is critical for susceptibility to repeated

social defeat stress in mice. J Neurosci 32, 4319-4329.

Tornatzky, W., and Miczek, K.A. (1993). Long-term impairment of autonomic circadian rhythms after brief intermittent social stress. Physiol Behav 53, 983-993.

Tsuda, M., Shigemoto-Mogami, Y., Koizumi, S., Mizokoshi, A., Kohsaka, S., Salter, M.W., and Inoue, K. (2003). P2X4 receptors induced in spinal microglia gate tactile allodynia after nerve injury. Nature 424, 778-783.

Vogl, T., Tenbrock, K., Ludwig, S., Leukert, N., Ehrhardt, C., van Zoelen, M.A., Nacken, W., Foell, D., van der Poll, T., Sorg, C., and Roth, J. (2007). Mrp8 and Mrp14 are endogenous activators of Toll-like receptor 4, promoting lethal, endotoxin-induced shock. Nat Med 13, 1042-1049.

Wohleb, E.S., Hanke, M.L., Corona, A.W., Powell, N.D., Stiner, L.M., Bailey, M.T., Nelson, R.J., Godbout, J.P., and Sheridan, J.F. (2011). β-Adrenergic receptor antagonism prevents anxiety-like behavior and microglial reactivity induced by repeated social defeat. J Neurosci 31, 6277-6288.

Wohleb, E.S., Powell, N.D., Godbout, J.P., and Sheridan, J.F. (2013). Stress-induced recruitment of bone marrow-derived monocytes to the brain promotes anxiety-like behavior. J Neurosci 33, 13820-13833.

Åkerblom, M., Sachdeva, R., Quintino, L., Wettergren, E.E., Chapman, K.Z., Manfre, G.,

Lindvall, O., Lundberg, C., and Jakobsson, J. (2013). Visualization and genetic modification of resident brain microglia using lentiviral vectors regulated by microRNA-9. Nat Commun 4, 1770.

FIGURE TITLES AND LEGENDS

Figure 1. TLR2/4 are crucial for R-SDS-induced social avoidance

(A) Schedule of behavioral experiments.

(B) Definitions of the social interaction zone and the social avoidance zone (green and red rectangles, respectively).

(C and D) The levels of social interaction (C) and social avoidance (D) in wild-type mice (WT) and TLR-DKO mice with or without prior R-SDS ("R-SDS" or "naïve", respectively). The durations in the interaction (C) or avoidance (D) zone without and with an ICR mouse and the differences between these durations without and with an ICR mouse (ΔTime [ICR(+)-ICR(-)]) were analyzed and are shown.

(E) The proportions of the time for the open arms in the elevated plus maze test as an index for anxiety of wild-type mice and TLR-DKO mice.

(F) The durations for the submissive posture during the first and tenth SDS ("single" and "R-SDS", respectively) in wild-type mice and TLR-DKO mice.

**P*<0.05, ***P*<0.01, ****P*<0.001 for Bonferroni's multiple comparison test. The number of mice is shown below each group. Data are shown as means ± SEM. See also Figure S1.

Figure 2. TLR2-KO mice and TLR4-KO mice, but not TLR-DKO littermates, show R-SDS-induced social avoidance

(A-D) The levels of social interaction (C) and social avoidance (D) in TLR2-KO and TLR-DKO littermates (A and B) or in TLR4-KO mice and TLR-DKO littermates (C and D) with or without prior R-SDS ("R-SDS" or "naïve", respectively). The data were analyzed and are shown as in Figure 1C and 1D.

(E and F) The traveling distances of TLR2-KO (E) or TLR4-KO mice (F) and TLR-DKO littermates in a novel open field with or without prior R-SDS.

*P<0.05, **P<0.01, ***P<0.001 for Bonferroni's multiple comparison test. The number of mice is shown below each group. Data are shown as means ± SEM. See also Figure S1.

Figure 3. TLR2/4 are crucial for R-SDS-induced activation of mPFC microglia

(A-D) Representative images (A and C) and quantitative analyses (B and D) of CD68 (A and B) and Iba-1 (C and D) immunostaining in the mPFC of wild-type mice (WT) and TLR-DKO mice without SDS ("naïve") and at 1.5 h and 4 h after S-SDS and the last session of R-SDS. For wild-type mice after R-SDS, the images were taken and analyzed only from susceptible mice ("R-SDS(sus)"). Scale bars, 50 μm.

(E) Quantitative analyses of CD11b immunostaining in the mPFC of wild-type mice (WT) and TLR-DKO mice without SDS ("naïve") and at 1.5 h after S-SDS and the last session of R-SDS. For wild-type mice after R-SDS, the images were taken and analyzed only from susceptible mice ("R-SDS(sus)").

(F-J) Representative images (F and I) and quantitative analyses (G, H and J) of immunostaining for CD68 and Iba-1 (F-H) or CD11b (I and J) in the mPFC of wild-type mice (WT) without SDS ("naïve") and susceptible and resilient mice at 1.5 h after the last session of R-SDS ("R-SDS(sus)" and "R-SDS(res)", respectively). In the merged images of Figure 3F, CD68 and Iba-1 signals are shown in green and red, respectively. CD68 signals in Iba-1 positive microglia are seen in yellow. Nuclei were counterstained with Hoechst33342 and are shown in blue. Scale bar, 25 μm.

(K and L) Quantitative analyses of CD68 (K) and Iba-1 (L) immunostaining in the mPFC

of wild-type mice (WT) and TLR-DKO mice without SDS (“naïve”) and at 1.5 h and 4 h after the last session of R-SDS for 4 days (“4× defeat”).

*P<0.05, **P<0.01, ***P<0.001 for Bonferroni’s multiple comparison test. The values of Iba-1 and CD11b intensity were normalized to those of naïve wild-type mice. The number of mice is shown below each group. Data are shown as means ± SEM. See also Figures S2 and S3.

Figure 4. R-SDS promotes monocyte infiltration into the ACC, but not to the mPFC, in a TLR2/4-independent manner

(A) Representative images of CD45-positive monocytes in the mPFC. Microglia were visualized by Iba-1 staining. Nuclei were counterstained with Hoechst33342. In the merged image, signals for Iba-1, CD45, and Hoechst33342 are shown in green, red, and blue, respectively. Scale bar, 25 μm.

(B and C) Regions of interest in the mPFC (B) and ACC (C).

(D-G) Representative images (D and E) and quantitative analyses (F and G) of CD45 immunostaining in the mPFC (D and F) and ACC (E and G) of wild-type mice (WT) and TLR-DKO mice without SDS (“naïve”) and at 1.5 h after S-SDS and the last session of R-SDS. Iba-1 and CD45 immunostaining and nuclear counterstaining with Hoechst33342 were performed as described in A. For wild-type mice after R-SDS, the images were taken and analyzed only from susceptible mice (“R-SDS(sus)”). Arrowheads in D and E indicate the representative CD45-positive cells. Scale bars, 100 μm.

*****P<0.05 for Bonferroni’s multiple comparison test. The number of mice is shown below each group. Data are shown as means ± SEM.

Figure 5. TLR2/4 are required for the attenuation of SDS-induced c-Fos expression and dendritic atrophy of mPFC neurons by R-SDS

(A) Representative images of double immunostaining of c-Fos and NeuN, a neuronal marker, in the mPFC. Nuclei were counterstained with Hoechst33342. In the merged image, signals for c-Fos, NeuN and Hoechst33342 are shown in green, red and blue, respectively. Scale bar, 25 μm.

(B and C) Representative images (B) and quantitative analyses (C) of c-Fos immunostaining in the mPFC of wild-type mice (WT) and TLR-DKO mice without SDS ("naïve") and at 1.5 h after S-SDS and R-SDS. For wild-type mice after R-SDS, the image was taken from susceptible mice ("R-SDS(sus)"). Scale bar, 200 μm.

(D and E) Representative images (D) and quantitative analyses (E) of c-Fos immunostaining in the mPFC of wild-type mice (WT) without SDS ("naïve") and susceptible mice and resilient mice at 1.5 h after the last session of R-SDS ("R-SDS(sus)" and "R-SDS(res)", respectively). Scale bar, 200 μm.

(F-H) Representative images of Golgi-Cox staining in the mPFC (F) and quantitative analyses of the lengths of apical dendrites of mPFC deep-layer pyramidal neurons (G and H) of wild-type mice (WT) and TLR-DKO mice with or without R-SDS ("R-SDS" or "naïve", respectively). Brain sections were counterstained with cresyl violet. For wild-type mice after R-SDS, the images were taken and analyzed only from susceptible mice ("R-SDS(sus)"). Scale bar, 100 μm.

$*P<0.05$, $**P<0.01$, $***P<0.001$ for Bonferroni's multiple comparison test. The orientations of the images (B-F) are indicated by arrows (L, lateral; M, medial; D, dorsal; V, ventral). The number of mice (C, E and H) or neurons (G) is shown below each group. Data are shown as means ± SEM. See also Figure S4.

Figure 6. TLR2/4 in mPFC microglia are crucial for R-SDS-induced social avoidance

(A) Experimental design for mPFC microglia-specific knockdown of TLR2/4.

(B) Schedule for behavioral experiments.

(C) Representative images of mCherry signals co-expressed with TLR2/4 microRNA in EYFP-positive microglia in the mPFC of CX3CR1-CreER mice infected with the lentiviral vector shown in A. EYFP and mCherry signals are shown in green and red, respectively. Scale bar, 25 μm.

(D-G) The proportions of mCherry-positive cells in EYFP-expressing cells (D), the proportions of EYFP-positive cells in mCherry-expressing cells (E), the numbers of cells expressing mCherry and EYFP (F) and the numbers of cells expressing mCherry and CD45 (G) in the mPFC of CX3CR1-CreER mice infected with lentiviral vectors expressing control microRNA (“Control”) and TLR2/4 microRNA (“TLR2/4KD”) with or without R-SDS (“R-SDS” or “naïve”, respectively).

(H-K) The levels of social interaction (H and J) and social avoidance (I and K) in CX3CR1-CreER mice which received an mPFC injection of the lentiviral vector expressing control microRNA (“Control”) or TLR2/4 microRNA (“TLR2/4KD”) with either microRNA-resistant TLR2 or TLR4 mutant (“TLR2mt7” or “TLR4mt8”, respectively) or mCherry with or without prior R-SDS (“R-SDS” or “naïve”, respectively). The data were analyzed and are shown as in Figure 1C and 1D.

(L) The time spent in the open arms in the elevated plus maze test as an index for anxiety in the same mice as in H and I.

(M) The numbers of c-Fos-positive mPFC neurons of CX3CR1-CreER mice which

received mPFC injections with a lentiviral vector expressing control microRNA (“Control, R-SDS(sus)”) or TLR2/4 microRNA (“TLR2/4KD, R-SDS”) at 1.5 h after R-SDS.

*P<0.05, **P<0.01, ***P<0.001 for Bonferroni’s multiple comparison test (H, I, K); *P<0.05 for unpaired t-test (M). The number of mice is shown below each group. Data are shown as means ± SEM. See also Figures S5-7.

Figure 7. R-SDS alters cytokine expression in mPFC microglia in a TLR2/4-dependent manner

(A) Design of transcriptome analysis of wild-type or TLR-DKO microglia isolated from the mPFC and NAc without or with R-SDS. Each sample was derived from total RNA from microglia in the mPFC or NAc of 3-6 mice, which was sufficient for transcriptome analysis using the DNA microarray in our experimental condition.

(B and C) The levels of social interaction (B) and social avoidance (C) in CX3CR1-EGFP mice and TLR-DKO; CX3CR1-EGFP mice with or without R-SDS (“R-SDS” or “naïve”, respectively). The mice used for this analysis are highlighted in red. The data were analyzed and are shown as in Figure 1C and 1D.

(D and E) Venn diagrams showing the numbers of DNA microarray probes which were significantly upregulated (D) or down-regulated (E) by R-SDS in wild-type microglia (“WT”) or TLR-DKO microglia isolated from the mPFC or NAc.

(F and G) A heat map (F) and bubble charts (G) showing R-SDS-induced changes in gene expressions of representative cytokines in microglia isolated from the mPFC and NAc of susceptible wild-type mice (“WT_R-SDS(sus)”) and TLR-DKO mice (“TLR-DKO_R-SDS”), compared with those with the respective genotypes without R-SDS (“WT_naïve” and “TLR-DKO_naïve”, respectively). In bubble charts, the size of a bubble indicates the

expression level of a respective gene in microglia isolated from the mPFC or NAc of susceptible wild-type mice after R-SDS.

(H-K) The expression levels of representative R-SDS-upregulated cytokines, namely IL-1α (H), TNFα (I), IL-1β (J) and IL-6 (K), in microglia isolated from the mPFC or NAc of wild-type mice (WT) and TLR-DKO mice with or without R-SDS ("R-SDS" or "naïve", respectively). Among defeated wild-type mice, only susceptible mice were analyzed ("R-SDS(s)").

***P<0.001 for Bonferroni's multiple comparison test (B, C); *P<0.05 for unpaired t-test (F, H-J). The number of mice (B and C) or samples (H-K) is shown below each group. Data are shown as means ± SEM.

Figure 8. IL-1α and TNFα in the mPFC are crucial for R-SDS-induced social avoidance

(A) Schedule of behavioral experiments.

(B-E) The levels of social interaction (B and D) and social avoidance (C and E) in wild-type mice which received mPFC infusions with a mixture of neutralizing antibodies ("anti-IL-1α anti-TNFα"), either of these antibodies added singly ("anti-IL-1α" or "anti-TNFα"), or control antibodies of the corresponding isotypes ("isotype") with or without R-SDS ("R-SDS" or "naïve", respectively). The data were analyzed and are shown as in Figure 1C and 1D.

*P<0.05, **P<0.01, ***P<0.001 for Bonferroni's multiple comparison test. The number of mice is shown below each group. Data are shown as means ± SEM. See also Figure S2.

STAR★METHODS

CONTACT FOR REAGENT AND RESOURCE SHARING

Further information and requests for reagents may be directed to, and will be fulfilled by, the Lead Contact and corresponding author, Tomoyuki Furuyashiki (tfuruya@med.kobe-u.ac.jp).

EXPERIMENTAL MODEL AND SUBJECT DETAILS

Mice

Tlr2 knockout (TLR2-KO) mice (RRID: IMSR_OBS:3) (Takeuchi et al., 1999), *Tlr4* knockout (TLR4-KO) mice (RRID:IMSR_OBS:4) (Hoshino et al., 1999)and *Tlr2/4* double knockout (TLR-DKO) mice in a C57BL/6N background were purchased from Oriental Bio Service. To make all the mice congenic to the C57BL/6N strain, these mice were backcrossed with C57BL/6N mice more than 10 times. These congenic TLR2-KO and TLR4-KO mice were used to generate TLR-DKO mice. From the crossing among TLR2-KO, TLR4-heterozygous mice (*Tlr2*(-/-);*Tlr4*(+/-)), only TLR2-KO (*Tlr2*(-/-);*Tlr4*(+/+)) and TLR-DKO (*Tlr2*(-/-);*Tlr4*(-/-)) littermates (but not TLR2-KO, TLR4-heterozygous (*Tlr2*(-/-);*Tlr4*(+/-)) littermates) were used. Likewise, only TLR4-KO (*Tlr2*(+/+);*Tlr4*(-/-)) and TLR-DKO (*Tlr2*(-/-);*Tlr4*(-/-)) littermates (but not TLR2-heterozygous, TLR4-KO (*Tlr2*(+/-);*Tlr4*(-/-)) littermates) were used from the crossing among TLR2-heterozygous, TLR4-KO mice. *Il1r1* knockout (IL-1RI-KO) mice (formally named B6.129S7-Il1r1tm1Imx/J (RRID:IMSR_JAX:003245)) (Glaccum et al., 1997), CX3CR1-EGFP mice (formally named B6.129P-Cx3cr1tm1Litt/J (RRID:IMSR_JAX:005582)) (Jung et al., 2000) and *Cx3cr1*-CreER mice (formally named B6.129P2(Cg)-Cx3cr1tm2.1(cre/ERT2)Litt/WganJ (RRID:IMSR_JAX:021160))

(Parkhurst et al., 2013) in the C57BL/6 strain background were purchased from Jackson Laboratory. Adult male C57BL/6N mice and male ICR mice retired from breeding were purchased from Japan SLC and CLEA Japan, respectively. Mice were housed in a group of four mice in a specific pathogen-free and temperature- and humidity-controlled vivarium under a 12-h light, 12-h dark cycle (light on between 0800 and 2000) with free access to chow and water. All procedures for animal care and use were in accordance with the National Institutes of Health Guide for the Care and Use of Laboratory Animals and were approved by the Animal Care and Use Committees of Kyoto University Graduate School of Medicine and Graduate School of Pharmaceutical Sciences and Kobe University Graduate School of Medicine.

METHOD DETAILS

Social defeat stress (SDS)

Single SDS (S-SDS) or repeated SDS (R-SDS) was applied as described previously (Tanaka et al., 2012) with minor modifications. Briefly, male ICR mice were screened based on their aggressiveness to a male C57BL/6N mouse, as measured by the latency and the number of attacks during the observation period (180 s), and were used as aggressor mice for SDS. Before SDS, 6~12-week-old male mice, were isolated with free access to chow and water for 1 week. Each of the isolated mice to be defeated was introduced and kept in the home cage of a resident aggressor ICR mouse for 10 min daily for 1 day (S-SDS) or 10 consecutive days (R-SDS), except that R-SDS was applied for 4 consecutive days (R-SDS for 4 days) in Figure 3K, 3L, S3F, S3G and S5D-G. The pairs of defeated and aggressor mice were randomized daily to minimize the variability in the aggressiveness of aggressor mice. To examine the time spent for a submissive posture

during SDS, behaviors of mice were video-recorded during SDS and analyzed post hoc in a manner blind to the mouse genotype. A submissive posture was defined as a posture of a defeated mouse standing upright with the belly exposed to an aggressor (Tornatzky and Miczek, 1993). SDS was applied between 1600 and 1900 h in a sound-attenuated room in dim light. Control mice were placed in a novel cage for 10 min daily for the same number of days as R-SDS. Each mouse was subjected to the social interaction test and the elevated plus maze test consecutively, with or without prior R-SDS. In Figure 8, to reduce the amounts of antibodies to be used, we employed a shorter version of R-SDS, which is composed of three exposures to social defeat for 10 min each, with 5 min intervals between each exposure.

Social interaction test

The social interaction test was performed as previously described (Tanaka et al., 2012), with minor modifications. A defeated or control mouse was kept for 150 s in an open field chamber (30 cm×40 cm) with a wire mesh cage (10 cm×6 cm) enclosing an unfamiliar ICR mouse located at one end of the field. Mouse behaviors were video-monitored, and the trajectory of mouse ambulation was automatically determined and recorded by a SMART video tracking system (Harvard Apparatus). A 30 cm×15 cm rectangular zone including the wire mesh cage was defined as the social interaction zone (Figure 1B). A 30 cm×9 cm rectangular zone opposite to the social interaction zone was defined as the social avoidance zone. The durations which each mouse spent in the respective zones were used as indices for the levels of social interaction and social avoidance, respectively. One day before the social interaction test, mice were habituated to the test chamber without an ICR mouse, except in Figure 8, in which the habituation and the social

interaction test were performed on the same day. Traveling distances during this habituation period were used to define novelty-induced locomotor activity. The social interaction test was performed between 1500 and 1700 h on the following days after R-SDS for 4 or 10 days, unless otherwise stated.

It has been reported that the level of social avoidance varies considerably across individual mice. In this study, we defined susceptible mice as those which showed social interaction and social avoidance for less than 40% and more than 60%, respectively, of the observation period. Resilient mice were defined as those which showed social interaction and social avoidance for more than 60% and less than 40%, respectively, of the observation period. These criteria excluded mice that spent most of the time in the middle zone and were thus difficult to categorize as either susceptible or resilient. Indeed, susceptible and resilient wild-type mice comprised most (77.8%) of the total of defeated wild-type mice prepared for the immunostaining (18/45 and 17/45, respectively).

Elevated plus maze test

The elevated plus maze test was performed as previously described (Tanaka et al., 2012), with minor modifications. An elevated plus maze is composed of two open arms (5 cm wide, 25 cm long, without walls) and two closed arms (5 cm wide, 25 cm long, with 15 cm walls) that are interconnected by a central area of 5 cm square, and it is maintained at a height of 50 cm from the floor. After acclimation to a test environment, a defeated or control mouse was transferred to the center of the elevated plus maze and kept on the maze for 5 min. Mouse behaviors were video-monitored, and the trajectory of mouse ambulation was automatically determined and recorded by the SMART video tracking system (Harvard Apparatus). The proportion of the time that the mouse spent in the open

arms during the observation period was determined.

Immunostaining

Immunofluorescent staining for c-Fos, Iba-1, CD68, CD11b, CD45, synaptophysin, and PSD-95 in the brain was performed without SDS, or at 1.5 h and 4 h after S-SDS or the last session of R-SDS. Susceptible mice and resilient mice were chosen according to the social interaction test after the last session of R-SDS for 10 days, and were subjected to an additional SDS at 1.5 h and 4 h prior to sacrifice. Immunofluorescent staining was performed as described previously (Tanaka et al., 2012) with minor modifications. Briefly, under deep anesthesia with intraperitoneal (i.p.) injection of sodium pentobarbital (50 mg/kg; Nacalai), mice were transcardially perfused with 20 ml Dulbecco's modified phosphate buffered saline (D-PBS) followed by 0.1M sodium phosphate buffer (pH 7.4) containing 4% paraformaldehyde. Brains were immersed in 0.1M sodium phosphate buffer (pH 7.4) containing 4% paraformaldehyde and 30% sucrose for 24 h. After the brains were rapidly frozen in OCT compound (Sakura Finetek), coronal brain sections of 30-μm thickness were made with a cryostat (Carl Zeiss MicroImaging). Immunofluorescent staining for HA tag and FLAG tag in cultured cells was performed as described below. The cells were washed with D-PBS and fixed with 0.1M sodium phosphate buffer (pH 7.4) containing 4% paraformaldehyde at RT for 30 min. After washed with D-PBS, the brain sections or the cells were incubated in blocking buffer composed of D-PBS containing 0.3% Triton X-100, 1% normal donkey serum and 0.125% carrageenan for 60 min at room temperature (RT). The sections or the cells were then incubated with appropriate primary antibodies in the blocking buffer at 4°C for 36 h. The primary antibodies used in this study were rabbit polyclonal anti-c-Fos (1:5000

dilution, Ab-5; Millipore, RRID: AB_2314043), rabbit anti-Iba-1 (1:500 dilution, 019-19741; Wako, RRID: AB_839504), mouse anti-NeuN (1:500 dilution, MAB377; Chemicon, RRID: AB_2298772), rat anti-CD68 (1:200 dilution, FA-11; AbD serotec, RRID: AB_322219), mouse anti-CD68 (1:500 dilution, KP1; Abcam, RRID: AB_307338), rat anti-CD45 (1:500 dilution, IBL-3/1; AbD serotec, RRID: AB_321729), rat anti-CD11b (1:500 dilution, 5C6; AbD serotec, RRID: AB_323135), rat anti-GFP (1:500 dilution, 04404-84, Nacalai, RRID: AB_10013361), rabbit anti-RFP (1:500 dilution, 600-401-379 ; Rockland, RRID: AB_2209751), mouse anti-RFP (1:500 dilution, M165-3; MBL, RRID: AB_1520843), rat anti-HA (1:500 dilution, 11867423001; Roche, RRID:AB_10094468), mouse anti-FLAG (1:1000 dilution, F1804; Sigma-Aldrich, RRID:AB_262044), rabbit anti-synaptophysin (1:1000 dilution, AB16659-1; Abcam, RRID: AB_443419) and mouse anti-PSD-95 (1:1000 dilution, MAB1596; Merck Millipore, RRID: AB_2092365). The sections were washed for 10 min three times at RT in D-PBS containing 0.3% Triton X-100. For immunofluorescent staining, the sections or the cells were incubated with Alexa Fluor 488-, Alexa Fluor 555- or Alexa Fluor 647-labeled secondary antibodies (1:500 dilution; Life Technologies) for 2 h at RT. The sections were mounted on APS-coated glass slides (Matsunami Glass). The sections or the cells were embedded in ProLong Gold Antifade Reagent (Life Technologies).

Analyses of immunofluorescent images

Immunofluorescent images for c-Fos staining were acquired through a 10x objective lens (N.A. 0.45) with a BIOREVO HS All-in-one Fluorescence Microscope (Keyence). Immunofluorescent images for synaptophysin and PSD-95 staining were acquired through a 63x oil-immersion objective lens (N.A. 1.40) and processed with channel

alignment using structured illumination microscopy (ELYRA PS.1, Carl Zeiss). Fluorescent images for the other signals were acquired through a 40x oil-immersion objective lens (N.A. 1.25) with a TCS-SP5 laser-scanning confocal microscope (Leica Microsystems). Confocal images were obtained at multiple Z planes and vertically projected. Six representative images for mPFC and 4 images for NAc were taken from each mouse. Images for c-Fos signals were analyzed using BZ-II Measurement Module software (Keyence). Images for synaptophysin and PSD-95 were processed using Imaris (Bitplane). Images for the other signals were analyzed using MetaMorph (Molecular Devices). Predetermined thresholds for the intensity and the size were applied to images to detect Iba-1-positive cells, CD68-positive puncta, CD11b-positive puncta, CD45-positive cells, c-Fos-positive nuclei, EYFP-positive cells, mCherry-positive cells, synaptophysin-positive puncta, and PSD-95-positive puncta as objects for subsequent image analyses. The same thresholds were applied to all the images in the same comparison groups. Most c-Fos signals detected using this method merged with DAPI-stained and NeuN-positive nuclei, indicating nuclear c-Fos staining of mPFC neurons (see Figure 5A). The intensity of immunofluorescent Iba-1 signals, the area of CD68-positive puncta, the intensity of CD11b-positive puncta, the number of c-Fos positive nuclei, the number of synaptophysin-positive puncta, and the number of PSD-95-positive puncta were determined for each image. The values of Iba-1 and CD11b intensities were normalized to those of corresponding control groups in respective figures. The numbers of EYFP-positive cells, mCherry-positive cells, CD45-positive cells, EYFP:mCherry-double-positive cells and CD45:mCherry-double-positive cells, as well as the proportion of EYFP:mCherry-double-positive cells in either mCherry-positive cells or EYFP-positive microglia were determined for each image. The resultant values were averaged

for respective brain areas of each mouse and statistically analyzed. For χ^2 analysis on the proportions of defeated wild-type and TLR-DKO mice with CD68 and c-Fos signals beyond the distributions of these signals in naïve mice, the threshold was determined to maximally discriminate the distributions of each signal between naïve and defeated mice of the respective genotypes.

Golgi-Cox staining

Golgi-Cox staining was performed using a FD Rapid GolgiStain Kit (FD Neuro Technologies) according to the manufacturer's instructions. Briefly, mice were sacrificed by decapitation at 24 h after the social interaction test, and the brains were quickly collected in MilliQ water. The anterior part of the brain was dissected and immersed in freshly prepared Golgi-Cox impregnation buffer included in the kit. The impregnation buffer was refreshed after 24 h, and the brains were incubated for 2 weeks. After cryoprotection with the cryoprotectant buffer included in the kit at 4°C for 1 week, each brain was frozen in isopentane kept at -80oC and cut into 200-μm sections with a cryostat (Carl Zeiss MicroImaging). The sections were mounted on gelatin-coated slides, dried at RT for 72 h, and stained according to the manufacturer's instructions. The sections were counterstained with Nissl staining. The slides were dehydrated in ethanol, cleared in xylene, and covered with Mount Quick (Daido Sangyo). Images were acquired with a BIOREVO HS All-in-one Fluorescence Microscope (Keyence). The lengths of apical dendrites of Golgi-impregnated pyramidal neurons in the mPFC were measured by Image J software post hoc in a manner blind to experimental conditions. Since many layer 6 pyramidal neurons possess short apical dendrites, which are much easier to trace than those of other neuronal populations, we chose layer 6 pyramidal neurons for this analysis.

Isolation of microglia from the brain

Since CX3CR1-EGFP mice were generated by replacing the open reading frame for CX3CR1 by that for EGFP (Jung et al., 2000), we used heterozygous CX3CR1-EGFP mice to preserve CX3CR1 function. Cell dissociation from the brain tissue was performed using the Papain Dissociation System (Worthington Biochemical Corporation). Briefly, under deep anesthesia with i.p. injection of sodium pentobarbital (50 mg/kg; Nacalai), CX3CR1-EGFP mice were transcardially perfused with D-PBS, and the brains were rapidly isolated. After the olfactory bulb and the cerebellum were removed, the brains were minced in Earle's Buffer containing papain and DNase I saturated with 95% O2 and 5% CO2 according to the manufacturer's protocol. The small brain tissues were incubated for 60 min at 37°C with rocking and triturated. The dissociated cells were passed through a cell strainer with 70-μm pores (BD Falcon). Myelin was removed using AutoMACS (Miltenyi Biotech) and myelin removal beads (Miltenyi Biotech). Cells were stained with propidium iodide (eBioscience) and subjected to cell sorting using a FACS AriaIII (BD Biosciences). EGFP-positive cells containing microglia and monocytes (a minor population) in the brain, and EGFP-negative cells containing other types of cells were collected. Dead cells were removed according to propidium iodide staining. Total RNA was extracted from the collected cells using an RNeasy Plus Mini kit (QIAGEN).

Quantitative RT-PCR

cDNA was obtained from total RNA using a High Capacity cDNA Reverse Transcription Kit (Life Technologies). All PCR experiments were conducted in duplicate using SYBR Premix Ex Taq (Takara Bio), and fluorescent SYBR Green signals were automatically

detected and analyzed with a CFX96 Touch Real-Time PCR Detection System (Bio-Rad) or Applied Biosystems 7500 (Applied Biosystems). Primers for PCR are as follows: for mouse *Actb* (β-actin), 5'-TGC GTG ACA TCA AAG AGA AG-3' and 5'-GAT GCC ACA GGA TTC CAT A-3'; for mouse *Cd11b*, 5'-CAA TAG CCA GCC TCA GTG C-3' and 5'- GAG CCC AGG GGA GAA GTG-3'; for mouse *Il1r1*, 5'-CGA ACC GTG AAC AAC ACA AA-3' and 5'-CAG AGG CAC CAT GAG ACA AA-3'; for mouse *Tlr1*, 5'-CTG AGG GTC CTG ATA ATG TCC T-3' and 5'-GAT GCC ACA GGA TTC CAT A-3'; for mouse *Tlr2*, 5'-TGG AAT GTC ACC AGG CTG C-3' and 5'- GTC CGT GGA AAT GGT GGC-3'; for mouse *Tlr3*, 5'-GAT ACA GGG ATT GCA CCC ATA-3' and 5'-TCC CCC AAA GGA GTA CAT TAG A-3'; for mouse *Tlr4*, 5'-ATG GAA AAG CCT CGA ATC CT-3' and 5'- TCC AAG TTG CCG TTT CTT GT-3'; for mouse *Tlr5*, 5'-GGC TGT AAC CTC ACC CAG AT-3' and 5'-CCA GGA GTG GAA ATG ATG TG-3'; for mouse *Tlr6*, 5'-ACC GTC AGT GCT GGA AAT AGA-3' and 5'-CGA TGG GTT TTC TGT CTT GG-3'; for mouse *Tlr7*, 5'-CTC CAG TCT TTC TGT ATT GCA CA-3' and 5'-GAA GTT AGT GCC AAG GTC AAG AA-3'; for mouse *Tlr8*, 5'-AAA TCC CAA ATG GAG CAT TC-3' and 5'-CAG CAA GTG AAG GTG AGG AA-3'; for mouse *Tlr9*, 5'-GAG AAT CCT CCA TCT CCC AAC-3' and 5'-CCA GAG TCT CAG CCA GCA C-3'; for mouse *Tlr11*, 5'-ATG GGG CTT TAT CCC TTT TG-3' and 5'-AGA TGT TAT TGC CAC TCA ACC A-3'; for mouse *Tlr12*, 5'-TCT GAG GGG TAA GGG AGA CA-3' and 5'-GCA GTG GGA CAC GAA TAC ATC-3'; for mouse *Tlr13*, 5'-ACT TGG CCG GAC AGT GTT-3' and 5'-GCC CAA CGC ATT TCT GAT-3'; for human *Actb* (β-actin), 5'-ATT GGC AAT GAG CGG TTC-3' and 5'-CGT GGA TGC CAC AGG ACT-3'. The values were normalized to those of β-actin mRNA in the same cDNA samples. The levels were then normalized to those of the control groups.

Transplantation of cultured microglia-like cells into the mPFC

Primary microglia were isolated as microglia-like cells, as described previously (Tsuda et al., 2003). Briefly, brains were removed from the skulls of wild-type neonates at postnatal day 2, and cortices were collected. The cortices were mashed by a cell scraper and passed through a cell strainer with 70-μm pores (BD Falcon). The cells were seeded in a 75-cm2 flask and incubated at 37oC and 5% CO2. After 7-10 days, floating microglia were collected from cultures by shaking a flask at 125 rpm for 60 min and plated on a new culture dish. After the incubation at 37oC and 5% CO2 for 30 min, culture medium was changed to remove unattached non-microglial cells, and adherent cells were maintained until transplantation. Immunofluorescent staining confirmed that more than 90% of adherent cells were Iba-1-positive cells. On the day of transplantation, adherent cells were collected by a cell scraper. The cell suspension was adjusted to 10,000 cells/μl with Hank's Balanced Salt Solution (HBSS; Life Technologies). The cell suspension of 500 nl per injection site was injected bilaterally into the mPFC through a 27-gauge stainless needle attached to a syringe pump (Eicom) while mice were kept under anesthesia with isoflurane (Wako). The stereotaxic coordinates were targeted to the infralimbic cortex: 1.9 mm anterior from the bregma, 0.4 mm lateral from the midline, and 3.0 mm ventral from the skull surface at the bregma according to a mouse brain atlas (Paxinos and Franklin, 2003). To visualize the distribution of injected microglia, microglia were labeled with carboxyfluorescein diacetate succinimidyl ester (CFSE; Life Technologies) before transplantation. Sham-operated mice received the same treatment, except that HBSS was injected into the mPFC. After a four-week recovery, the mice were subjected to R-SDS for 4 or 10 days. The transplanted cells typically spread around 500

μm from the injection site. The percentage of CFSE/Iba-1 cells over total Iba1 cells was about 50% around the injection site, regardless of whether wild-type or TLR-DKO microglia were transplanted, or whether the mice were defeated or not.

Lentiviral vectors

A lentiviral vector expressing artificial microRNA targeting TLR2/4 with mCherry only in cells expressing Cre recombinase was generated as follows. We designed the sequences for the artificial microRNAs for *Tlr2* and *Tlr4* according to the website for the BLOCK-iT RNAi Designer (Thermo Fisher Scientific). First, the DNA fragment encoding microRNA (miR) for either *Tlr2* (5'-TGC TGT GAA GAG TCA GGT GAT GGA TGG TTT TGG CCA CTG ACT GAC CAT CCA TCC TGA CTC TTC A-3' and 5'-CCT GTG AAG AGT CAG GAT GGA TGG TCA GTC AGT GGC CAA AAC CAT CCA TCA CCT GAC TCT TCA C-3') or *Tlr4* (5'-TGC TGT TCA CGT AGA AAC TGT AAG TCG TTT TGG CCA CTG ACT GAC GAC TTA CAT TCT ACG TGA A-3' and 5'-CCT GTT CAC GTA GAA TGT AAG TCG TCA GTC AGT GGC CAA AAC GAC TTA CAG TTT CTA CGT GAA C-3') was subcloned into pcDNA6.2-GW/EmGFP-miR (Life Technologies). The resultant vectors were named pcDNA6.2-GW/EmGFP-TLR2miR and pcDNA6.2-GW/EmGFP-TLR4miR, respectively. The open reading frame of EmGFP in pcDNA6.2-GW/EmGFP-TLR4miR was replaced with that of mCherry to generate pcDNA6.2-GW/mCherry-TLR4miR. The fragment encoding *Tlr2*miR was obtained from pcDNA6.2-GW/EmGFP-TLR2miR and inserted between the BglII and XhoI sites downstream of *Tlr4*miR of pcDNA6.2-GW/mCherry-TLR4miR. The fragment encoding mCherry plus *Tlr4*miR and *Tlr2*miR in tandem (TLR2/4 microRNA) was obtained from the resultant construct and inserted between AscI and NheI sites of pAAV-

EF1α-DIO-EYFP vector (Addgene). The resultant vector was digested with AgeI and SphI to obtain a fragment containing loxP/lox2272 sequences for the FLEx switch, the open reading frame of mCherry, and the sequence encoding TLR2/4 microRNA, and this fragment was used to replace the open reading frame of GFP in pLV-PGK-GFP (Åkerblom et al., 2013) (a kind gift from Dr. Johan Jakobsson at Lund University). The resultant plasmid was named pLV-PGK-DIO-mCherry-TLR4miR-TLR2miR, and was used to generate the lentiviral vector expressing TLR2/4 microRNA and mCherry specifically in cells expressing Cre recombinase. For simultaneous knockdown of endogenous *Tlr2* and *Tlr4* in the N9 microglial cells (a kind gift from Dr. Makoto Tsuda at Kyushu University), the fragment encoding mCherry and TLR2/4 microRNA was obtained from pLV-PGK-DIO-mCherry-TLR4miR-TLR2miR by PCR and inserted between SphI and AgeI sites of pLV-PGK-Sph/Pst, a plasmid derived from pLV-PGK-GFP containing an additional multiple cloning site. Then, the fragment containing the PGK promoter and blasticidin-resistance gene (blasticidin S deaminase, bsd) was obtained from pLenti6.4/R4R2/V5-DEST (Life Technologies) and inserted into the KpnI site. The resultant plasmid was named pLV-PGK-mCherry-TLR4miR-TLR2miR-PGK-bsd, and was used to generate the lentiviral vector expressing TLR2/4 microRNA, mCherry and the blasticidin-resistance gene constitutively.

To generate a lentiviral vector expressing control microRNA, the DNA fragment encoding control microRNA (5’-TGC TGA AAT GTA CTG CGC GTG GAG ACG TTT TGG CCA CTG ACT GAC GTC TCC ACG CAG TAC ATT T-3’ and 5’-CCT GAA ATG TAC TGC GTG GAG ACG TCA GTC AGT GGC CAA AAC GTC TCC ACG CGC AGT ACA TTT C-3’), which can form a hairpin structure processed into mature microRNA, but is predicted not to target any known vertebrate gene, was used instead of

those encoding *Tlr2* microRNA and *Tlr4* microRNA. The resultant plasmid contains loxP/lox2272 sequences for the FLEx switch, the open reading frame of mCherry, and the sequences encoding two copies of control miRNA in tandem, and was used to generate the lentiviral vector expressing control miRNA and mCherry only in the presence of Cre recombinase.

A lentiviral vector expressing either a *Tlr2* or *Tlr4* synonymous mutant resistant to the respective miRNA simultaneously with TLR2/4 microRNA specifically in cells expressing Cre recombinase was generated as follows. The open reading frames of *Tlr2* and *Tlr4* attached with HA-tag and FLAG-tag at the C-terminals, respectively, were PCR-amplified from pCMV-SPORT-mTLR2 and pCMV-SPORT6-mTLR4 using primers containing sequences for the respective tags (for HA, 5'-TAT CCC TAT GAT GTG CCA GAC TAT GCT-3' and for FLAG, 5'-GAC TAC AAG GAT GAC GAT GAC AAG-3'). The amplified open reading frames were inserted between AgeI and SalI sites of pLV-PGK-Sph/Pst to generate pLV-PGK-TLR2-HA and pLV-PGK-TLR4-FLAG. Seven or 8 nucleotides within the microRNA-targeting regions of *Tlr2* and *Tlr4* in these plasmids were substituted without changing their amino acid sequences (see Figure S6C and S6D) by PCR to generate pLV-PGK-TLR2mt7-HA and pLV-PGK-TLR4mt8-FLAG, respectively. The open reading frames of the mutated *Tlr2* and *Tlr4* (TLR2mt7-HA and TLR4mt8-FLAG, respectively) were obtained from pLV-PGK-TLR2mt7-HA or pLV-PGK-TLR4mt8-FLAG by PCR and inserted between the NheI and BsstBI sites of pLV-PGK-DIO-mCherry-TLR2/4 miRNA to replace the open reading frame of mCherry in this plasmid. The resultant plasmids were named pLV-PGK-DIO-TLR2mt7-HA-TLR2/4 miRNA and pLV-PGK-DIO-TLR4mt8-FLAG-TLR2/4 miRNA.

Lentiviral vectors were produced as described previously (Hioki et al., 2007). The

plasmids generated above and helper plasmids from a Lenti-X HTX packaging System (Clontech) were transfected into Lenti-X 293T cells (a derivative of HEK293T cells; Clontech) with Xfect Polymer (Clontech). At 8 h after transfection, the medium was replaced with virus production medium containing UltraCULTURE (Cambrex), 0.1 M MEM Non-Essential Amino Acids (NEAA; Life Technologies), 4 mM L-glutamine (Life Technologies), 2 mM GlutaMAX (Life Technologies) and 1 mM sodium pyruvate (Nacalai). The medium was collected at 48 h after transfection and concentrated with an Amicon Ultra-15 Centrifugal Filter Unit (Millipore). To determine the titer of the generated lentiviral vectors, genomic RNA was extracted from the lentiviral vectors and subjected to quantitative RT-PCR analysis using a Lenti-X qRT-PCR Titration Kit (Clontech).

Knockdown of TLR2/4 in cultured cells

Plasmids containing cDNA clones encoding mouse *Tlr1*, *Tlr2*, *Tlr 3*, *Tlr4*, *Tlr5*, *Tlr6*, *Tlr7*, *Tlr8*, *Tlr9*, *Tlr11*, *Tlr12* and *Tlr13* were obtained from GE Dharmacon, Addgene, and R&D Systems. The plasmids containing mouse *Tlr1*, *Tlr2*, *Tlr4*, *Tlr6* and *Tlr9* have the CMV promoter, so that the respective genes are constitutively expressed. Since the other plasmids do not have any promoter sequence, the open reading frames of the respective genes were subcloned into pcDNA3.1 to generate the mammalian expression plasmids with a CMV promoter. To quantify the knockdown efficiency of TLR2/4 microRNA, both a TLR-expressing plasmid and a microRNA-expressing plasmid were transfected into Lenti-X 293T cells with Lipofectamine 2000 (Thermo Fisher Scientific). At 48 h after transfection, the cells were harvested to purify total RNA using a Nucleospin RNA kit (Macherey-Nagal). For simultaneous knockdown of endogenous *Tlr2* and *Tlr4* in the

N9 microglial cells, the cells were infected with the lentivirus vector which expresses TLR2/4 microRNA, mCherry, and the blasticidin-resistance gene (pLV-PGK-mCherry-TLR4miR-TLR2miR-PGK-bsd). From the next day, the cells were incubated with blasticidin (final concentration; 5μg/ml) for two days. After blasticidin was removed, the cells were cultured for 4 days, and then harvested to purify total RNA. The specificity and efficiency of the knockdown were validated using quantitative RT-PCR, as described above.

Injection of lentiviral vectors into the mPFC

Under anesthesia with isoflurane, a lentiviral solution of 500 nl per injection site at 2 x 10^9 copies/ml was stereotaxically pressure-injected at two sites in each hemisphere, bilaterally, into the mPFC using a PV-830 Pneumatic PicoPump (World Precision Instruments) through a glass micropipette made with a PN-30 micropipette puller (Narishige). The stereotaxic coordinates were targeted to the infralimbic cortex: 1.9 mm anterior from the bregma, 0.3 and 0.5 mm lateral from the midline, and 3.0 mm ventral from the skull surface at the bregma according to a mouse brain atlas (Paxinos and Franklin, 2003).

Transcriptome analyses

For transcriptome analysis in mPFC tissue, wild-type mice were subjected to R-SDS. At 4 h after the last stress exposure, mice were transcardially perfused with ice-cold D-PBS under deep anesthesia with i.p. injection of sodium pentobarbital. Brains were sliced at 0.5-mm intervals using a mouse brain slicer matrix. mPFC was collected in RNA Later (Life Technologies) using a 1.5 mm biopsy punch (Kai Industries). Total RNA was

prepared using an RNeasy Plus Mini kit (QIAGEN). The resultant RNA (35 ng per array isolated from the mPFC of an individual mouse) was converted to cDNA using a Low Input Quick Amp Labeling Kit (Agilent Technologies). The cDNA samples were used to synthesize Cy3-labeled cRNA using a Low Input Quick Amp Labeling Kit (Agilent Technologies). The resultant Cy3-labeled cRNA was fragmented and hybridized with a SurePrint G3 Mouse GE 8×60K Microarray (Agilent Technologies).

For mPFC microglia- or NAc microglia-specific transcriptome analyses, CX3CR1-EGFP mice and TLR-DKO mice were crossed to generate CX3CR1-EGFP mice lacking TLR2 and TLR4 (TLR-DKO; CX3CR1-EGFP mice). CX3CR1-EGFP mice and TLR-DKO; CX3CR1-EGFP mice were subjected to R-SDS. At 90 min after the last stress exposure, mice were transcardially perfused with ice-cold D-PBS under deep anesthesia with i.p. injection of sodium pentobarbital. Brains were sliced at 0.5-mm intervals using a mouse brain slicer matrix. The mPFC and NAc were collected using a 1.5 mm biopsy punch (Kai Industries). EGFP-positive cells were isolated as described above. To ensure that each sample had 500 pg of total RNA, which was sufficient for subsequent processing, microglia isolated from the mPFC or NAc of 3-6 mice were pooled for each sample. Total RNA was prepared using an RNeasy Plus Mini kit (QIAGEN). The resultant RNA was amplified and converted to cDNA using an Ovation RNA Amplification System V2 (NuGEN). The cDNA samples were used to synthesize Cy3-labeled cDNA using a SureTag DNA labeling kit (Agilent Technologies). The resultant Cy3-labeled cDNA was hybridized with a SurePrint G3 Mouse GE 8×60K Microarray (Agilent Technologies). Signal values were normalized to the average across all probes on each chip. Signals for a given probe were considered to be significantly different between two groups if the difference was larger than two-fold and significant for an unpaired t-test at the 5% false

positive rate. These analyses were performed using Gene Spring 12.6 (Agilent Technologies).

Local infusion of neutralizing antibodies into the mPFC

Under anesthesia with isoflurane, cannulas were implanted into the mPFC. The stereotaxic coordinates were targeted to the infralimbic cortex as described above. After a 7-day recovery, 1 μl of PBS containing a mixture of neutralizing antibodies to IL-1α (16-7011-85; eBioscience, RRID:AB_469199) and TNFα (506331; BioLegend, RRID:AB_11147367) (0.25 μg each) per injection site was pressure-injected bilaterally into the mPFC using a microsyringe pump (Eicom). For a negative control, either or both of the two antibodies were replaced by the same amount of corresponding isotype antibodies (16-4888-85; eBioscience, RRID:AB_470172 and 400431; BioLegend, RRID:AB_11150233). At 2 h after the infusion, mice were subjected to a shorter version of R-SDS, followed by the social interaction test, as described above.

QUANTIFICATION AND STATISTICAL ANALYSIS

We did not exclude any samples (e.g., mice and neurons) from our statistical analyses. Data are shown as means ± SEM. Comparison of two groups was analyzed by a two-sided unpaired t-test, with Welch's correction if the assumption of equal variance was violated. For comparison of more than two groups, multiple comparison tests with Bonferroni correction were used. For correlative analyses, a Pearson correlation was performed. The analyses were performed with PRISM 7.0 software (GraphPad). *P* values less than 0.05 were considered to be significant. All the statistical details can be found in Table S1.

DATA AND SOFTWARE AVAILABILITY

The raw data have been deposited in the Mendeley Data under the following URL: https://data.mendeley.com/datasets/2tyyncv6rm/draft?a=1b61fbd5-1bd0-475e-97bd-da0e80ce94eb.

The accession number for the DNA microarray data reported in this paper is GEO: GSE115996.

SUPPLEMENTAL FIGURES

Figure S1, related to Figures 1 and 2. Behavioral and gene expression analyses of TLR2, TLR4, and IL-1RI

(A) A heat map showing R-SDS-induced changes in gene expression of the top 25 most upregulated genes in the mPFC from susceptible and resilient wild-type mice ("WT_R-SDS(sus)" and "WT_R-SDS(res)", respectively). **P*<0.05 for unpaired *t*-test for the changes in gene expression for the indicated probes. (**B** and **C**) The expression levels of S100A8 (**B**) and S100A9 (**C**) in the mPFC of susceptible and resilient wild-type mice ("R-SDS(sus)" and "R-SDS(res)", respectively) at 4 h after R-SDS as well as wild-type mice without SDS ("naïve"). **P*<0.05, ***P*<0.01, ****P*<0.001 for Bonferroni's multiple comparison test. (**D** and **E**) The durations for presence in the interaction (**D**) or avoidance (**E**) zone without and with an ICR mouse and the differences between these durations without and with an ICR mouse (ΔTime [ICR(+)-ICR(-)]), for wild-type mice ("WT") with or without prior R-SDS ("R-SDS" and "naïve"). Red dots in right panels indicate the data from susceptible mice. **P*<0.05 for Bonferroni's multiple comparison test (left panels) or unpaired *t*-test (right panels). (**F**-**I**) mRNA levels of *Cd11b* (**F**), *Tlr2* (**G**), *Tlr4*

(**H**) and *Il1r1* (**I**) in EGFP-positive cells ("EGFP(+)") and EGFP-negative cells ("EGFP(-)") isolated from CX3CR1-EGFP mice, in which EGFP is selectively expressed in microglia and monocytes (a minor population) in the brain, with or without prior R-SDS ("R-SDS" or "naïve", respectively). The levels were normalized to that of *Actb* (β-actin) to minimize sample variance. The levels were further normalized to those of the control groups, namely EGFP(-) in Figure S1F and naïve EGFP(-) in Figure S1G-I, and are shown. ***P<0.001 for unpaired *t*-test (**F**) and *P<0.05 for Bonferroni's multiple comparison test (**I**). (**J** and **K**) The durations for presence in the interaction (**J**) or avoidance (**K**) zone with an ICR mouse for wild-type mice (WT), TLR2-KO mice, and TLR4-KO mice before and after R-SDS ("naïve" and "R-SDS", respectively). The same individuals were analyzed and statistically compared before and after R-SDS. *P<0.05 for Bonferroni's multiple comparison test. (**L** and **M**) The durations within the interaction (**L**) or avoidance (**M**) zone without and with an ICR mouse and the differences between these durations without and with an ICR mouse (ΔTime [ICR(+)-ICR(-)]) in IL-1RI-KO mice with or without prior R-SDS ("R-SDS" or "naïve", respectively). *P<0.05 for Bonferroni's multiple comparison test (left panels) or unpaired *t*-test (right panels). (**N**) The level of anxiety of IL-1RI-KO mice with or without prior R-SDS ("R-SDS" or "naïve", respectively). The proportion of the time spent in the open arms in the elevated plus maze was measured as an index of anxiety. The number of mice is shown below each group. Data are shown as means ± SEM.

Figure S2, related to Figures 3 and 8. TLR2 and TLR4 deficiency attenuates R-SDS-induced activation of mPFC microglia

(**A**-**F**) Representative images (**A** and **D**) and quantitative analyses (**B**, **C**, **E** and **F**) of

immunostaining for CD68 and Iba-1 in the mPFC of TLR2-KO mice (**A**-**C**) and TLR4-KO mice (**D**-**F**) without SDS ("naïve"), susceptible and resilient mice ("R-SDS(sus)" and R-SDS(res)", respectively) with the respective genotypes, and TLR-DKO littermates (**B**, **C**, **E** and **F**) with or without R-SDS ("R-SDS" and "naïve", respectively) at 1.5 h after the last session of R-SDS. The images from TLR-DKO littermates are not shown in this figure, since these images are similar to those from TLR-DKO mice shown in Figure 3A and 3C. In the merged images, CD68 and Iba-1 signals are shown in green and red, respectively. CD68 signals in Iba-1 positive microglia are seen in yellow. Nuclei were counterstained with Hoechst 33342 and are shown in blue. The values of Iba-1 intensity were normalized to that of naïve TLR2-KO or TLR4-KO mice for Figure S2C or S2F, respectively. (**G**-**J**) Representative images (**G** and **I**) and quantitative analyses (**H** and **J**) of immunostaining of CD68 in the mPFC (**G** and **H**) and NAc (**I** and **J**) of wild-type mice which received mPFC infusions with a mixture of neutralizing antibodies for IL-1α and TNFα ("anti-IL-1α anti-TNFα") or control antibodies of the corresponding isotypes ("isotype") without SDS ("naïve"), and at 1.5 h and 4 h after the last session of a shorter version of R-SDS (see Figure 8A). Scale bars, 20 μm. $^{**}P<0.01$, $^{***}P<0.001$ for Bonferroni's multiple comparison test. The number of mice is shown below each group. Data are shown as means ± SEM.

Figure S3, related to Figure 3. R-SDS does not induce activation of NAc microglia in wild-type mice or TLR-DKO mice

(**A**) Colocalization of CD68 signals with FA-11, a monoclonal anti-CD68 antibody which was mainly used in this study, and those with KP1, another monoclonal anti-CD68 antibody. This colocalization with the two independent antibodies confirmed the

specificity of CD68 signals. Scale bar, 50 μm. (**B**-**E**) Representative images (**B** and **D**) and quantitative analyses (**C** and **E**) of CD68 (**B** and **C**) and Iba-1 (**D** and **E**) immunostaining in the NAc of wild-type mice (WT) and TLR-DKO mice without SDS ("naïve"), and at 1.5 h and 4 h after S-SDS and the last session of R-SDS. For wild-type mice after R-SDS, the images were taken and analyzed only from susceptible mice ("R-SDS(sus)"). Scale bars, 50 μm. (**F** and **G**) Quantitative analyses of CD68 (**F**) and Iba-1 (**G**) immunostaining in the NAc of wild-type mice (WT) and TLR-DKO mice without SDS ("naïve") and at 1.5 h and 4 h after the last session of R-SDS for 4 days ("4× defeat"). The values of Iba-1 intensity were normalized to that of naïve wild-type mice. The number of mice is shown below each group. Data are shown as means ± SEM.

Figure S4, related to Figure 5. SDS-induced c-Fos expression in mPFC neurons of TLR2-KO mice and TLR4-KO mice as well as TLR-DKO littermates

Representative images (**A** and **B**) and quantitative analyses (**C** and **D**) of c-Fos immunostaining in mPFC of TLR2-KO mice (**A** and **C**) and TLR4-KO mice (**B** and **D**) without SDS ("naïve"), susceptible and resilient mice ("R-SDS(sus)" and "R-SDS(res)", respectively) of the respective genotypes, and TLR-DKO mice (**C** and **D**) with or without R-SDS ("R-SDS" and "naïve", respectively) at 1.5 h after the last session of R-SDS. The images from TLR-DKO littermates are not shown in this figure, since these images are similar to those from TLR-DKO mice shown in Figure 5B. The orientations of the images are indicated by arrows (L, lateral; M, medial; D, dorsal; V, ventral). Scale bars, 100 μm. **P*<0.05, ***P*<0.01, ****P*<0.001 for Bonferroni's multiple comparison test. The number of mice is shown below each group. Data are shown as means ± SEM.

Figure S5, related to Figure 6. Transplantation of wild-type microglia-like cells into the mPFC of TLR-DKO mice transiently restores social avoidance induced by R-SDS

(**A**) Design of behavioral experiments with transplantation of microglia-like cells. Primary microglia-like cells were obtained from wild-type (WT) and TLR-DKO neonates, and were transplanted to the mPFC of TLR-DKO mice. After a four-week recovery, the mice were subjected to R-SDS. (**B**) Representative images of transplanted microglia-like cells in the mPFC. Wild-type microglia-like cells were labeled with CFSE and locally infused into the mPFC of TLR-DKO mice. Fluorescence images were taken after the four-week recovery. Microglia were visualized by Iba-1 staining. CFSE and Iba-1 signals are shown in green and red, respectively. Nuclei counterstained with Hoechst 33342 are shown in blue. The orientations of the images are indicated by arrows (L, lateral; M, medial; D, dorsal; V, ventral). Scale bars, 500 μm and 25 μm for the lower and higher magnifications, respectively. (**C**) The numbers of CFSE-positive cells in TLR-DKO mice that received transplantation of wild-type (WT) or TLR-DKO (DKO) microglia-like cells into the mPFC with or without prior R-SDS for 10 days ("10×" or "(-)", respectively). (**D**-**K**) The durations for presence in the interaction (**D**, **E**, **H** and **I**) or avoidance (**F**, **G**, **J** and **K**) zone without and with an ICR mouse and the differences between these durations without and with an ICR mouse (ΔTime [ICR(+)-ICR(-)]) in wild-type recipient mice (WT) that received a sham operation ("(-)") (**D**, **F**, **H** and **J**), and in TLR-DKO recipient mice which received a sham operation ("(-)"), or transplantation of wild-type (WT) or TLR-DKO (DKO) microglia-like cells into the mPFC (**E**, **G**, **I** and **K**) with or without prior R-SDS for 4 days ("4×" or "(-)", respectively; **D**-**G**) or for 10 days ("10×" or "(-)", respectively; **H**-**K**). n.s. (not significant), **P*<0.05, ***P*<0.01, ****P*<0.001 for

unpaired *t*-test for pairwise comparisons, or for Bonferroni's multiple comparison test for comparisons among more than two groups. The number of mice is shown below each group. Data are shown as means ± SEM.

Figure S6, related to Figure 6. TLR2/4 microRNA selectively suppresses mRNA expression of TLR2 and TLR4 *in vitro*

(**A**) RNA interference with TLR2 or TLR4 microRNA efficiently and specifically suppresses mRNA expression of the corresponding TLR isoform in Lenti-X 293T cells. Various mouse TLR isoforms (*Tlr1* to *Tlr13*) were overexpressed with *Tlr2* or *Tlr4* microRNA (miR) as well as control microRNA, and their expression levels were quantified by real-time RT-PCR. ***$P<0.001$ for Bonferroni's multiple comparison test. (**B**) Lentivirus-delivered TLR2/4 microRNA, in which *Tlr4* microRNA and *Tlr2* microRNA are tandemly connected, simultaneously suppressed endogenous mRNA expression of *Tlr2* and *Tlr4* in the N9 microglial cells. The values were normalized to those with control microRNA. **$P<0.01$, ***$P<0.001$ for unpaired *t*-test. (**C** and **D**) DNA sequences for microRNA-targeting regions of *Tlr2* (**C**) and *Tlr4* (**D**) and the corresponding regions of microRNA-resistant mutant cDNAs of these genes ("TLR2mt7" and "TLR4mt8", respectively) with no change in the amino acid sequences. Mutations in these mutants are highlighted in red. (**E** and **F**) Representative images of immunostaining for TLR2 (**E**), TLR4 (**F**) or the respective microRNA-resistant mutants ("TLR2mt7" and "TLR4mt8") with the corresponding microRNA or control microRNA in Lenti-X 293T cells. TLR2 and TLR2mt7 cDNAs were tagged with HA and detected by HA immunostaining. TLR4 and TLR4mt8 cDNAs were tagged with FLAG and detected by FLAG immunostaining. mCherry was simultaneously expressed with TLR2 or TLR4

microRNA to identify cells expressing these miRNAs. HA or FLAG signals and mCherry are shown in green and red, respectively, in the merged images. Nuclear counterstaining with Hoechst 33342 is shown in blue. Scale bars, 25 μm. (**G** and **H**) The fluorescent intensities of HA (**G**) and FLAG (**H**) tags in the experimental conditions shown in **E** and **F**, respectively. The values were normalized to those with control microRNA. ***P<0.001 for unpaired t-test. The number of analyzed wells is shown below each group. Data are shown as means ± SEM.

Figure S7, related to Figure 6. R-SDS increases the number of PSD-95-positive puncta in the mPFC in a manner dependent on TLR2/4 expressed in mPFC microglia

Representative SIM images (**A**) and quantitative analyses (**B** and **C**) of immunostaining for synaptophysin (green in **A**) and PSD-95 (red in **A**) in the deep layer of the mPFC of CX3CR1-CreER mice that received mPFC injections of lentiviral vectors expressing control microRNA ("Control") or TLR2/4 microRNA ("TLR2/4KD"). The images were taken from susceptible and resilient CX3CR1-CreER mice ("R-SDS(sus)" and "R-SDS(res)", respectively) expressing control microRNA, and those expressing TLR2/4 microRNA ("R-SDS") at 1.5 h after R-SDS, as well as those expressing control or TLR2/4 microRNA without R-SDS ("naïve"). Arrowheads in **A** indicate the juxtaposition of synaptophysin and PSD-95 punctate signals reminiscent of excitatory synapses. Scale bar, 5 μm. *P<0.05 for Bonferroni's multiple comparison test. The number of mice is shown below each group. Data are shown as means ± SEM.

Figure S8, related to all Figures. The role of TLR2/4 in mPFC microglia for R-SDS-

induced neuronal and behavioral changes

Our findings demonstrate that R-SDS induces activation of mPFC microglia through TLR2/4 for neuronal and behavioral changes, although the endogenous TLR2/4 ligand for this microglial activation remains to be identified. We also suggest that IL-1α and TNFα derived from the activated mPFC microglia mediate neuronal response attenuation and dendritic atrophy in the mPFC, thereby leading to social avoidance.

SUPPLEMENTAL TABLE

Table S1. A comprehensive table of statistical analyses, Related to the "Quantification and Statistical Analysis" subsection in the STAR Methods section.

Figure 1

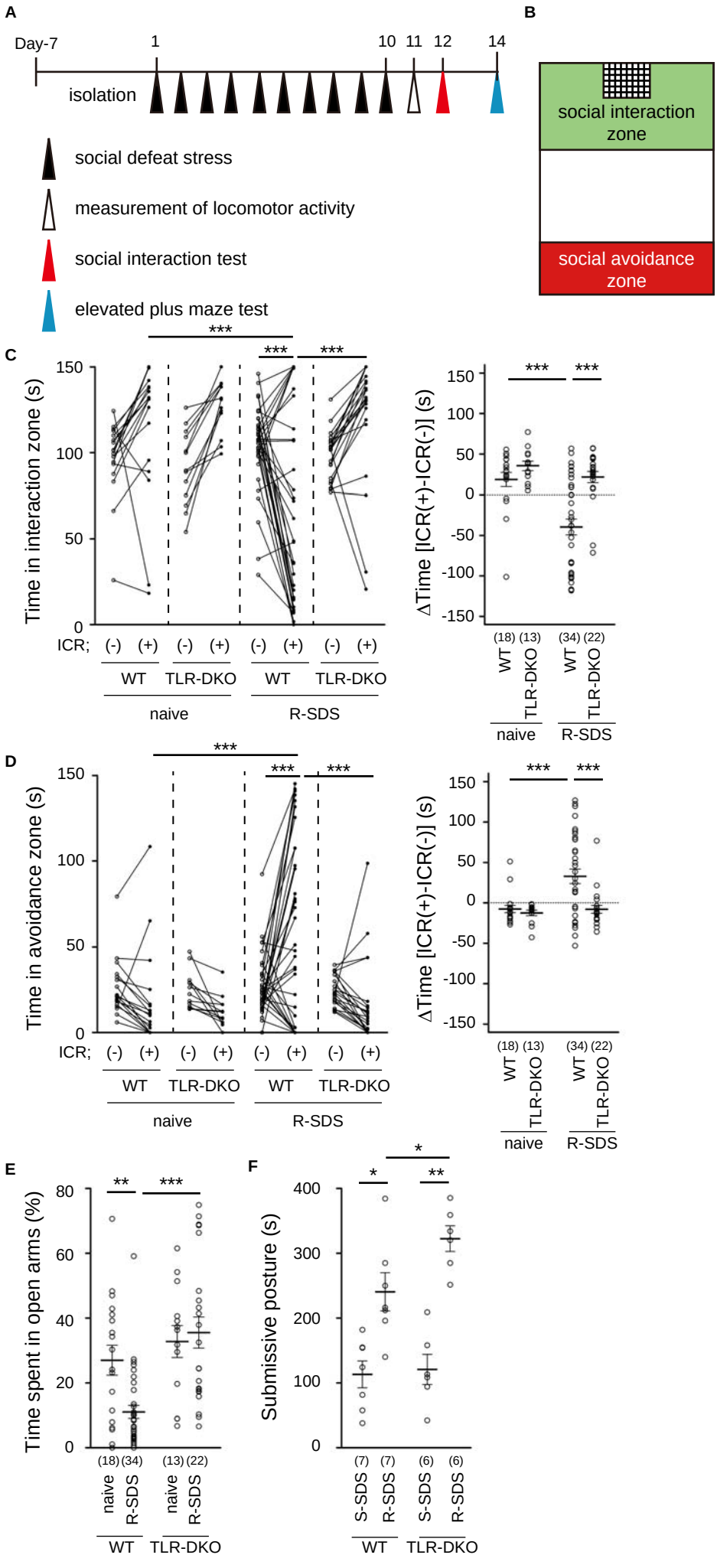
A
Day-7
1
10
11
12
14
isolation
social defeat stress
measurement of locomotor activity
social interaction test
elevated plus maze test
B
social interaction zone
social avoidance zone
C
Time in interaction zone (s)
ICR; (-) (+) (-) (+) (-) (+) (-) (+)
WT
TLR-DKO
WT
TLR-DKO
naive
R-SDS
ΔTime [ICR(+)-ICR(-)] (s)
(18) (13) (34) (22)
WT
TLR-DKO
WT
TLR-DKO
naive
R-SDS
D
Time in avoidance zone (s)
ICR; (-) (+) (-) (+) (-) (+) (-) (+)
WT
TLR-DKO
WT
TLR-DKO
naive
R-SDS
ΔTime [ICR(+)-ICR(-)] (s)
(18) (13) (34) (22)
WT
TLR-DKO
WT
TLR-DKO
naive
R-SDS
E
Time spent in open arms (%)
(18) (34) (13) (22)
naive
R-SDS
naive
R-SDS
WT
TLR-DKO
F
Submissive posture (s)
(7) (7) (6) (6)
S-SDS
R-SDS
S-SDS
R-SDS
WT
TLR-DKO

Figure 2

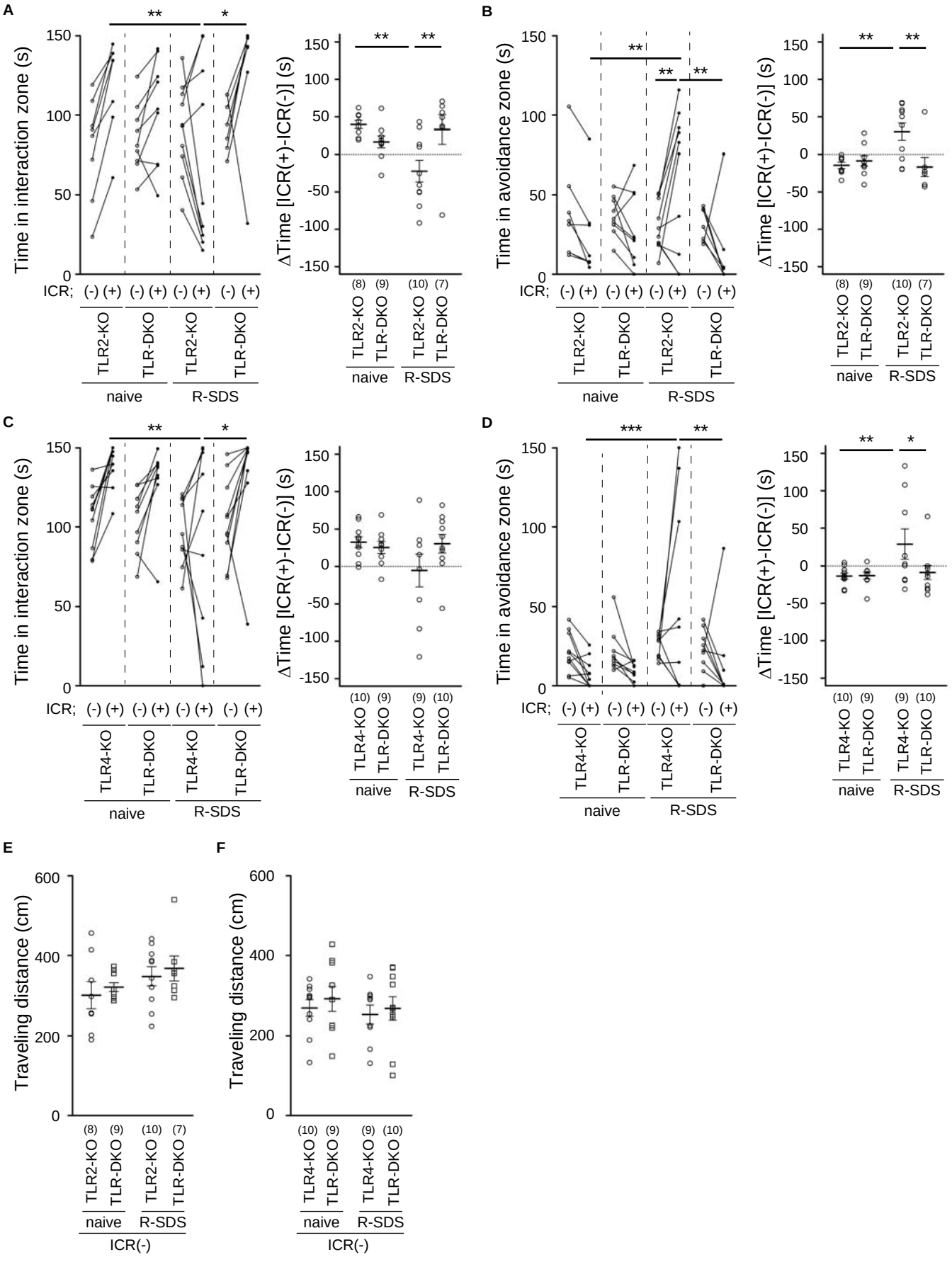
A
B
C
D
E
F
Time in interaction zone (s)
Time in avoidance zone (s)
ΔTime [ICR(+)-ICR(-)] (s)
Traveling distance (cm)
ICR; (-) (+) (-) (+) (-) (+) (-) (+)
TLR2-KO
TLR-DKO
TLR4-KO
naive
R-SDS
ICR(-)
(8) (9) (10) (7)
(10) (9) (9) (10)
**
*
***

Figure 3

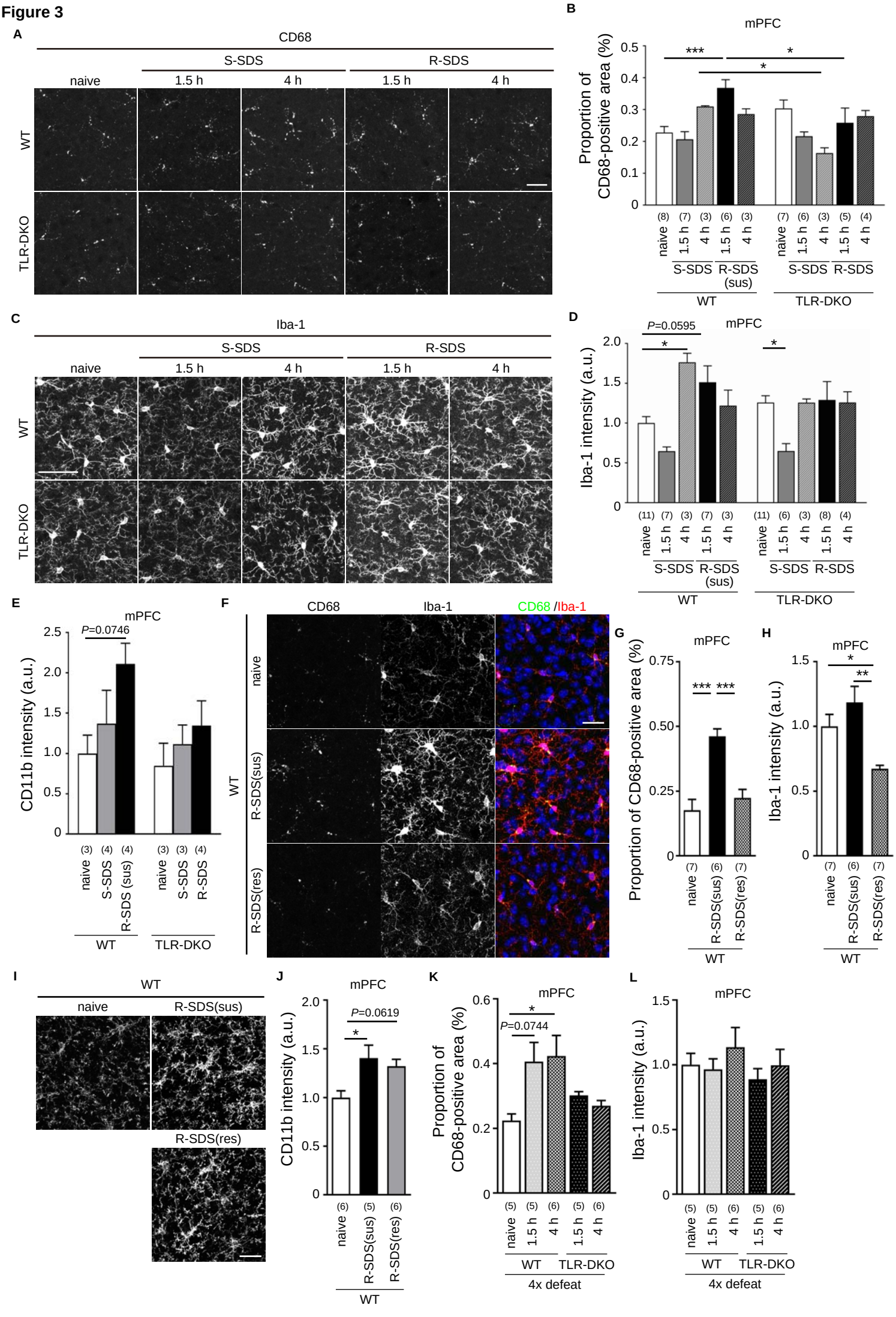
A
CD68
S-SDS
R-SDS
naive
1.5 h
4 h
1.5 h
4 h
WT
TLR-DKO
B
mPFC
Proportion of CD68-positive area (%)
0.5
0.4
0.3
0.2
0.1
0
***
*
*
(8) (7) (3) (6) (3) (7) (6) (3) (5) (4)
naive
1.5 h
4 h
1.5 h
4 h
naive
1.5 h
4 h
1.5 h
4 h
S-SDS
R-SDS (sus)
S-SDS
R-SDS
WT
TLR-DKO
C
Iba-1
S-SDS
R-SDS
naive
1.5 h
4 h
1.5 h
4 h
WT
TLR-DKO
D
P=0.0595
mPFC
Iba-1 intensity (a.u.)
2.0
1.5
1.0
0.5
0
*
*
(11) (7) (3) (7) (3) (11) (6) (3) (8) (4)
naive
1.5 h
4 h
1.5 h
4 h
naive
1.5 h
4 h
1.5 h
4 h
S-SDS
R-SDS (sus)
S-SDS
R-SDS
WT
TLR-DKO
E
mPFC
P=0.0746
CD11b intensity (a.u.)
2.5
2.0
1.5
1.0
0.5
0
(3) (4) (4) (3) (3) (4)
naive
S-SDS
R-SDS (sus)
naive
S-SDS
R-SDS
WT
TLR-DKO
F
CD68
Iba-1
CD68 /Iba-1
WT
naive
R-SDS(sus)
R-SDS(res)
G
mPFC
Proportion of CD68-positive area (%)
0.75
0.50
0.25
0
*** ***
(7) (6) (7)
naive
R-SDS(sus)
R-SDS(res)
WT
H
mPFC
Iba-1 intensity (a.u.)
1.5
1.0
0.5
0
*
**
(7) (6) (7)
naive
R-SDS(sus)
R-SDS(res)
WT
I
WT
naive
R-SDS(sus)
R-SDS(res)
J
mPFC
P=0.0619
*
CD11b intensity (a.u.)
2.0
1.5
1.0
0.5
0
(6) (5) (6)
naive
R-SDS(sus)
R-SDS(res)
WT
K
mPFC
*
P=0.0744
Proportion of CD68-positive area (%)
0.6
0.4
0.2
0
(5) (5) (6) (5) (6)
naive
1.5 h
4 h
1.5 h
4 h
WT
TLR-DKO
4x defeat
L
mPFC
Iba-1 intensity (a.u.)
1.5
1.0
0.5
0
(5) (5) (6) (5) (6)
naive
1.5 h
4 h
1.5 h
4 h
WT
TLR-DKO
4x defeat

Figure 4

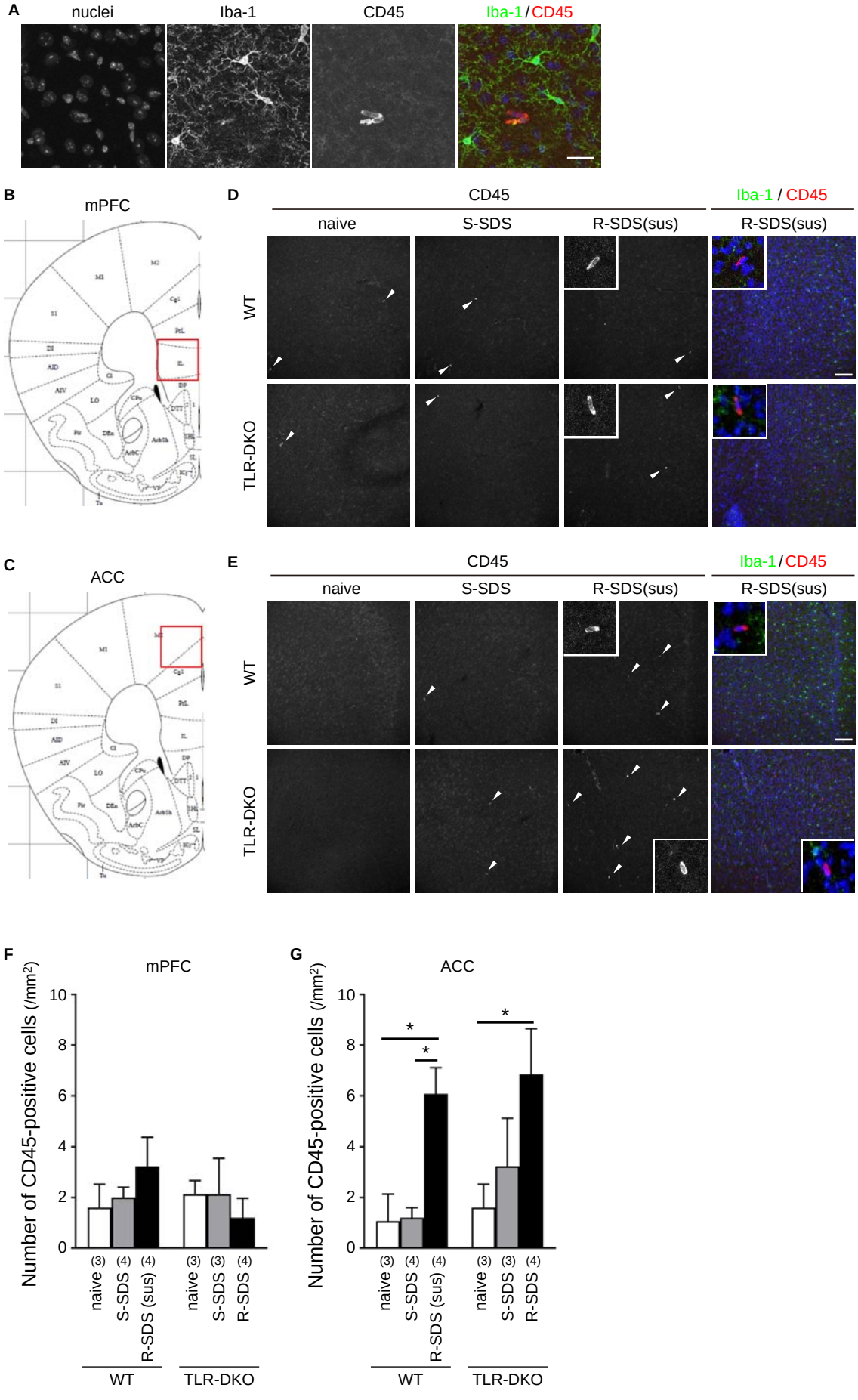
A
nuclei
Iba-1
CD45
Iba-1 / CD45
B
mPFC
C
ACC
D
CD45
Iba-1 / CD45
naive
S-SDS
R-SDS(sus)
R-SDS(sus)
WT
TLR-DKO
E
CD45
Iba-1 / CD45
naive
S-SDS
R-SDS(sus)
R-SDS(sus)
WT
TLR-DKO
F
mPFC
Number of CD45-positive cells (/mm²)
10
8
6
4
2
0
(3) (4) (4)
naive
S-SDS
R-SDS (sus)
(3) (3) (4)
naive
S-SDS
R-SDS
WT
TLR-DKO
G
ACC
Number of CD45-positive cells (/mm²)
10
8
6
4
2
0
*
*
*
(3) (4) (4)
naive
S-SDS
R-SDS (sus)
(3) (3) (4)
naive
S-SDS
R-SDS
WT
TLR-DKO

Figure 5

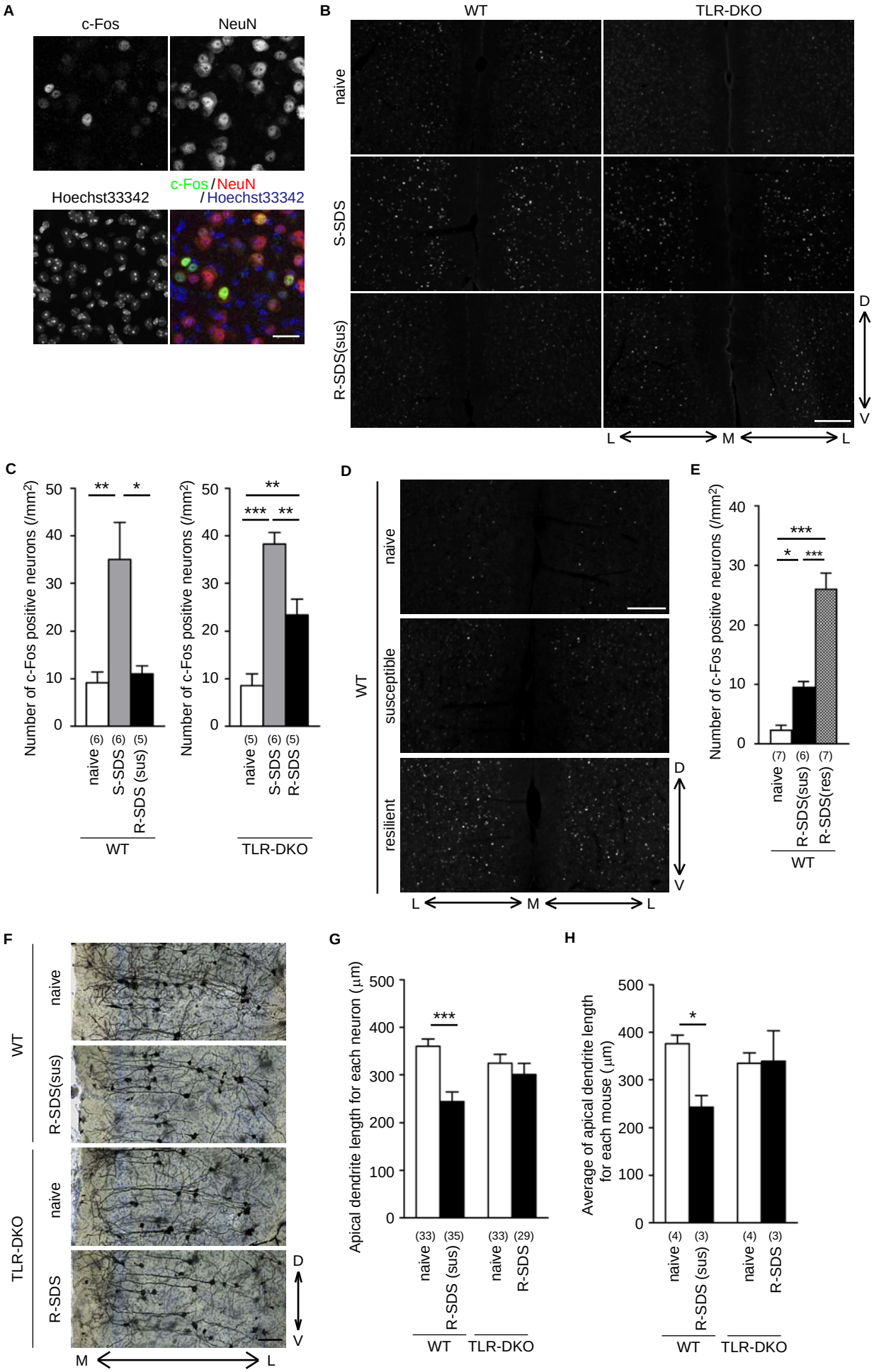
A
c-Fos
NeuN
Hoechst33342
c-Fos / NeuN / Hoechst33342
B
WT
TLR-DKO
naive
S-SDS
R-SDS(sus)
D
V
L
M
L
C
Number of c-Fos positive neurons (/mm²)
naive
S-SDS
R-SDS (sus)
R-SDS
WT
TLR-DKO
D
WT
susceptible
resilient
E
naive
R-SDS(sus)
R-SDS(res)
F
WT
TLR-DKO
naive
R-SDS(sus)
R-SDS
G
Apical dendrite length for each neuron (μm)
H
Average of apical dendrite length for each mouse (μm)

Figure 6

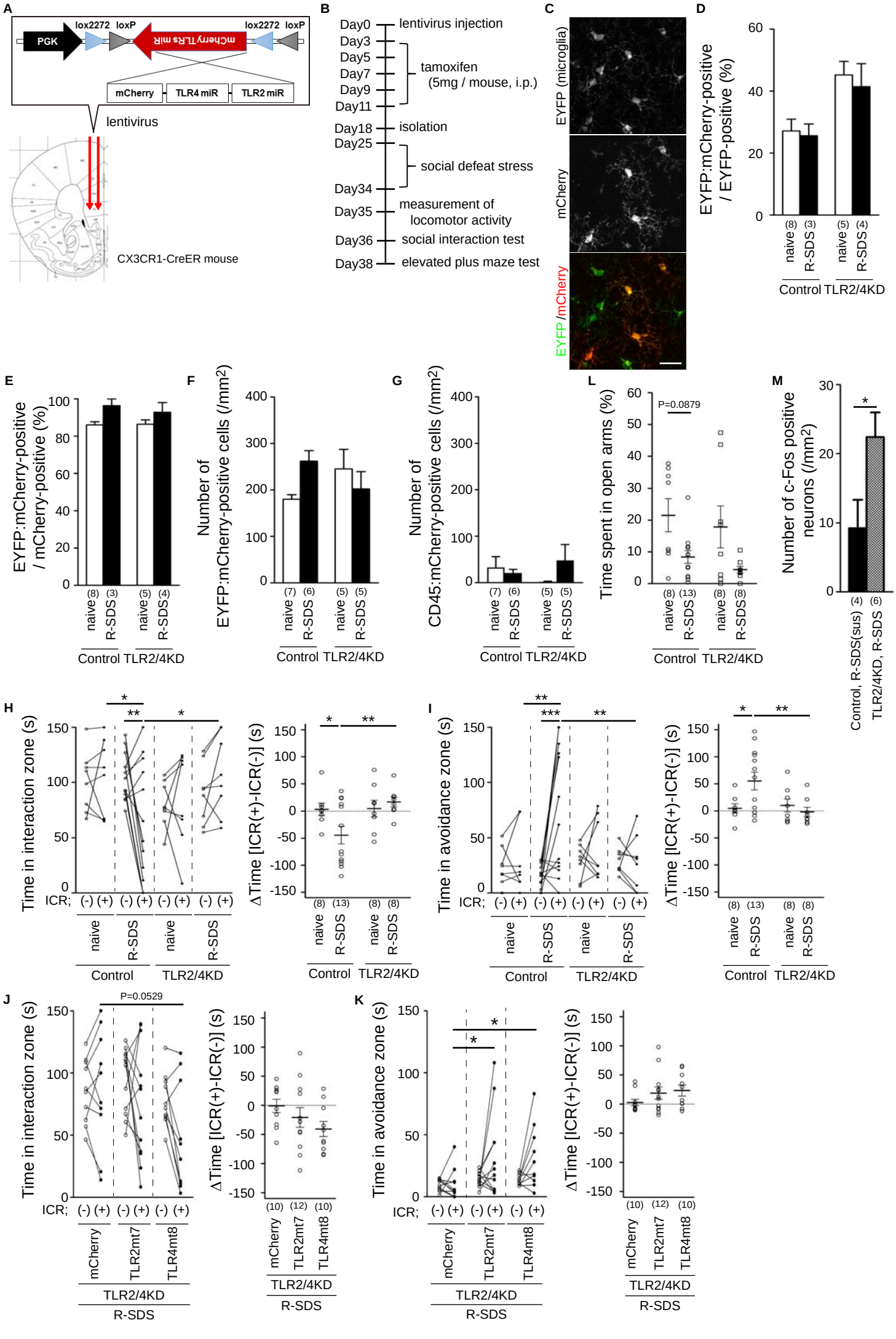
A
lox2272 loxP
PGK
mCherry-TLRs miR
lox2272 loxP
mCherry
TLR4 miR
TLR2 miR
lentivirus
CX3CR1-CreER mouse
B
Day0 lentivirus injection
Day3
Day5
Day7
Day9 tamoxifen (5mg / mouse, i.p.)
Day11
Day18 isolation
Day25
social defeat stress
Day34
Day35 measurement of locomotor activity
Day36 social interaction test
Day38 elevated plus maze test
C
EYFP (microglia)
mCherry
EYFP /mCherry
D
EYFP:mCherry-positive / EYFP-positive (%)
naive R-SDS naive R-SDS
Control TLR2/4KD
E
EYFP:mCherry-positive / mCherry-positive (%)
F
Number of EYFP:mCherry-positive cells (/mm2)
G
Number of CD45:mCherry-positive cells (/mm2)
L
Time spent in open arms (%)
P=0.0879
M
Number of c-Fos positive neurons (/mm2)
Control, R-SDS(sus) TLR2/4KD, R-SDS
H
Time in interaction zone (s)
ICR; (-) (+) (-) (+) (-) (+) (-) (+)
naive R-SDS naive R-SDS
Control TLR2/4KD
ΔTime [ICR(+)-ICR(-)] (s)
I
Time in avoidance zone (s)
J
P=0.0529
mCherry TLR2mt7 TLR4mt8
TLR2/4KD
R-SDS
K

Figure 7

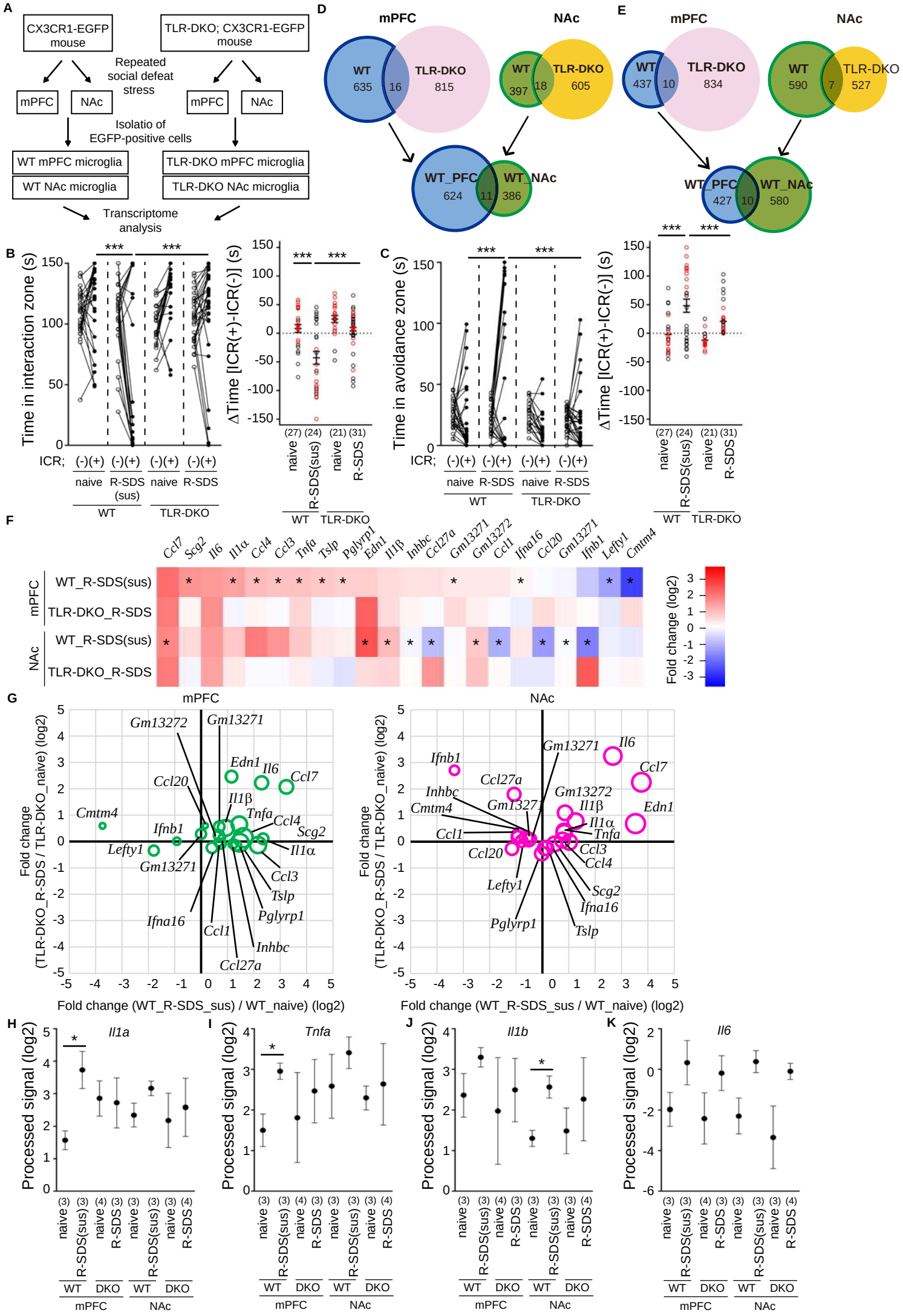
A
CX3CR1-EGFP mouse
TLR-DKO; CX3CR1-EGFP mouse
Repeated social defeat stress
mPFC
NAc
mPFC
NAc
Isolatio of EGFP-positive cells
WT mPFC microglia
WT NAc microglia
TLR-DKO mPFC microglia
TLR-DKO NAc microglia
Transcriptome analysis
D
mPFC
NAc
WT 635 16 TLR-DKO 815
WT 397 18 TLR-DKO 605
WT_PFC 624 11 WT_NAc 386
E
mPFC
NAc
WT 437 10 TLR-DKO 834
WT 590 7 TLR-DKO 527
WT_PFC 427 10 WT_NAc 580
B
Time in interaction zone (s)
ΔTime [ICR(+)-ICR(-)] (s)
ICR; (-)(+) (-)(+) (-)(+) (-)(+)
naive R-SDS (sus) naive R-SDS
WT TLR-DKO
(27) (24) (21) (31)
naive R-SDS(sus) naive R-SDS
C
Time in avoidance zone (s)
ΔTime [ICR(+)-ICR(-)] (s)
F
Ccl7 Scg2 Il6 Il1α Ccl4 Ccl3 Tnfa Tslp Pglyrp1 Edn1 Il1β Inhbc Ccl27a Gm13271 Gm13272 Ccl1 Ifna16 Ccl20 Gm13271 Ifnb1 Lefty1 Cmtm4
mPFC
WT_R-SDS(sus)
TLR-DKO_R-SDS
NAc
WT_R-SDS(sus)
TLR-DKO_R-SDS
Fold change (log2)
G
mPFC
NAc
Fold change (TLR-DKO_R-SDS / TLR-DKO_naive) (log2)
Fold change (WT_R-SDS_sus) / WT_naive) (log2)
Fold change (WT_R-SDS_sus / WT_naive) (log2)
H
Il1a
I
Tnfa
J
Il1b
K
Il6
Processed signal (log2)
naive R-SDS(sus) naive R-SDS naive R-SDS(sus) naive R-SDS
WT DKO WT DKO
mPFC NAc

Figure 8

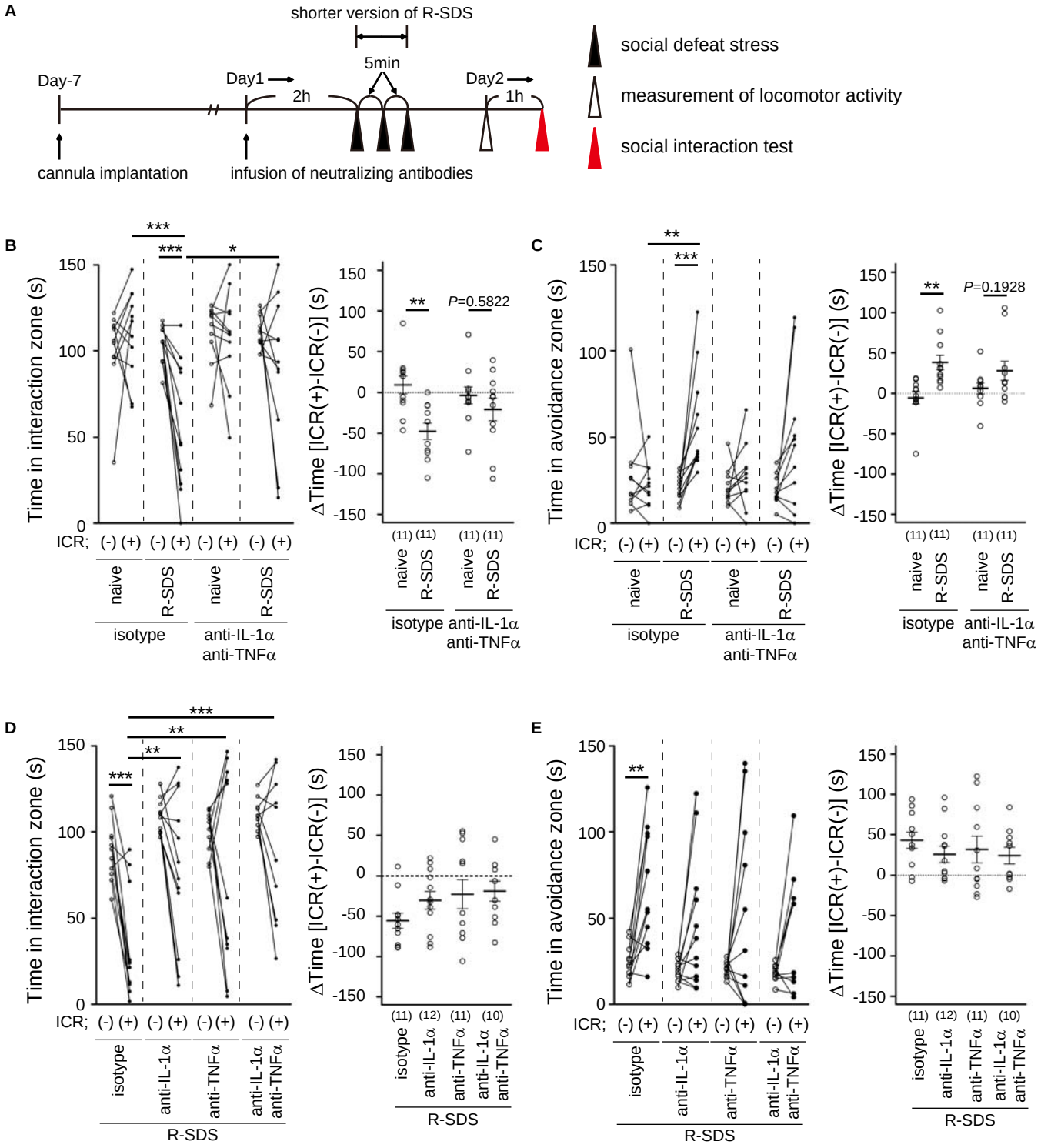
A
shorter version of R-SDS
5min
Day-7
Day1
2h
Day2
1h
cannula implantation
infusion of neutralizing antibodies
social defeat stress
measurement of locomotor activity
social interaction test
B
Time in interaction zone (s)
ICR; (-) (+) (-) (+) (-) (+) (-) (+)
naive
R-SDS
isotype
anti-IL-1α
anti-TNFα
ΔTime [ICR(+)-ICR(-)] (s)
P=0.5822
C
Time in avoidance zone (s)
P=0.1928
D
isotype
anti-IL-1α
anti-TNFα
R-SDS
E

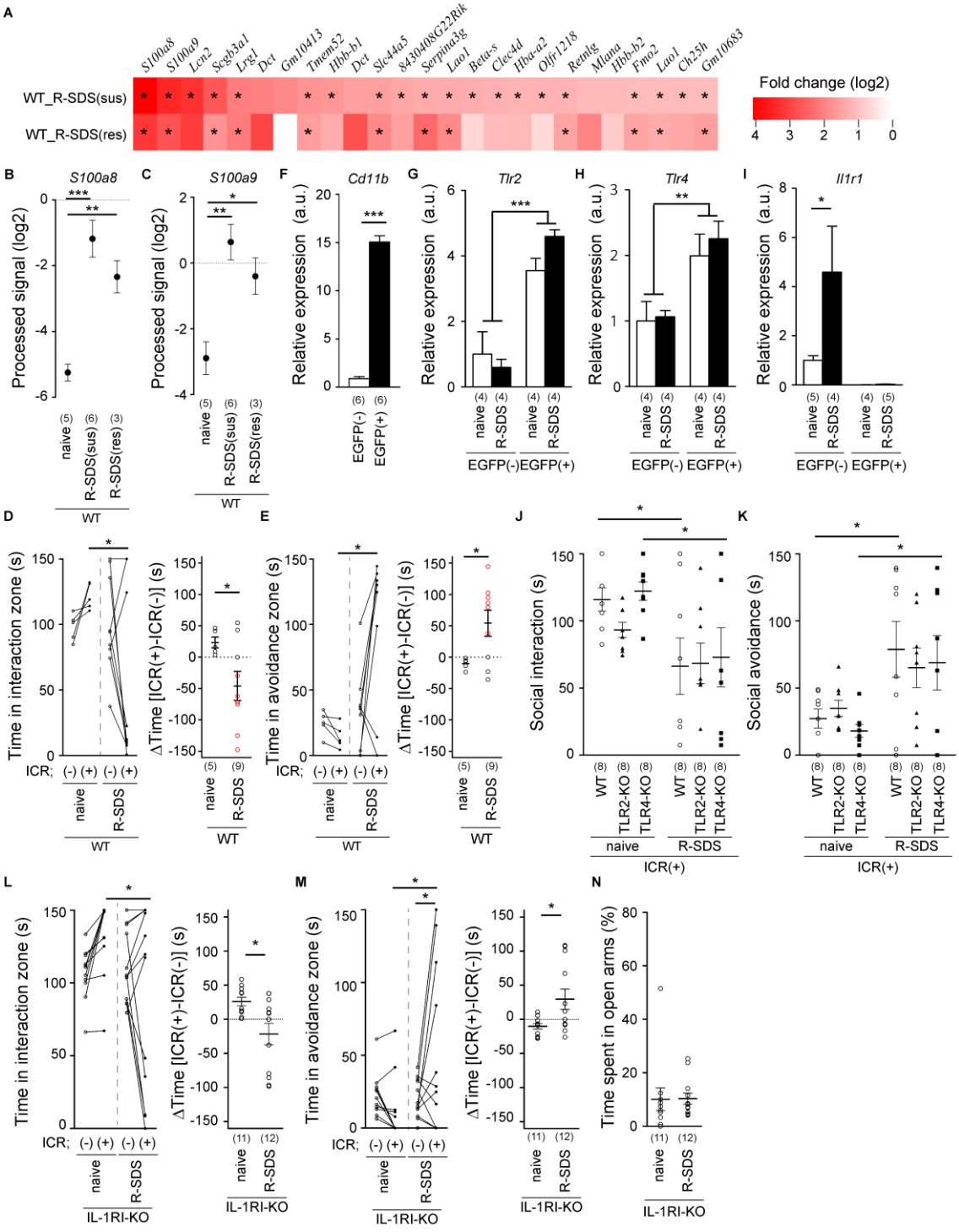

Figure S1, related to Figures 1 and 2.

Behavioral and gene expression analyses of TLR2, TLR4, and IL-1RI

(A) A heat map showing R-SDS-induced changes in gene expression of the top 25 most upregulated genes in the mPFC from susceptible and resilient wild-type mice ("WT_R-SDS(sus)" and "WT_R-SDS(res)",

respectively). *P<0.05 for unpaired *t*-test for the changes in gene expression for the indicated probes. (**B** and **C**) The expression levels of S100A8 (**B**) and S100A9 (**C**) in the mPFC of susceptible and resilient wild-type mice ("R-SDS(sus)" and "R-SDS(res)", respectively) at 4 h after R-SDS as well as wild-type mice without SDS ("naïve"). *P<0.05, **P<0.01, ***P<0.001 for Bonferroni's multiple comparison test. (**D** and **E**) The durations for presence in the interaction (**D**) or avoidance (**E**) zone without and with an ICR mouse and the differences between these durations without and with an ICR mouse (ΔTime [ICR(+)-ICR(-)]), for wild-type mice ("WT") with or without prior R-SDS ("R-SDS" and "naïve"). Red dots in right panels indicate the data from susceptible mice. *P<0.05 for Bonferroni's multiple comparison test (left panels) or unpaired *t*-test (right panels). (**F**-**I**) mRNA levels of CD11b (**F**), TLR2 (**G**), TLR4 (**H**) and IL-1RI (**I**) in EGFP-positive cells ("EGFP(+)") and EGFP-negative cells ("EGFP(-)") isolated from CX3CR1-EGFP mice, in which EGFP is selectively expressed in microglia and monocytes (a minor population) in the brain, with or without prior R-SDS ("R-SDS" or "naïve", respectively). The levels were normalized to that of β-actin to minimize sample variance. The levels were further normalized to those of the control groups, namely EGFP(-) in Figure S1F and naïve EGFP(-) in Figure S1G-I, and are shown. ***P<0.001 for unpaired *t*-test (**F**) and *P<0.05 for Bonferroni's multiple comparison test (**I**). (**J** and **K**) The durations for presence in the interaction (**J**) or avoidance (**K**) zone with an ICR mouse for wild-type mice (WT), TLR2-KO mice, and TLR4-KO mice before and after R-SDS ("naïve" and "R-SDS", respectively). The same individuals were analyzed and statistically compared before and after R-SDS. *P<0.05 for Bonferroni's multiple comparison test. (**L** and **M**) The durations within the interaction (**L**) or avoidance (**M**) zone without and with an ICR mouse and the differences between these durations without and with an ICR mouse (ΔTime [ICR(+)-ICR(-)]) in IL-1RI-KO mice with or without prior R-SDS ("R-SDS" or "naïve", respectively). *P<0.05 for Bonferroni's multiple comparison test (left panels) or unpaired *t*-test (right panels). (**N**) The level of anxiety of IL-1RI-KO mice with or without prior R-SDS ("R-SDS" or "naïve", respectively). The proportion of the time spent in the open arms in the elevated plus maze was measured as an index of anxiety. The number of mice is shown below each group. Data are shown as means ± SEM.

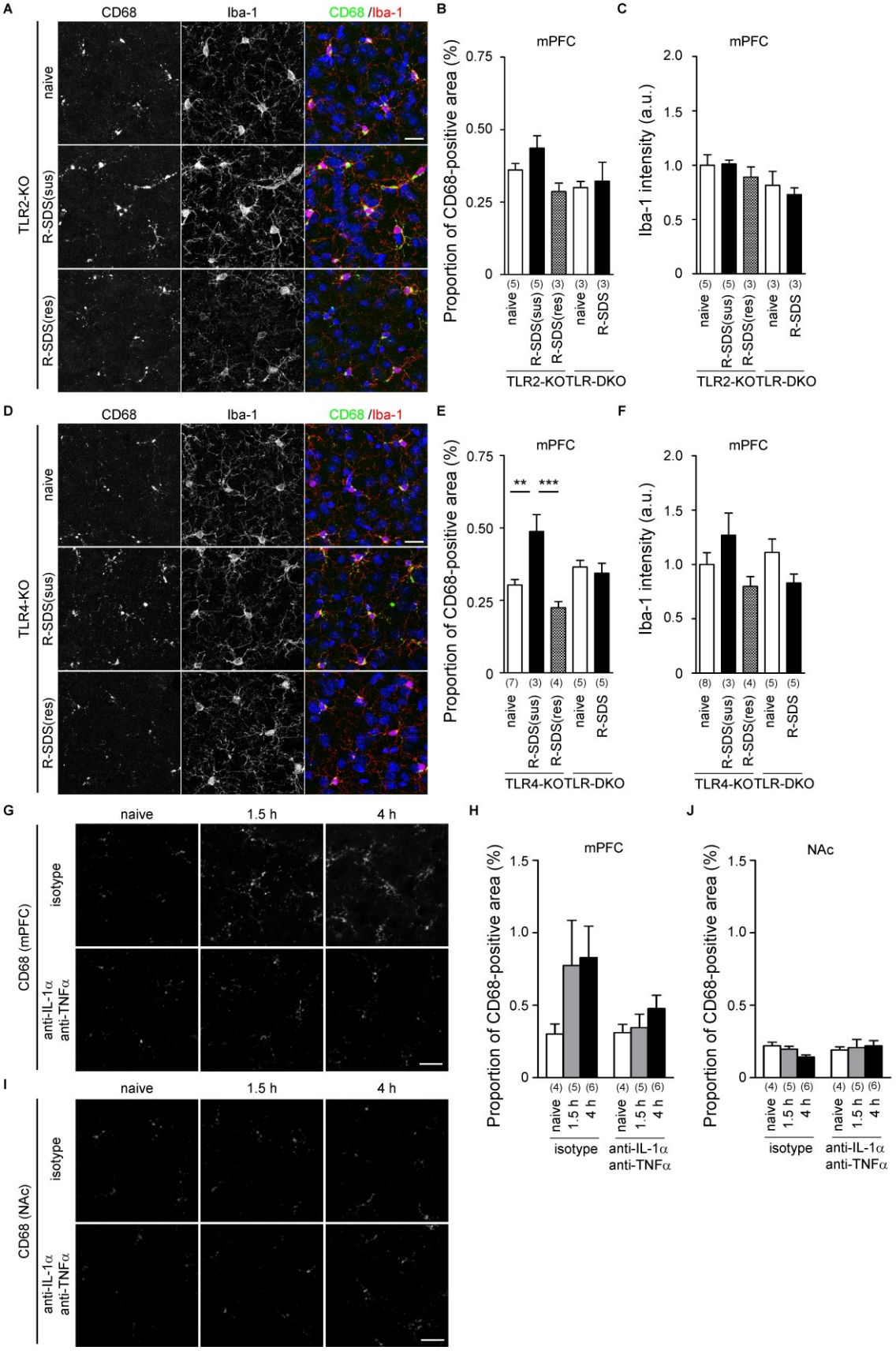
A
CD68
Iba-1
CD68 /Iba-1
TLR2-KO
naive
R-SDS(sus)
R-SDS(res)
B
mPFC
Proportion of CD68-positive area (%)
0.75
0.50
0.25
0
(5) (5) (3) (3) (3)
naive
R-SDS(sus)
R-SDS(res)
naive
R-SDS
TLR2-KO
TLR-DKO
C
mPFC
Iba-1 intensity (a.u.)
2.0
1.5
1.0
0.5
0
(5) (5) (3) (3) (3)
naive
R-SDS(sus)
R-SDS(res)
naive
R-SDS
TLR2-KO
TLR-DKO
D
CD68
Iba-1
CD68 /Iba-1
TLR4-KO
naive
R-SDS(sus)
R-SDS(res)
E
mPFC
Proportion of CD68-positive area (%)
**
***
0.75
0.50
0.25
0
(7) (3) (4) (5) (5)
naive
R-SDS(sus)
R-SDS(res)
naive
R-SDS
TLR4-KO
TLR-DKO
F
mPFC
Iba-1 intensity (a.u.)
2.0
1.5
1.0
0.5
0
(8) (3) (4) (5) (5)
naive
R-SDS(sus)
R-SDS(res)
naive
R-SDS
TLR4-KO
TLR-DKO
G
naive
1.5 h
4 h
CD68 (mPFC)
isotype
anti-IL-1α
anti-TNFα
H
mPFC
Proportion of CD68-positive area (%)
1.5
1.0
0.5
0
(4) (5) (6) (4) (5) (6)
naive
1.5 h
4 h
naive
1.5 h
4 h
isotype
anti-IL-1α
anti-TNFα
I
naive
1.5 h
4 h
CD68 (NAc)
isotype
anti-IL-1α
anti-TNFα
J
NAc
Proportion of CD68-positive area (%)
1.5
1.0
0.5
0
(4) (5) (6) (4) (5) (6)
naive
1.5 h
4 h
naive
1.5 h
4 h
isotype
anti-IL-1α
anti-TNFα

Figure S2, related to Figures 3 and 8.

TLR2 and TLR4 deficiency attenuates R-SDS-induced activation of mPFC microglia

(**A**-**F**) Representative images (**A** and **D**) and quantitative analyses (**B**, **C**, **E** and **F**) of immunostaining for CD68 and Iba-1 in the mPFC of TLR2-KO mice (**A**-**C**) and TLR4-KO mice (**D**-**F**) without SDS ("naïve"), susceptible and resilient mice ("R-SDS(sus)" and R-SDS(res)", respectively) with the respective genotypes, and TLR-DKO littermates (**B**, **C**, **E** and **F**) with or without R-SDS ("R-SDS" and "naïve", respectively) at 1.5 h after the last session of R-SDS. The images from TLR-DKO littermates are not shown in this figure, since these images are similar to those from TLR-DKO mice shown in Figure 3A and 3C. In the merged images, CD68 and Iba-1 signals are shown in green and red, respectively. CD68 signals in Iba-1 positive microglia are seen in yellow. Nuclei were counterstained with Hoechst 33342 and are shown in blue. The values of Iba-1 intensity were normalized to that of naïve TLR2-KO or TLR4-KO mice for Figure S2C or S2F, respectively. (**G**-**J**) Representative images (**G** and **I**) and quantitative analyses (**H** and **J**) of immunostaining of CD68 in the mPFC (**G** and **H**) and NAc (**I** and **J**) of wild-type mice which received mPFC infusions with a mixture of neutralizing antibodies for IL-1α and TNFα ("anti-IL-1α anti-TNFα") or control antibodies of the corresponding isotypes ("isotype") without SDS ("naïve"), and at 1.5 h and 4 h after the last session of a shorter version of R-SDS (see Figure 8A). Scale bars, 20 μm. $^{**}P<0.01$, $^{***}P<0.001$ for Bonferroni's multiple comparison test. The number of mice is shown below each group. Data are shown as means ± SEM.

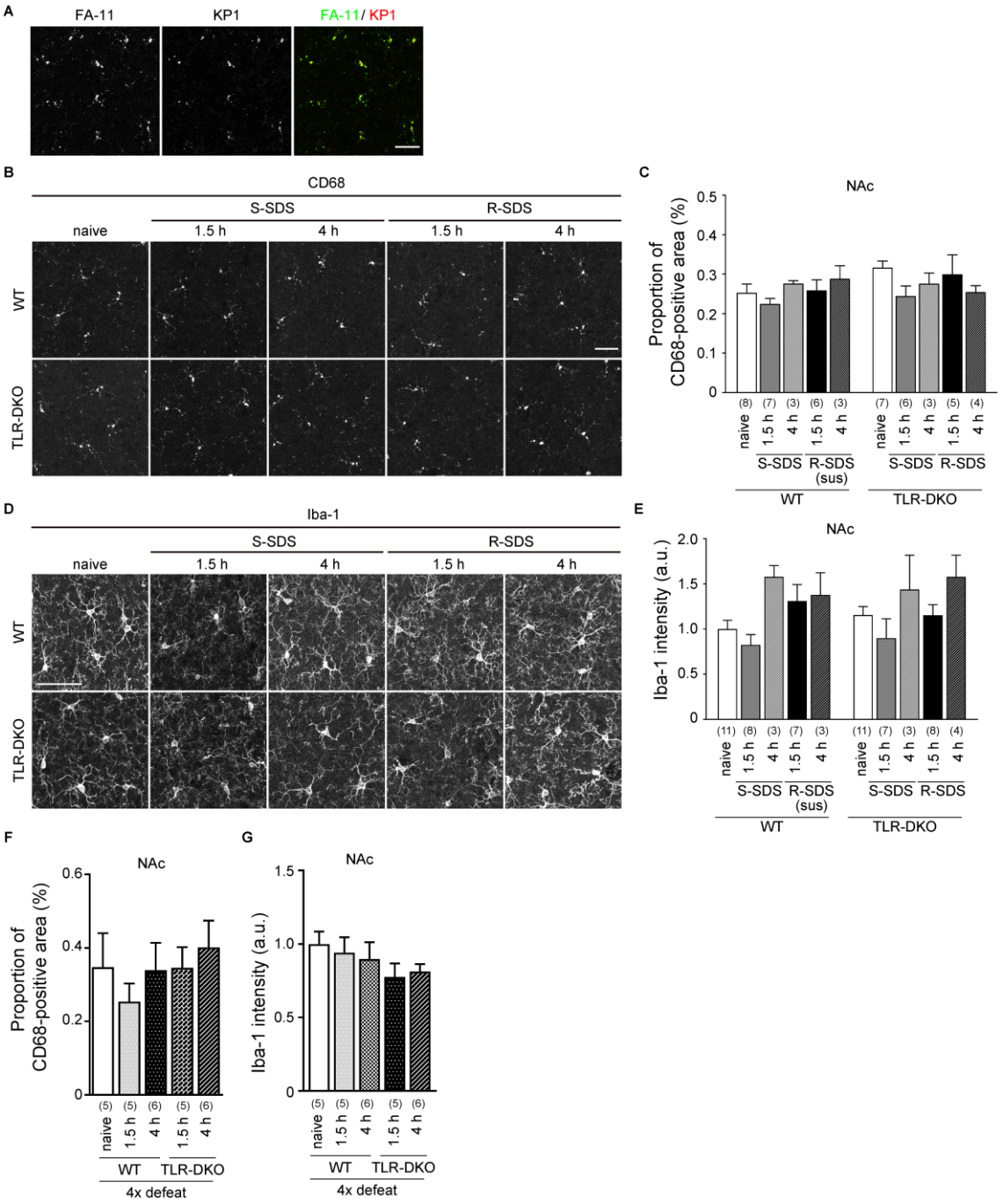

Figure S3, related to Figure 3.

R-SDS does not induce activation of NAc microglia in wild-type mice or TLR-DKO mice

(**A**) Colocalization of CD68 signals with FA-11, a monoclonal anti-CD68 antibody which was mainly used in this study, and those with KP1, another monoclonal anti-CD68 antibody. This colocalization with the two independent antibodies confirmed the specificity of CD68 signals. Scale bar, 50 μm. (**B**-**E**) Representative images (**B** and **D**) and quantitative analyses (**C** and **E**) of CD68 (**B** and **C**) and Iba-1 (**D** and

E) immunostaining in the NAc of wild-type mice (WT) and TLR-DKO mice without SDS ("naïve"), and at 1.5 h and 4 h after S-SDS and the last session of R-SDS. For wild-type mice after R-SDS, the images were taken and analyzed only from susceptible mice ("R-SDS(sus)"). Scale bars, 50 μm. (**F** and **G**) Quantitative analyses of CD68 (**F**) and Iba-1 (**G**) immunostaining in the NAc of wild-type mice (WT) and TLR-DKO mice without SDS ("naïve") and at 1.5 h and 4 h after the last session of R-SDS for 4 days ("4× defeat"). The values of Iba-1 intensity were normalized to that of naïve wild-type mice. The number of mice is shown below each group. Data are shown as means ± SEM.

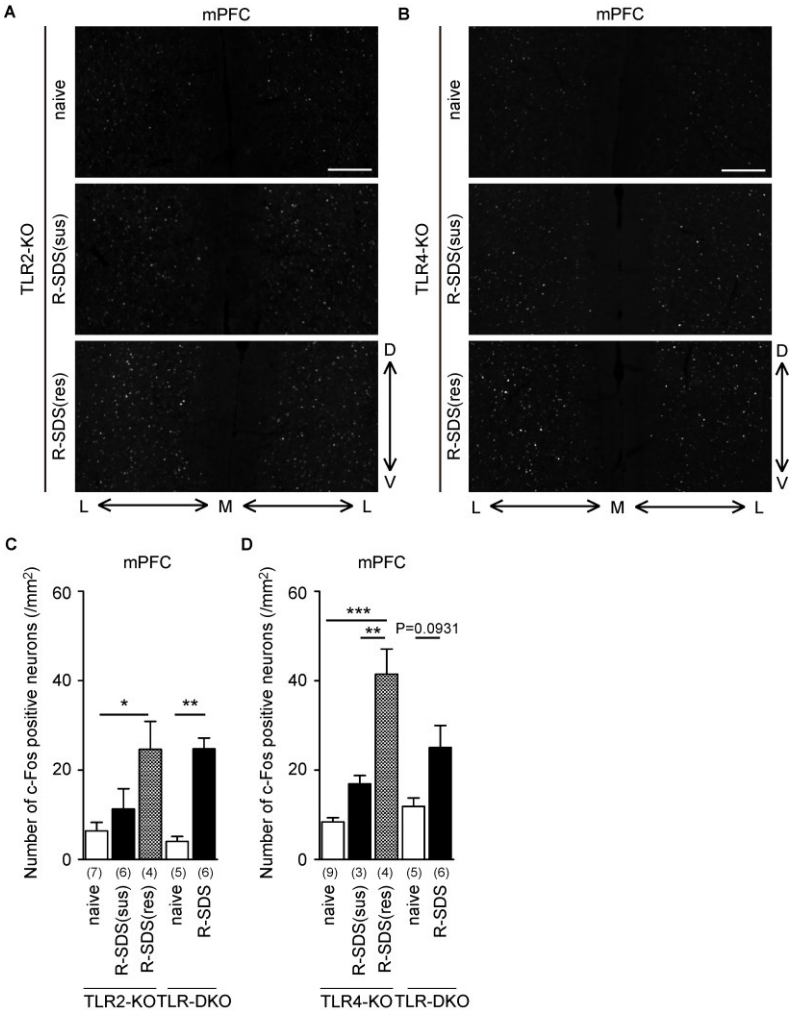

Figure S4, related to Figure 5.

SDS-induced c-Fos expression in mPFC neurons of TLR2-KO mice and TLR4-KO mice as well as TLR-DKO littermates

Representative images (**A** and **B**) and quantitative analyses (**C** and **D**) of c-Fos immunostaining in mPFC of TLR2-KO mice (**A** and **C**) and TLR4-KO mice (**B** and **D**) without SDS ("naïve"), susceptible and resilient mice ("R-SDS(sus)" and "R-SDS(res)", respectively) of the respective genotypes, and TLR-DKO mice (**C** and **D**) with or without R-SDS ("R-SDS" and "naïve", respectively) at 1.5 h after the last session of R-SDS. The images from TLR-DKO littermates are not shown in this figure, since these images are similar to those from TLR-DKO mice shown in Figure 5B. The orientations of the images are indicated by arrows (L, lateral; M, medial; D, dorsal; V, ventral). Scale bars, 100 μm. **P*<0.05, ***P*<0.01, ****P*<0.001 for Bonferroni's multiple comparison test. The number of mice is shown below each group. Data are shown as means ± SEM.

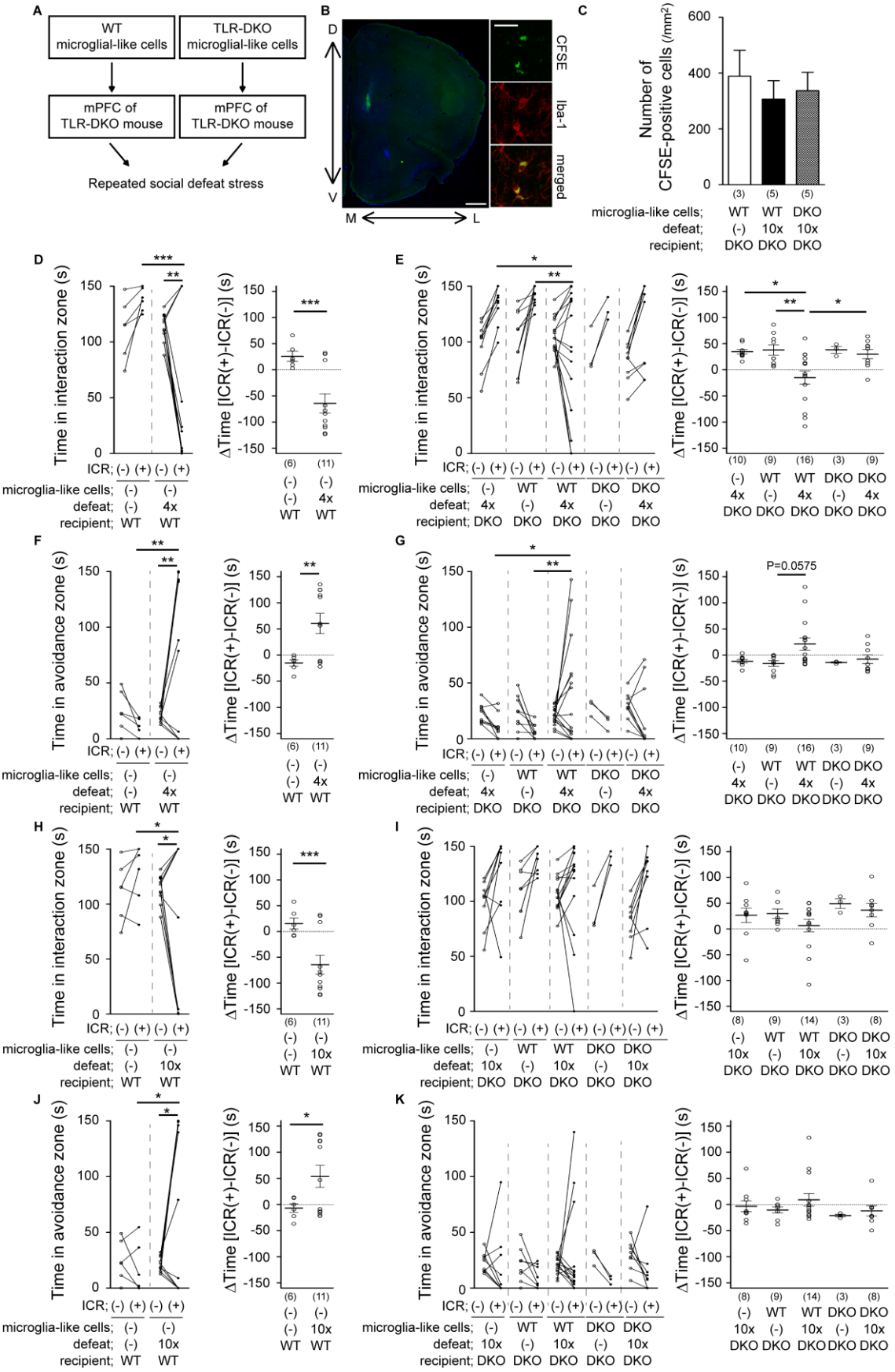
A
WT microglial-like cells
TLR-DKO microglial-like cells
mPFC of TLR-DKO mouse
mPFC of TLR-DKO mouse
Repeated social defeat stress
B
D
V
M
L
CFSE
Iba-1
merged
C
Number of CFSE-positive cells (/mm2)
microglia-like cells; WT WT DKO
defeat; (-) 10x 10x
recipient; DKO DKO DKO
D
Time in interaction zone (s)
ΔTime [ICR(+)-ICR(-)] (s)
microglia-like cells; (-) (-)
defeat; (-) 4x
recipient; WT WT
E
microglia-like cells; (-) WT WT DKO DKO
defeat; 4x (-) 4x (-) 4x
recipient; DKO DKO DKO DKO DKO
F
Time in avoidance zone (s)
G
P=0.0575
H
Time in interaction zone (s)
microglia-like cells; (-) (-)
defeat; (-) 10x
recipient; WT WT
I
microglia-like cells; (-) WT WT DKO DKO
defeat; 10x (-) 10x (-) 10x
recipient; DKO DKO DKO DKO DKO
J
Time in avoidance zone (s)
K

Figure S5, related to Figure 6.

Transplantation of wild-type microglia-like cells into the mPFC of TLR-DKO mice transiently restores social avoidance induced by R-SDS

(**A**) Design of behavioral experiments with transplantation of microglia-like cells. Primary microglia-like cells were obtained from wild-type (WT) and TLR-DKO neonates, and were transplanted to the mPFC of TLR-DKO mice. After a four-week recovery, the mice were subjected to R-SDS. (**B**) Representative images of transplanted microglia-like cells in the mPFC. Wild-type microglia-like cells were labeled with CFSE and locally infused into the mPFC of TLR-DKO mice. Fluorescence images were taken after the four-week recovery. Microglia were visualized by Iba-1 staining. CFSE and Iba-1 signals are shown in green and red, respectively. Nuclei counterstained with Hoechst 33342 are shown in blue. The orientations of the images are indicated by arrows (L, lateral; M, medial; D, dorsal; V, ventral). Scale bars, 500 μm and 25 μm for the lower and higher magnifications, respectively. (**C**) The numbers of CFSE-positive cells in TLR-DKO mice that received transplantation of wild-type (WT) or TLR-DKO (DKO) microglia-like cells into the mPFC with or without prior R-SDS for 10 days ("10×" or "(-)", respectively). (**D**-**K**) The durations for presence in the interaction (**D**, **E**, **H** and **I**) or avoidance (**F**, **G**, **J** and **K**) zone without and with an ICR mouse and the differences between these durations without and with an ICR mouse (ΔTime [ICR(+)-ICR(-)]) in wild-type recipient mice (WT) that received a sham operation ("(-)") (**D**, **F**, **H** and **J**), and in TLR-DKO recipient mice which received a sham operation ("(-)"), or transplantation of wild-type (WT) or TLR-DKO (DKO) microglia-like cells into the mPFC (**E**, **G**, **I** and **K**) with or without prior R-SDS for 4 days ("4×" or "(-)", respectively; **D**-**G**) or for 10 days ("10×" or "(-)", respectively; **H**-**K**). n.s. (not significant), **P*<0.05, ***P*<0.01, ****P*<0.001 for unpaired *t*-test for pairwise comparisons, or for Bonferroni's multiple comparison test for comparisons among more than two groups. The number of mice is shown below each group. Data are shown as means ± SEM.

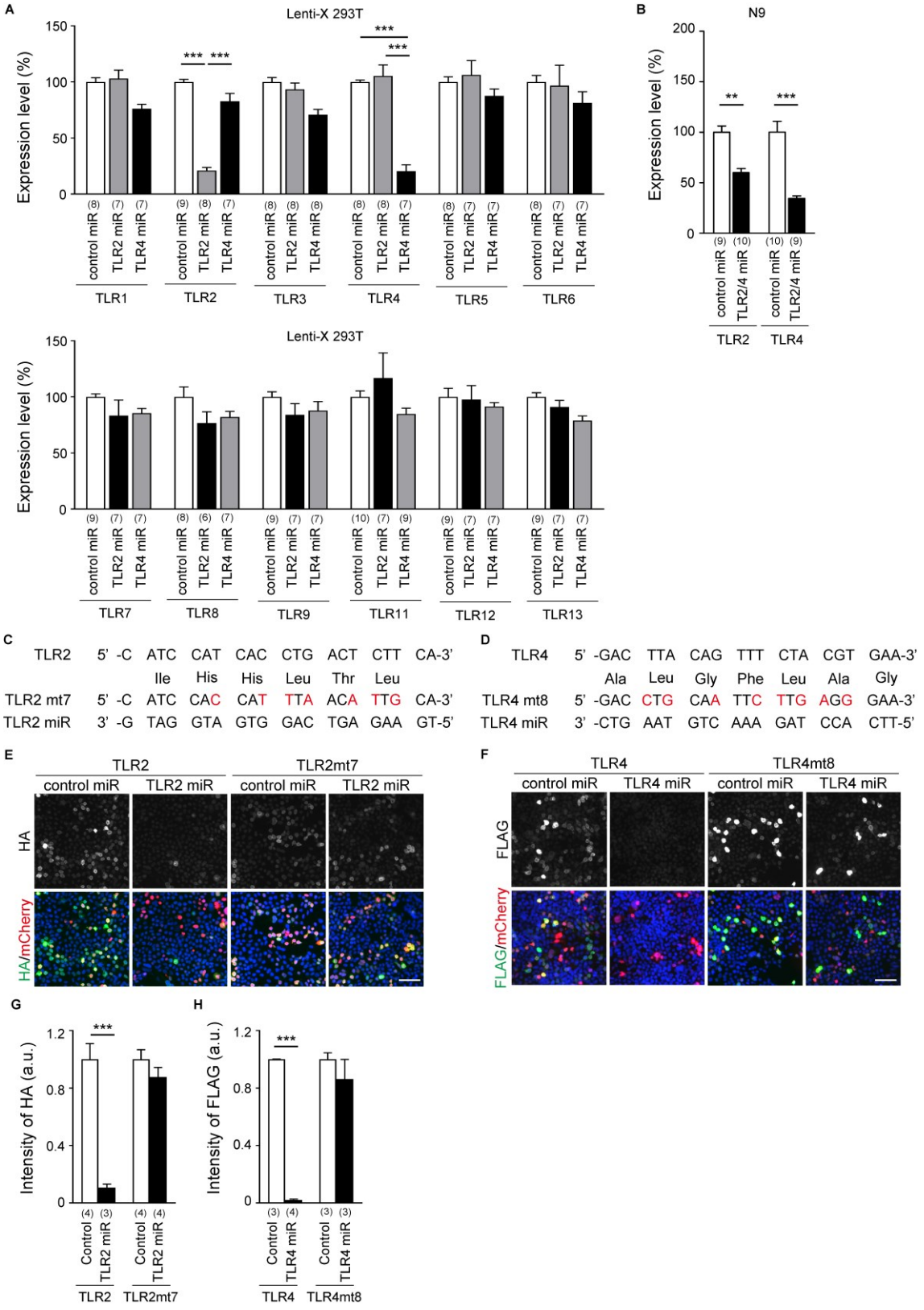
A
Lenti-X 293T
Expression level (%)
control miR
TLR2 miR
TLR4 miR
TLR1
TLR2
TLR3
TLR4
TLR5
TLR6
Lenti-X 293T
TLR7
TLR8
TLR9
TLR11
TLR12
TLR13
B
N9
control miR
TLR2/4 miR
TLR2
TLR4
C
TLR2 5' -C ATC CAT CAC CTG ACT CTT CA-3'
Ile His His Leu Thr Leu
TLR2 mt7 5' -C ATC CAC CAT TTA ACA TTG CA-3'
TLR2 miR 3' -G TAG GTA GTG GAC TGA GAA GT-5'
D
TLR4 5' -GAC TTA CAG TTT CTA CGT GAA-3'
Ala Leu Gly Phe Leu Ala Gly
TLR4 mt8 5' -GAC CTG CAA TTC TTG AGG GAA-3'
TLR4 miR 3' -CTG AAT GTC AAA GAT CCA CTT-5'
E
TLR2
TLR2mt7
control miR
TLR2 miR
HA
HA/mCherry
F
TLR4
TLR4mt8
TLR4 miR
FLAG
FLAG/mCherry
G
Intensity of HA (a.u.)
Control
TLR2mt7
H
Intensity of FLAG (a.u.)
TLR4mt8

Figure S6, related to Figure 6.

TLR2/4 microRNA selectively suppresses mRNA expression of TLR2 and TLR4 *in vitro*

(**A**) RNA interference with TLR2 or TLR4 microRNA efficiently and specifically suppresses mRNA expression of the corresponding TLR isoform in Lenti-X 293T cells. Various mouse TLR isoforms (TLR1 to TLR13) were overexpressed with TLR2 or TLR4 microRNA (miR) as well as control microRNA, and their expression levels were quantified by real-time RT-PCR. ***P<0.001 for Bonferroni's multiple comparison test. (**B**) Lentivirus-delivered TLR2/4 microRNA, in which TLR4 microRNA and TLR2 microRNA are tandemly connected, simultaneously suppressed endogenous mRNA expression of TLR2 and TLR4 in the N9 microglial cells. The values were normalized to those with control microRNA. **P<0.01, ***P<0.001 for unpaired t-test. (**C** and **D**) DNA sequences for microRNA-targeting regions of TLR2 (**C**) and TLR4 (**D**) and the corresponding regions of microRNA-resistant mutant cDNAs of these genes ("TLR2mt7" and "TLR4mt8", respectively) with no change in the amino acid sequences. Mutations in these mutants are highlighted in red. (**E** and **F**) Representative images of immunostaining for TLR2 (**E**), TLR4 (**F**) or the respective microRNA-resistant mutants ("TLR2mt7" and "TLR4mt8") with the corresponding microRNA or control microRNA in Lenti-X 293T cells. TLR2 and TLR2mt7 cDNAs were tagged with HA and detected by HA immunostaining. TLR4 and TLR4mt8 cDNAs were tagged with FLAG and detected by FLAG immunostaining. mCherry was simultaneously expressed with TLR2 or TLR4 microRNA to identify cells expressing these miRNAs. HA or FLAG signals and mCherry are shown in green and red, respectively, in the merged images. Nuclear counterstaining with Hoechst 33342 is shown in blue. Scale bars, 25 μm. (**G** and **H**) The fluorescent intensities of HA (**G**) and FLAG (**H**) tags in the experimental conditions shown in **E** and **F**, respectively. The values were normalized to those with control microRNA. ***P<0.001 for unpaired t-test. The number of analyzed wells is shown below each group. Data are shown as means ± SEM.

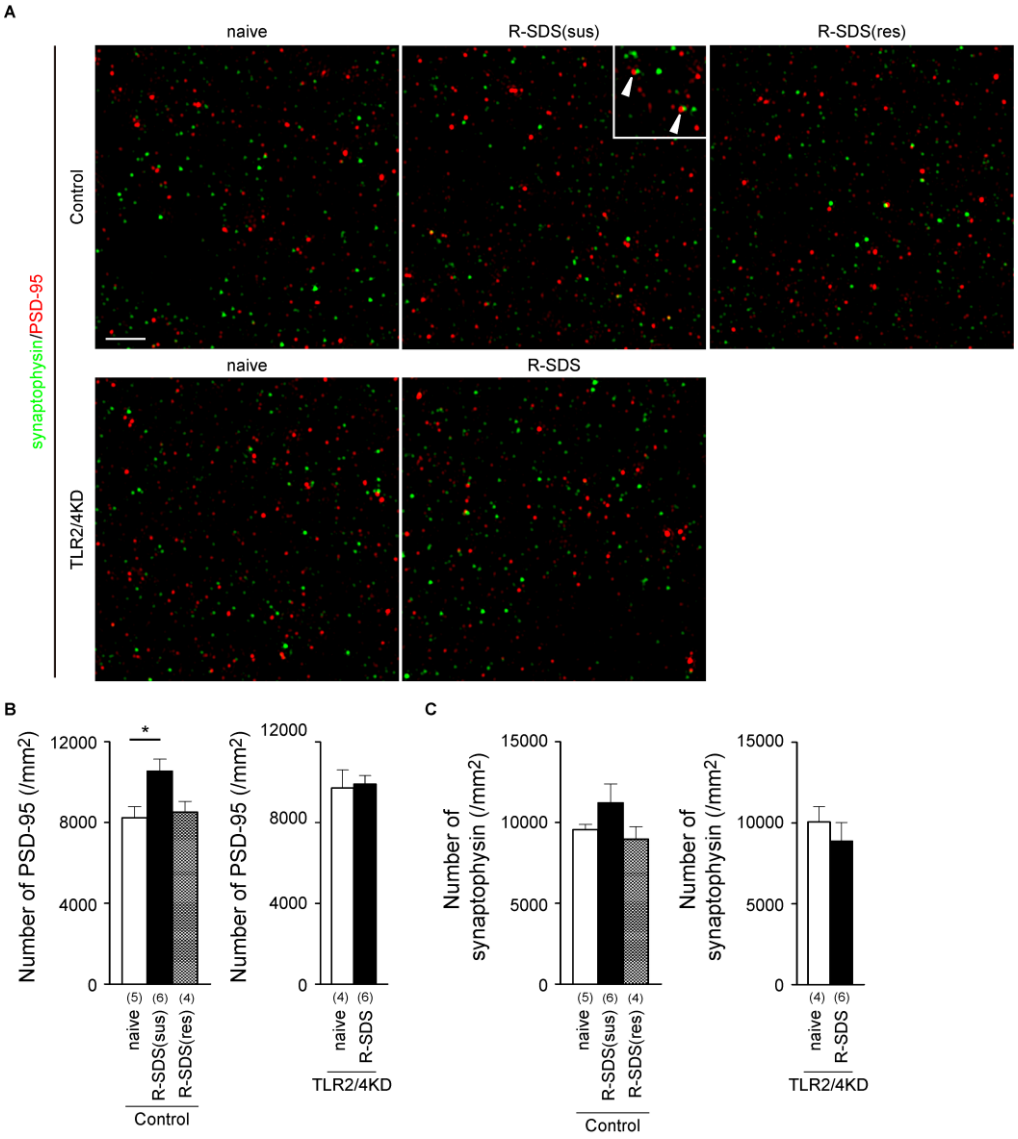

Figure S7, related to Figure 6.

R-SDS increases the number of PSD-95-positive puncta in the mPFC in a manner dependent on TLR2/4 expressed in mPFC microglia

Representative SIM images (**A**) and quantitative analyses (**B** and **C**) of immunostaining for synaptophysin (green in **A**) and PSD-95 (red in **A**) in the deep layer of the mPFC of CX3CR1-CreER mice that received mPFC injections of lentiviral vectors expressing control microRNA ("Control") or TLR2/4 microRNA ("TLR2/4KD"). The images were taken from susceptible and resilient CX3CR1-CreER mice ("R-SDS(sus)" and "R-SDS(res)", respectively) expressing control microRNA, and those expressing TLR2/4 microRNA ("R-SDS") at 1.5 h after R-SDS, as well as those expressing control or TLR2/4 microRNA without R-SDS ("naïve"). Arrowheads in **A** indicate the juxtaposition of synaptophysin and PSD-95 punctate signals reminiscent of excitatory synapses. Scale bar, 5 μm. **P*<0.05 for Bonferroni's multiple comparison test.

The number of mice is shown below each group. Data are shown as means ± SEM.

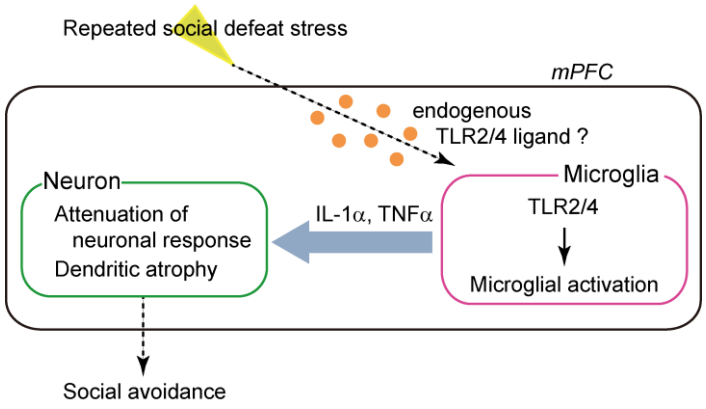

Figure S8, related to all Figures.

The role of TLR2/4 in mPFC microglia for R-SDS-induced neuronal and behavioral changes

Our findings demonstrate that R-SDS induces activation of mPFC microglia through TLR2/4 for neuronal and behavioral changes, although the endogenous TLR2/4 ligand for this microglial activation remains to be identified. We also suggest that IL-1α and TNFα derived from the activated mPFC microglia mediate neuronal response attenuation and dendritic atrophy in the mPFC, thereby leading to social avoidance.

KEY RESOURCES TABLE

REAGENT or RESOURCE	SOURCE	IDENTIFIER
Antibodies		
Rabbit polyclonal anti-c-Fos	Merck Millipore	Cat#PC38-100µl; RRID: AB_2314043
Rabbit polyclonal anti- Iba-1	Wako	Cat#019-19741; RRID: AB_839504
Mouse monoclonal anti-NeuN	Chemicon	Cat#MAB377; RRID: AB_2298772
Rat monoclonal anti-CD68	AbD serotec	Cat#ABD-MCA1957; RRID:AB_322219
Mouse monoclonal anti-CD68	Abcam	Cat#ab955; RRID: AB_307338
Rat monoclonal anti-CD45	AbD serotec	Cat# ABD-MCA1388; RRID:AB_321729
Rat monoclonal anti-CD11b	AbD serotec	Cat#ABD-MCA711FT-25; RRID: AB_323135
Rat monoclonal anti-GFP	Nacalai	Cat#04404-84; RRID: AB_10013361
Rabbit polyclonal anti-RFP	Rockland,	Cat#600-401-379; RRID: AB_2209751
Mouse monoclonal anti-RFP	MBL	Cat#M165-3; RRID: AB_1520843
Rat monoclonal anti-HA	Roche	Cat#11867423001; RRID: AB_10094468
Mouse monoclonal anti-FLAG	Sigma-Aldrich	Cat#F1804; RRID:AB_262044
Rabbit monoclonal anti-synaptophysin	Abcam	Cat# AB16659-1; RRID: AB_443419
Mouse monoclonal anti-PSD-95	Merck Millipore	Cat#MAB1596; RRID: AB_2092365
Armenian hamster monoclonal anti-IL-1 alpha	eBioscience,	Cat#16-7011-85; RRID: AB_469199

Rat monoclonal anti-TNF-α	BioLegend,	Cat#506331; RRID:AB_11147367
Bacterial and Virus Strains		
pLV-PGK-GFP	Dr. Johan Jakobsson	N/A
Lenti-X HTX packaging System	Clontech	Cat#631247
Biological Samples		
None		
Chemicals, Peptides, and Recombinant Proteins		
blasticidin	Wako	Cat#029-18701; CAS: 3513-03-9
Armenian Hamster IgG Isotype Control	eBioscience	Cat#16-4888-85; RRID:AB_470172
Rat IgG1, κ Isotype Ctrl Antibody	BioLegend	Cat#400431; RRID:AB_11150233
Critical Commercial Assays		
FD Rapid GolgiStain Kit	FD Neuro Technologies	Cat# PK401
Ovation RNA Amplification System V2	NuGEN	Cat#3100-12
Low Input Quick Amp Labeling Kit	Agilent Technologies	Cat#5190-2305
SurePrint G3 Mouse GE 8×60K Microarray	Agilent Technologies	Cat#G4852B
Deposited Data		
Raw microarray data	This paper	GSE115996
Experimental Models: Cell Lines		
Mouse: N9 cells	Laboratory of Dr. Makoto Tsuda	RRID:CVCL_0452
Human: Lenti-X 293T cells	Clontech	Cat#632180 RRID:CVCL_4401
Experimental Models: Organisms/Strains		
Mouse: TLR2 knockout mice	Oriental Bio Service	RRID:IMSR_OBS:3
Mouse: TLR4 knockout mice	Oriental Bio Service	RRID:IMSR_OBS:4
Mouse: B6.129S7-Il1r1tm1Imx/J	The Jackson Laboratory	RRID:IMSR_JAX:003245
Mouse: B6.129P-Cx3cr1tm1Litt/J	The Jackson Laboratory	RRID:IMSR_JAX:005582

Mouse: B6.129P2(Cg)-Cx3cr1tm2.1(cre/ERT2)Litt/WganJ	The Jackson Laboratory	RRID:IMSR_JAX:021160
Oligonucleotides		
Primers for quantitative RT-PCR, see Supplemental Experimental Procedures	This paper	N/A
miRNA target sequence, see Supplemental Experimental Procedures	This paper	N/A
Recombinant DNA		
mTLR1	Addgene	Cat #13080
pCMV-SPORT-mTLR2	Dharmacon	Cat#MMM1013-202763576
pCMV-SPORT6-mTLR3	Dharmacon	Cat#MMM1013-202709109
pCMV-SPORT6-mTLR4	Dharmacon	Cat#MMM1013-202761834
pCR-BluntII-TOPO-mTLR5	Dharmacon	Cat#MMM1013-211692986
pCMV-SPORT6-mTLR6	Dharmacon	Cat#MMM1013-202709109
pCR4-TOPO-mTLR7	Dharmacon	Cat#MMM1013-211691472
mTLR8 cDNA Plasmid	R&D SYSTEMS	Cat# RDC0786
mTLR9	Addgene	Cat#13091
pCR-BluntII-TOPO-mTLR11	Dharmacon	Cat#MMM1013-211692974
pCR4-TOPO-mTLR12	Dharmacon	Cat#MMM1013-211691876
pCR-BluntII-TOPO-mTLR13	Dharmacon	Cat#MMM1013-211693738
Software and Algorithms		
BZ-II Measurement Module software	Keyence	RRID: SCR_016348
Imaris	Bitplane	RRID:SCR_007370
MetaMorph	Molecular Devices	RRID:SCR_002368

BLOCK-iT RNAi Designer	Thermo Fisher Scientific	https://rnaidesigner.thermofisher.com/rnaiexpress/
PRISM 7.0 software	GraphPad	RRID:SCR_002798
Other		
None		

Panel	Behavior	Group	N value	Replicate	Statistical test	ANOVA	P value	F value	Multiple comparison test	Comparison	P value	t value	df (between)
1C, Left	interaction	WT, naïve	18	mouse	Two-way RM ANOVA	interaction	***<0.0001	F (3,83)=15.51	Bonferroni	WT, naïve, ICR(+) vs WT, R-SDS, ICR(+)	***<0.0001	5.034	166
		TLR-DKO, naïve	13	mouse		group	**0.0018	F (3,83)=5.444		WT, R-SDS, ICR(-) vs WT, R-SDS, ICR(+)	***<0.0001	5.33	83
		WT, R-SDS	34	mouse		within subject effect (ICR(-), (+))	0.0609	F (1,83)=3.611		WT, R-SDS, ICR(+) vs TLR-DKO, R-SDS, ICR(+)	***<0.0001	5.928	166
		TLR-DKO, R-SDS	22	mouse		Subjects (matching)	*0.0208	F (83, 83) = 1.569					

Panel	Behavior	Group	N value	Replicate	Statistical test	ANOVA	P value	F value	Multiple comparison test	Comparison	P value	t value	df (between)
1C, Right	interaction	WT, naïve	18	mouse	Two-way ANOVA	interaction	*0.0237	F (1, 83) = 5.308	Bonferroni	WT, naïve vs WT, R-SDS	***<0.0001	4.657	83
		TLR-DKO, naïve	13	mouse		defeat	***0.0004	F (1, 83) = 13.38		WT, R-SDS vs TLR-DKO, R-SDS	***<0.0001	5.219	83
		WT, R-SDS	34	mouse		genotype	***0.0002	F (1, 83) = 15.75					
		TLR-DKO, R-SDS	22	mouse									

Panel	Behavior	Group	N value	Replicate	Statistical test	ANOVA	P value	F value	Multiple comparison test	Comparison	P value	t value	df (between)
1D, Left	avoidance	WT, naïve	18	mouse	Two-way RM ANOVA	interaction	***<0.0001	F (3, 83) = 9.243	Bonferroni	WT, naïve, ICR(+) vs WT, R-SDS, ICR(+)	***<0.0001	5.027	166
		TLR-DKO, naïve	13	mouse		group	***0.0001	F (3, 83) = 7.751		WT, R-SDS, ICR(-) vs WT, R-SDS, ICR(+)	***<0.0001	5.284	83
		WT, R-SDS	34	mouse		within subject effect (ICR(-), (+))	0.774	F (1, 83) = 0.08298		WT, R-SDS, ICR(+) vs TLR-DKO, R-SDS, ICR(+)	***<0.0001	5.605	166
		TLR-DKO, R-SDS	22	mouse		Subjects (matching)	*0.0416	F (83, 83) = 1.466					

Panel	Behavior	Group	N value	Replicate	Statistical test	ANOVA	P value	F value	Multiple comparison test	Comparison	P value	t value	df (between)
1D, Right	avoidance	WT, naïve	18	mouse	Two-way ANOVA	interaction	*0.0318	F (1, 83) = 4.77	Bonferroni	WT, naïve vs WT, R-SDS	***0.0005	3.834	83
		TLR-DKO, naïve	13	mouse		defeat	**0.0078	F (1, 83) = 7.424		WT, R-SDS vs TLR-DKO, R-SDS	***0.0002	4.117	83
		WT, R-SDS	34	mouse		genotype	**0.007	F (1, 83) = 7.64					
		TLR-DKO, R-SDS	22	mouse									

Panel	Behavior	Group	N value	Replicate	Statistical test	χ^2	P value
1C, 1D	susceptible/resilient	WT, R-SDS	24	mouse	chi square	10.062	**0.0015
		TLR-DKO, R-SDS	19	mouse			

Panel	Behavior	Group	N value	Replicate	Statistical test	ANOVA	P value	F value	Multiple comparison test	Comparison	P value	t value	df (between)
1E	elevated plus maze	WT, naïve	18	mouse	Two-way ANOVA	Interaction	*0.0212	F (1, 83) = 5.517	Bonferroni	WT, naïve vs WT, R-SDS	**0.0048	3.129	83
		TLR-DKO, naïve	13	mouse		defeat	***0.0003	F (1, 83) = 14.43		WT, R-SDS vs TLR-DKO, R-SDS	***<0.0001	5.116	83
		WT, R-SDS	34	mouse		genotype	0.1012	F (1, 83) = 2.747					
		TLR-DKO, R-SDS	22	mouse									

Panel	Behavior	Group	N value	Replicate	Statistical test	ANOVA	P value	F value	Multiple comparison test	Comparison	P value	t value	df (between)
1F	submissive posture	WT, S-SDS	7	mouse	Two-way RM ANOVA	Interaction	0.2223	F (1, 11) = 1.673	Bonferroni	WT, S-SDS vs WT, R-SDS	*0.0154	3.254	11
		TLR-DKO, S-SDS	6	mouse		genotype	*0.0312	F (1, 11) = 6.097		TLR-DKO, S-SDS vs TLR-DKO, R-SDS	**0.0012	4.775	11
		WT, R-SDS	7	mouse		Time	***0.0001	F (1, 11) = 32.65		WT, R-SDS vs TLR-DKO, R-SDS	*0.0493	2.412	22
		TLR-DKO, R-SDS	6	mouse		Subjects (matching)	0.929	F (11, 11) = 0.3981					

Panel	Behavior	Group	N value	Replicate	Statistical test	ANOVA	P value	F value	Multiple comparison test	Comparison	P value	t value	df (between)
2A, Left	interaction	TLR2KO, naïve	8	mouse	Two-way RM ANOVA	interaction	**0.0056	F (3, 30) = 5.114	Bonferroni	TLR2KO, naïve, ICR(+) vs TLR2KO, R-SDS, ICR(+)	*0.0219	3.025	60
		TLR-DKO, naïve	9	mouse		group	0.229	F (3, 30) = 1.522		TLR2KO, R-SDS, ICR(+) vs TLR-DKO, R-SDS, ICR(+)	**0.0084	3.35	60
		TLR2KO, R-SDS	10	mouse		within subject effect (ICR(-), (+))	*0.0136	F (1, 30) = 6.87					
		TLR-DKO, R-SDS	7	mouse		Subjects (matching)	**0.0053	F (30, 30) = 2.604					

Panel	Behavior	Group	N value	Replicate	Statistical test	ANOVA	P value	F value	Multiple comparison test	Comparison	P value	t value	df (between)
2A, Right	interaction	TLR2KO, naïve	8	mouse	Two-way ANOVA	interaction	**0.0047	F (1, 30) = 9.343	Bonferroni	TLR2KO, naïve vs TLR2KO, R-SDS	**0.0027	3.527	30
		TLR-DKO, naïve	9	mouse		defeat	0.0854	F (1, 30) = 3.164		TLR2KO, R-SDS vs TLR-DKO, R-SDS	**0.01	3.032	30
		TLR2KO, R-SDS	10	mouse		genotype	0.2172	F (1, 30) = 1.589					
		TLR-DKO, R-SDS	7	mouse									

Panel	Behavior	Group	N value	Replicate	Statistical test	ANOVA	P value	F value	Multiple comparison test	Comparison	P value	t value	df (between)
2B, Left	avoidance	TLR2KO, naïve	8	mouse	Two-way RM ANOVA	interaction	**0.0027	F (3, 30) = 5.931	Bonferroni	TLR2KO, naïve, ICR(+) vs TLR2KO, R-SDS, ICR(+)	*0.0272	2.95	60
		TLR-DKO, naïve	9	mouse		group	0.2349	F (3, 30) = 1.499		TLR2KO, R-SDS, ICR(-) vs TLR2KO, R-SDS, ICR(+)	**0.0062	3.481	30
		TLR2KO, R-SDS	10	mouse		within subject effect (ICR(-), (+))	0.6218	F (1, 30) = 0.2484		TLR2KO, R-SDS, ICR(+) vs TLR-DKO, R-SDS, ICR(+)	**0.0046	3.545	60
		TLR-DKO, R-SDS	7	mouse		Subjects (matching)	*0.0041	F (30, 30) = 2.696					

Panel	Behavior	Group	N value	Replicate	Statistical test	ANOVA	P value	F value	Multiple comparison test	Comparison	P value	t value	df (between)
2B, Right	avoidance	TLR2KO, naïve	8	mouse	Two-way ANOVA	interaction	**0.0092	F (1, 30) = 7.741	Bonferroni	TLR2KO, naïve vs TLR2KO, R-SDS	**0.0035	3.436	30
		TLR-DKO, naïve	9	mouse		defeat	0.0635	F (1, 30) = 3.713		TLR2KO, R-SDS vs TLR-DKO, R-SDS	**0.0032	3.464	30
		TLR2KO, R-SDS	10	mouse		genotype	*0.0397	F (1, 30) = 4.627					
		TLR-DKO, R-SDS	7	mouse									

Panel	Behavior	Group	N value	Replicate	Statistical test	ANOVA	P value	F value	Multiple comparison test	Comparison	P value	t value	df (between)
2C, Left	interaction	TLR4KO, naïve	10	mouse	Two-way RM ANOVA	interaction	0.1867	F (3, 34) = 1.694	Bonferroni	TLR4KO, naïve, ICR(+) vs TLR4KO, R-SDS, ICR(+)	**0.0072	3.38	68
		TLR-DKO, naïve	9	mouse		group	*0.0429	F (3, 34) = 3.024		TLR4KO, R-SDS, ICR(+) vs TLR-DKO, R-SDS, ICR(+)	*0.0189	3.062	68
		TLR4KO, R-SDS	9	mouse		within subject effect (ICR(-), (+))	**0.004	F (1, 34) = 9.528					
		TLR-DKO, R-SDS	10	mouse		Subjects (matching)	0.3253	F (34, 34) = 1.169					

Panel	Behavior	Group	N value	Replicate	Statistical test	ANOVA	P value	F value
2C, Right	interaction	TLR4KO, naïve	10	mouse	Two-way ANOVA	interaction	0.1198	F (1, 34) = 2.546
		TLR-DKO, naïve	9	mouse		defeat	0.2894	F (1, 34) = 1.158
		TLR4KO, R-SDS	9	mouse		genotype	0.2276	F (1, 34) = 1.51
		TLR-DKO, R-SDS	10	mouse				

Panel	Behavior	Group	N value	Replicate	Statistical test	ANOVA	P value	F value	Multiple comparison test	Comparison	P value	t value	df (between)
2D, Left	avoidance	TLR4KO, naïve	10	mouse	Two-way RM ANOVA	interaction	*0.0322	F (3, 34) = 3.291	Bonferroni	TLR4KO, naïve, ICR(+) vs TLR4KO, R-SDS, ICR(+)	***0.0009	4.029	68
		TLR-DKO, naïve	9	mouse		group	*0.0148	F (3, 34) = 4.029		TLR4KO, R-SDS, ICR(+) vs TLR-DKO, R-SDS, ICR(+)	**0.0026	3.695	68
		TLR4KO, R-SDS	9	mouse		within subject effect (ICR(-), (+))	0.7991	F (1, 34) = 0.0658					
		TLR-DKO, R-SDS	10	mouse		Subjects (matching)	0.3578	F (34, 34) = 1.134					

Panel	Behavior	Group	N value	Replicate	Statistical test	ANOVA	P value	F value	Multiple comparison test	Comparison	P value	t value	df (between)
2D, Right		TLR4KO, naïve	10	mouse	Two-way ANOVA	interaction	*0.0494	F (1, 34) = 4.152	Bonferroni	TLR4KO, naïve vs TLR4KO, R-SDS	**0.0089	3.047	34
	avoidance	TLR-DKO, naïve	9	mouse		genotype	0.0641	F (1, 34) = 3.663		TLR4KO, R-SDS vs TLR-DKO, R-SDS	*0.017	2.794	34
		TLR4KO, R-SDS	9	mouse		defeat	*0.0296	F (1, 34) = 5.158					
		TLR-DKO, R-SDS	10	mouse									

Panel	Behavior	Group	N value	Replicate	Statistical test	ANOVA	P value	F value
2E		TLR2KO, naïve	8	mouse	Two-way ANOVA	interaction	0.9857	F (1, 30) = 0.000328
	traveling distance	TLR-DKO, naïve	9	mouse		defeat	0.0776	F (1, 30) = 3.339
		TLR2KO, R-SDS	10	mouse		genotype	0.4395	F (1, 30) = 0.6137
		TLR-DKO, R-SDS	7	mouse				

Panel	Behavior	Group	N value	Replicate	Statistical test	ANOVA	P value	F value
2F		TLR4KO, naïve	10	mouse	Two-way ANOVA	interaction	0.8811	F (1, 34) = 0.02271
	traveling distance	TLR-DKO, naïve	9	mouse		defeat	0.4558	F (1, 34) = 0.5692
		TLR4KO, R-SDS	9	mouse		genotype	0.4798	F (1, 34) = 0.5106
		TLR-DKO, R-SDS	10	mouse				

Panel	IHC	Group	N value	Replicate	Statistical test	ANOVA	P value	F value	Multiple comparison test	Comparison	P value	t value	df (between)
3B		WT. naïve	8	mouse	Two-way ANOVA	interaction	***0.0009	F (4, 42) = 5.756	Bonferroni	WT, naïve vs WT, R-SDS, 1.5h	***0.0009	4.323	42
		WT, S-SDS, 1.5h	7	mouse		genotype	0.053	F (1, 42) = 3.966		WT, S-SDS, 4h vs TLR-DKO, S-SDS, 4h	*0.0234	2.988	42
		WT, S-SDS, 4h	3	mouse		defeat	**0.0029	F (4, 42) = 4.773		WT, R-SDS, 1.5h vs TLR-DKO, R-SDS, 1.5h	*0.0218	3.013	42
		WT, R-SDS (sus), 1.5h	6	mouse									
		WT, R-SDS (sus), 4h	3	mouse									
	mPFC, CD68	TLR-DKO. naïve	7	mouse									
		TLR-DKO, S-SDS, 1.5h	6	mouse									
		TLR-DKO, S-SDS, 4h	3	mouse									
		TLR-DKO, R-SDS, 1.5h	5	mouse									
		TLR-DKO, R-SDS, 4h	4	mouse									

Panel	IHC	Group	N value	Replicate	Statistical test	χ^2	P value
3B, 3G		WT, R-SDS	19	mouse	chi square	5.776	*0.016
S2B, S2E	mPFC, CD68	TLR-DKO, R-SDS	13	mouse			

Panel	IHC	Group	N value	Replicate	Statistical test	ANOVA	P value	F value	Multiple comparison test	Comparison	P value	t value	df (between)
3D		WT. naïve	11	mouse	Two-way ANOVA	interaction	0.1608	F (4, 53) = 1.713	Bonferroni	WT, naïve vs WT, S-SDS, 4h	*0.0254	3.169	53
		WT, S-SDS, 1.5h	7	mouse		genotype	0.4175	F (1, 53) = 0.6677		TLR-DKO, naïve vs TLR-DKO, S-SDS, 1.5h	*0.0204	3.245	53
		WT, S-SDS, 4h	3	mouse		defeat	***<0.001	F (4, 53) = 9.218		WT, naïve vs WT, R-SDS, 1.5h	#0.0595	2.866	53
		WT, R-SDS (sus), 1.5h	7	mouse									
		WT, R-SDS (sus), 4h	3	mouse									
	mPFC, Iba-1	TLR-DKO. naïve	11	mouse									
		TLR-DKO, S-SDS, 1.5h	6	mouse									
		TLR-DKO, S-SDS, 4h	3	mouse									
		TLR-DKO, R-SDS, 1.5h	8	mouse									
		TLR-DKO, R-SDS, 4h	4	mouse									

Panel	IHC	Group	N value	Replicate	Statistical test	ANOVA	P value	F value	Multiple comparison test	Comparison	P value	t value	df (between)
3E		WT. naïve	3	mouse	Two-way ANOVA	interaction	0.3007	F (1, 10) = 1.191	Bonferroni	WT, naïve vs WT, R-SDS(sus)	#0.0746	2.493	15
		WT, S-SDS	4	mouse		genotype	0.133	F (1, 10) = 2.675					
		WT, R-SDS (sus)	4	mouse		defeat	*0.017	F (1, 10) = 8.173					
	mPFC, CD11b	TLR-DKO. naïve	3	mouse									
		TLR-DKO, S-SDS	3	mouse									
		TLR-DKO, R-SDS	4	mouse									

Panel	IHC	Group	N value	Replicate	Statistical test	P value	F value	Multiple comparison test	Comparison	P value	t value	df (between)
3G		WT, naïve	7	mouse	One-way ANOVA	***P<0.0001	F (2, 17) = 17.64	Bonferroni	WT, naïve vs WT, R-SDS(sus)	***<0.0001	5.604	17
	mPFC, CD68	WT, R-SDS(sus)	6	mouse					WT, R-SDS(sus) vs WT, R-SDS(res)	***0.0007	4.674	17
		WT, R-SDS(res)	7	mouse								

Panel	IHC	Group	N value	Replicate	Statistical test	P value	F value	Multiple comparison test	Comparison	P value	t value	df (between)
3H		WT, naïve	7	mouse	One-way ANOVA	**0.0023	F (2, 17) = 8.889	Bonferroni	WT, naïve vs WT, R-SDS(res)	*0.0419	2.739	17
	mPFC, Iba-1	WT, R-SDS(sus)	6	mouse					WT, R-SDS(sus) vs WT, R-SDS(res)	**0.0021	4.127	17
		WT, R-SDS(res)	7	mouse								

Panel	IHC	Group	N value	Replicate	Statistical test	P value	F value	Multiple comparison test	Comparison	P value	t value	df (between)
3J		WT, naïve	6	mouse	One-way ANOVA	*0.0153	F (2, 14) = 5.718	Bonferroni	WT, naïve vs WT, R-SDS(sus)	*0.0219	3.136	14
	mPFC, CD11b	WT, R-SDS(sus)	5	mouse					WT, naïve vs WT, R-SDS(res)	#0.0619	2.608	14
		WT, R-SDS(res)	6	mouse								

Panel	IHC	Group	N value	Replicate	Statistical test	P value	F value	Multiple comparison test	Comparison	P value	t value	df (between)
3K		WT. naïve	5	mouse	One-way ANOVA	*0.0105	F (4, 22) = 4.264	Bonferroni	WT, naïve vs WT, 1.5h	#0.0744	2.948	22
		WT, 1.5h	5	mouse					WT, naïve vs WT, 4h	*0.0275	3.372	22
	mPFC,CD68	WT, 4h	6	mouse								
		TLR-DKO, 1.5h	5	mouse								
		TLR-DKO, 4h	6	mouse								

Panel	IHC	Group	N value	Replicate	Statistical test	P value	F value
3L		WT. naïve	5	mouse	One-way ANOVA	0.6439	F (4, 22) = 0.6336
		WT, 1.5h	5	mouse			
	mPFC,	WT, 4h	6	mouse			
	lba-1	TLR-DKO, 1.5h	5	mouse			
		TLR-DKO, 4h	6	mouse			

Panel	correlation	Group	N value	Replicate	Statistical test	P value	R squared
	mPFC, CD68 vs avoidan	WT. naïve	60	mouse	Pearson	***<0.0001	0.5375
		WT. R-SDS					

		TLR2KO, naïve						
		TLR2KO, R-SDS						
		TLR4KO, naïve						
		TLR4KO, R-SDS						
		TLR-DKO, naïve						
		TLR-DKO, R-SDS						
Panel	correlation	Group	N value	Replicate	Statistical test	P value	R squared	
	mPFC, Iba-1 vs avoidanc	WT. naïve	61	mouse	Pearson	***0.0002	0.2072	
		WT. R-SDS						
		TLR2KO, naïve						
		TLR2KO, R-SDS						
		TLR4KO, naïve						
		TLR4KO, R-SDS						
		TLR-DKO, naïve						
		TLR-DKO, R-SDS						
Panel	IHC	Group	N value	Replicate	Statistical test	ANOVA	P value	F value
4F		WT. naïve	3	mouse	Two-way ANOVA	interaction	0.333	F (2, 15) = 1.184
		WT, S-SDS	4	mouse		genotype	0.5566	F (1, 15) = 0.3616
	mPFC,	WT, R-SDS (sus)	4	mouse		defeat	0.9324	F (2, 15) = 0.07032
	CD45	TLR-DKO. naïve	3	mouse				
		TLR-DKO, S-SDS	3	mouse				
		TLR-DKO, R-SDS	4	mouse				

Panel	IHC	Group	N value	Replicate	Statistical test	ANOVA	P value	F value	Multiple comparison test	Comparison	P value	t value	df (between)
4G		WT. naïve	3	mouse	Two-way ANOVA	interaction	0.8296	F (2, 15) = 0.1892	Bonferroni	WT, naïve vs WT, R-SDS(sus)	*0.0466	2.729	15
		WT, S-SDS	4	mouse		genotype	0.3098	F (1, 15) = 1.105		WT, S-SDS vs WT, R-SDS(sus)	*0.0351	2.869	15
		WT, R-SDS (sus)	4	mouse		defeat	**0.0022	F (2, 15) = 9.482		TLR-DKO, naïve vs TLR-DKO, R-SDS	*0.0357	2.861	15
	ACC,CD45	TLR-DKO. naïve	3	mouse									
		TLR-DKO, S-SDS	3	mouse									
		TLR-DKO, R-SDS	4	mouse									

Panel	IHC	Group	N value	Replicate	Statistical test	P value	F value	Multiple comparison test	Comparison	P value	t value	df (between)
5C		WT. naïve	6	mouse	One-way ANOVA	**0.004	F (2, 14) = 8.431	Bonferroni	WT, naïve vs WT, S-SDS	**0.0068	3.725	14
	c-Fos	WT, S-SDS	6	mouse					WT, S-SDS vs WT, R-SDS(sus)	*0.0159	3.295	14
		WT, R-SDS (sus)	5	mouse								

Panel	IHC	Group	N value	Replicate	Statistical test	P value	F value	Multiple comparison test	Comparison	P value	t value	df (between)
5C		TLR-DKO. naïve	5	mouse	One-way ANOVA	***<0.0001	F (2, 13) = 30.59	Bonferroni	TLRDKO, naïve vs TLR-DKO, S-SDS	***<0.0001	7.812	13
	c-Fos	TLR-DKO, S-SDS	6	mouse					TLRDKO, naïve vs TLR-DKO, R-SDS	**0.0073	3.748	13
		TLR-DKO, R-SDS	5	mouse					TLR-DKO, S-SDS vs TLR-DKO, R-SDS	**0.0055	3.897	13

Panel	IHC	Group	N value	Replicate	Statistical test	χ^2	P value
5C, 5E		WT, R-SDS	18	mouse	chi square	4.118	*0.042
S4C, S4D	c-Fos	TLR-DKO, R-SDS	17	mouse			

Panel	IHC	Group	N value	Replicate	Statistical test	P value	F value	Multiple comparison test	Comparison	P value	t value	df (between)
5E		WT, naïve	7	mouse	One-way ANOVA	***P<0.0001	F (2, 17) = 52.96	Bonferroni	WT, naïve vs WT, R-SDS(sus)	*0.0271	2.946	17
	c-Fos	WT, R-SDS(sus)	6	mouse					WT, naïve vs WT, R-SDS(res)	***<0.0001	10.06	17
		WT, R-SDS(res)	7	mouse					WT, R-SDS(sus) vs WT, R-SDS(res)	***<0.0001	6.723	17

Panel	Golgi-Cox	Group	N value	Replicate	Statistical test	ANOVA	P value	F value	Multiple comparison test	Comparison	P value	t value	df (between)
5G		WT, naïve	33	neuron	Two-way ANOVA	interaction	*0.0197	F (1, 126) = 5.576	Bonferroni	WT, naïve vs WT, R-SDS(sus)	***<0.0001	4.309	126
	dendrite length	WT, R-SDS (sus)	35	neuron		genotype	0.6092	F (1, 126) = 0.2627					
		TLR-DKO, naïve	33	neuron		defeat	***0.0005	F (1, 126) = 12.85					
		TLR-DKO, R-SDS	29	neuron									

Panel	Golgi-Cox	Group	N value	Replicate	Statistical test	ANOVA	P value	F value	Multiple comparison test	Comparison	P value	t value	df (between)
5H		WT, naïve	4	mouse	Two-way ANOVA	interaction	0.0653	F (1, 10) = 4.286	Bonferroni	WT, naïve vs WT, R-SDS(sus)	*0.0357	2.831	10
	dendrite length	WT, R-SDS (sus)	3	mouse		genotype	0.428	F (1, 10) = 0.6824					
		TLR-DKO, naïve	4	mouse		defeat	0.082	F (1, 10) = 3.736					
		TLR-DKO, R-SDS	3	mouse									

Panel	IHC	Group	N value	Replicate	Statistical test	ANOVA	P value	F value
6D		Control, naïve	8	mouse	Two-way ANOVA	interaction	0.8348	F (1, 16) = 0.04495
	EYFP:	Control, R-SDS	3	mouse		genotype	**0.0051	F (1, 16) = 10.49
	mCherry	TLR2/4KD, naïve	5	mouse		defeat	0.6183	F (1, 16) = 0.2582
		TLR2/4KD, R-SDS	4	mouse				

Panel	IHC	Group	N value	Replicate	Statistical test	ANOVA	P value	F value
6E		Control, naïve	8	mouse	Two-way ANOVA	interaction	0.5388	F (1, 16) = 0.3944
	EYFP:	Control, R-SDS	3	mouse		genotype	0.6224	F (1, 16) = 0.2522
	mCherry	TLR2/4KD, naïve	5	mouse		defeat	*0.0165	F (1, 16) = 7.174
		TLR2/4KD, R-SDS	4	mouse				

Panel	IHC	Group	N value	Replicate	Statistical test	ANOVA	P value	F value
6F		Control, naïve	7	mouse	Two-way ANOVA	interaction	*0.0357	F (1, 19) = 5.109
	EYFP:	Control, R-SDS	6	mouse		genotype	0.9234	F (1, 19) = 0.009494
	mCherry	TLR2/4KD, naïve	5	mouse		defeat	0.4892	F (1, 19) = 0.4974
		TLR2/4KD, R-SDS	5	mouse				

Panel	IHC	Group	N value	Replicate	Statistical test	ANOVA	P value	F value
6G		Control, naïve	7	mouse	Two-way ANOVA	interaction	0.186	F (1, 19) = 1.883
	CD45:	Control, R-SDS	6	mouse		genotype	0.9289	F (1, 19) = 0.008182
	mCherry	TLR2/4KD, naïve	5	mouse		defeat	0.4306	F (1, 19) = 0.6485
		TLR2/4KD, R-SDS	5	mouse				

Panel	Behavior	Group	N value	Replicate	Statistical test	ANOVA	P value	F value	Multiple comparison test	Comparison	P value	t value	df (between)
6H, Left		Control, naïve	8	mouse	Two-way RM ANOVA	interaction	*0.0148	F (3, 33) = 4.05	Bonferroni	Control, naïve, ICR(+) vs Conrol, R-SDS, ICR(+)	*0.0463	2.749	66
	interaction	Control, R-SDS	13	mouse		group	0.3026	F (3, 33) = 1.264		Control, R-SDS, ICR(-) vs Control, R-SDS, ICR(+)	**0.0045	3.569	33
		TLR2/4KD, naïve	8	mouse		within subject effect (ICR(-), (+))	0.5319	F (1, 33) = 0.3991		Control, R-SDS, ICR(+) vs TLR2/4KD, R-SDS, ICR(+)	*0.0349	2.851	66
		TLR2/4KD, R-SDS	8	mouse		Subjects (matching)	0.1132	F (33, 33) = 1.531					

Panel	Behavior	Group	N value	Replicate	Statistical test	ANOVA	P value	F value	Multiple comparison test	Comparison	P value	t value	df (between)
6H, Right		Control, naïve	8	mouse	Two-way ANOVA	interaction	0.0663	F (1, 36) = 3.588	Bonferroni	Control, naïve vs Control, R-SDS	*0.0468	2.367	36
	interaction	Control, R-SDS	13	mouse		genotype	0.054	F (1, 36) = 3.968		Control, R-SDS vs TLR2/4KD, R-SDS	**0.0082	3.066	36
		TLR2/4KD, naïve	8	mouse		defeat	0.1708	F (1, 36) = 1.953					
		TLR2/4KD, R-SDS	8	mouse									

Panel	Behavior	Group	N value	Replicate	Statistical test	ANOVA	P value	F value	Multiple comparison test	Comparison	P value	t value	df (between)
6I, Left		Control, naïve	8	mouse	Two-way RM ANOVA	interaction	*0.0113	F (3, 33) = 4.316	Bonferroni	Control, naïve, ICR(+) vs Conrol, R-SDS, ICR(+)	*0.0102	3.273	66
	avoidance	Control, R-SDS	13	mouse		group	0.1949	F (3, 33) = 1.659		Control, R-SDS, ICR(-) vs Control, R-SDS, ICR(+)	***0.0001	4.785	33
		TLR2/4KD, naïve	8	mouse		within subject effect (ICR(-), (+))	*0.0204	F (1, 33) = 5.939		Control, R-SDS, ICR(+) vs TLR2/4KD, R-SDS, ICR(+)	**0.0079	3.357	66
		TLR2/4KD, R-SDS	8	mouse		Subjects (matching)	0.3775	F (33, 33) = 1.116					

Panel	Behavior	Group	N value	Replicate	Statistical test	ANOVA	P value	F value	Multiple comparison test	Comparison	P value	t value	df (between)
6I, Right		Control, naïve	8	mouse	Two-way ANOVA	interaction	*0.0327	F (1, 33) = 4.969	Bonferroni	Control, naïve vs Control, R-SDS	*0.0218	2.698	33
	avoidance	Control, R-SDS	13	mouse		genotype	0.073	F (1, 33) = 3.431		Control, R-SDS vs TLR2/4KD, R-SDS	**0.0089	3.053	33
		TLR2/4KD, naïve	8	mouse		defeat	0.1775	F (1, 33) = 1.899					
		TLR2/4KD, R-SDS	8	mouse									

Panel	Behavior	Group	N value	Replicate	Statistical test	ANOVA	P value	F value	Multiple comparison test	Comparison	P value	t value	df (between)
6J, Left		TLR2/4KD, mCherry	10	mouse	Two-way RM ANOVA	interaction	0.2423	F (2, 29) = 1.489	Bonferroni	TLR2/4KD, mCherry, ICR(+) vs TLR2/4KD, TLR4mt8, ICR(+)	#0.0529	2.443	58
	interaction	TLR2/4KD, TLR2mt7	12	mouse		group	0.1474	F (2, 29) = 2.047					
		TLR2/4KD, TLR4mt8	10	mouse		within subject effect (ICR(-), (+))	*0.0418	F (1, 29) = 4.534					
						Subjects (matching)	0.0508	F (29, 29) = 1.855					

Panel	Behavior	Group	N value	Replicate	Statistical test	P value	F value
6J, Right		TLR2/4KD, mCherry	10	mouse	One-way ANOVA	0.1863	F (2, 29) = 1.782
	interaction	TLR2/4KD, TLR2mt7	12	mouse			
		TLR2/4KD, TLR4mt8	10	mouse			

Panel	Behavior	Group	N value	Replicate	Statistical test	ANOVA	P value	F value	Multiple comparison test	Comparison	P value	t value	df (between)
6K, Left		TLR2/4KD, mCherry	10	mouse	Two-way RM ANOVA	Interaction	0.2645	F (2, 29) = 1.393	Bonferroni	TLR2/4KD, mCherry, ICR(+) vs TLR2/4KD, TLR2mt7, ICR(+)	*0.0308	2.653	58
	avoidance	TLR2/4KD, TLR2mt7	12	mouse		group	0.0587	F (2, 29) = 3.132		TLR2/4KD, mCherry, ICR(+) vs TLR2/4KD, TLR4mt8, ICR(+)	*0.0473	2.487	58
		TLR2/4KD, TLR4mt8	10	mouse		within subject effect (ICR(-), (+))	*0.0166	F (1, 29) = 6.46					
						Subjects (matching)	0.4939	F (29, 29) = 1.006					

Panel	Behavior	Group	N value	Replicate	Statistical test	P value	F value
6K, Right		TLR2/4KD, mCherry	10	mouse	One-way ANOVA	0.2732	F (2, 29) = 1.357
	avoidance	TLR2/4KD, TLR2mt7	12	mouse			
		TLR2/4KD, TLR4mt8	10	mouse			

Panel	Behavior	Group	N value	Replicate	Statistical test	ANOVA	P value	F value	Multiple comparison test	Comparison	P value	t value	df (between)
6L		Control, naïve	8	mouse	Two-way ANOVA	interaction	0.8656	F (1, 24) = 0.02927	Bonferroni	Control, naïve vs Control, R-SDS	#0.0879	2.127	24
	elevated plus maze	Control, R-SDS	13	mouse		defeat	*0.0256	F (1, 24) = 5.668					
		TLR2/4KD, naïve	8	mouse		genotype	0.3057	F (1, 24) = 1.095					
		TLR2/4KD, R-SDS	8	mouse									

Panel	IHC	Group	N value	Replicate	Statistical test	P value	t value	df (between)	F test to compare variances
6M		Control, R-SDS(sus)	4	mouse	Two-tailed t-test	*0.0443	2.384	8	p=0.9865
	c-Fos	TLR2/4KD, R-SDS	6	mouse					

Panel	Behavior	Group	N value	Replicate	Statistical test	ANOVA	P value	F value	Multiple comparison test	Comparison	P value	t value	df (between)
7B, Left		WT, naïve	27	mouse	Two-way RM ANOVA	interaction	***<0.0001	F (3, 99) = 10.74	Bonferroni	WT, naïve, ICR(+) vs WT, R-SDS, ICR(+)	***<0.0001	5.399	198
	interaction	WT, R-SDS	24	mouse		group	**0.0021	F (3, 99) = 5.244		WT, R-SDS, ICR(+) vs TLR-DKO, R-SDS, ICR(+)	***<0.0001	4.789	198
		TLR-DKO, naïve	21	mouse		within subject effect (ICR(-), (+))	0.6948	F (1, 99) = 0.1549					
		TLR-DKO, R-SDS	31	mouse		Subjects (matching)	**0.0021	F (99, 99) = 1.787					

Panel	Behavior	Group	N value	Replicate	Statistical test	ANOVA	P value	F value	Multiple comparison test	Comparison	P value	t value	df (between)
7B, Right		WT, naïve	27	mouse	Two-way ANOVA	Interaction	0.0827	F (1, 99) = 3.073	Bonferroni	WT, naïve vs WT, R-SDS(sus)	***<0.0001	4.275	99
	interaction	WT, R-SDS	24	mouse		genotype	***0.0004	F (1, 99) = 13.48		WT, R-SDS(sus) vs TLR-DKO, R-SDS	***0.0003	3.973	99
		TLR-DKO, naïve	21	mouse		defeat	***<0.0001	F (1, 99) = 18.24					
		TLR-DKO, R-SDS	31	mouse									

Panel	Behavior	Group	N value	Replicate	Statistical test	ANOVA	P value	F value	Multiple comparison test	Comparison	P value	t value	df (between)
7C, Left		WT, naïve	27	mouse	Two-way RM ANOVA	interaction	***<0.0001	F (3, 99) = 11.96	Bonferroni	WT, naïve, ICR(+) vs WT, R-SDS, ICR(+)	***<0.0001	5.939	198
	avoidance	WT, R-SDS	24	mouse		group	***<0.0001	F (3, 99) = 8.174		WT, R-SDS, ICR(+) vs TLR-DKO, R-SDS, ICR(+)	***<0.0001	6.26	198
		TLR-DKO, naïve	21	mouse		within subject effect (ICR(-), (+))	*0.022	F (1, 99) = 5.413					
		TLR-DKO, R-SDS	31	mouse		Subjects (matching)	0.1246	F (99, 99) = 1.262					

Panel	Behavior	Group	N value	Replicate	Statistical test	ANOVA	P value	F value	Multiple comparison test	Comparison	P value	t value	df (between)
7C, Right		WT, naïve	27	mouse	Two-way ANOVA	Interaction	*0.0158	F (1, 99) = 6.034	Bonferroni	WT, naïve vs WT, R-SDS(sus)	***<0.0001	4.733	99
	avoidance	WT, R-SDS	24	mouse		genotype	***0.0003	F (1, 99) = 14.33		WT, R-SDS(sus) vs TLR-DKO, R-SDS	***<0.0001	4.571	99
		TLR-DKO, naïve	21	mouse		defeat	***<0.0001	F (1, 99) = 17.74					
		TLR-DKO, R-SDS	31	mouse									

Panel	Gene	Group	N value	Replicate	Statistical test	P value	t value	df (between)	F test to compare variances
7F		NAc, WT, naïve	3	group	Two-tailed t-test	*0.0377	3.06	4	p=0.5068
	Ccl7	NAc, WT, R-SDS (sus)	3	group					

Panel	Gene	Group	N value	Replicate	Statistical test	P value	t value	df (between)	F test to compare variances
7F		mPFC, WT, naïve	3	group	Two-tailed t-test	*0.0369	3.082	4	p=0.5128
	Scg2	mPFC, WT, R-SDS (sus)	3	group					

Panel	Gene	Group	N value	Replicate	Statistical test	P value	t value	df (between)	F test to compare variances
7F		mPFC, WT, naïve	3	group	Two-tailed t-test	*0.0283	3.359	4	p=0.4046
	Il1a	mPFC, WT, R-SDS (sus)	3	group					

Panel	Gene	Group	N value	Replicate	Statistical test	P value	t value	df (between)	F test to compare variances
7F		mPFC, WT, naïve	3	group	Two-tailed t-test	**0.0074	5.01	4	p=0.1965
	Ccl4	mPFC, WT, R-SDS (sus)	3	group					

Panel	Gene	Group	N value	Replicate	Statistical test	P value	t value	df (between)	F test to compare variances
7F		mPFC, WT, naïve	3	group	Two-tailed t-test	*0.0116	4.416	4	p=0.5542
	Ccl3	mPFC, WT, R-SDS (sus)	3	group					

Panel	Gene	Group	N value	Replicate	Statistical test	P value	t value	df (between)	F test to compare variances
7F		mPFC, WT, naïve	3	group	Two-tailed t-test	*0.0319	3.234	4	p=0.3931
	Tnf	mPFC, WT, R-SDS (sus)	3	group					

Panel	Gene	Group	N value	Replicate	Statistical test	P value	t value	df (between)	F test to compare variances
7F	Tslp	mPFC, WT, naïve mPFC, WT, R-SDS (sus)	3 3	group group	Two-tailed t-test	*0.0448	2.884	4	p=0.3535
7F	Pglyrp1	mPFC, WT, naïve mPFC, WT, R-SDS (sus)	3 3	group group	Two-tailed t-test	*0.0315	3.244	4	p=0.0558
7F	Edn1	NAc, WT, naïve NAc, WT, R-SDS (sus)	3 3	group group	Two-tailed t-test	*0.0286	3.35	4	p=0.2849
7F	Il1b	NAc, WT, naïve NAc, WT, R-SDS (sus)	3 3	group group	Two-tailed t-test	*0.0203	3.731	4	p=0.69
7F	Inhbc	NAc, WT, naïve NAc, WT, R-SDS (sus)	3 3	group group	Two-tailed t-test	*0.012	4.368	4	p=0.3968
7F	Ccl27a	NAc, WT, naïve NAc, WT, R-SDS (sus)	3 3	group group	Two-tailed t-test	*0.0306	3.276	4	p=0.4167
7F	Gm13271	mPFC, WT, naïve mPFC, WT, R-SDS (sus)	3 3	group group	Two-tailed t-test	*0.0494	2.788	4	p=0.7758
7F	Gm13272	NAc, WT, naïve NAc, WT, R-SDS (sus)	3 3	group group	Two-tailed t-test	*0.0211	3.684	4	p=0.9489
7F	Ccl1	NAc, WT, naïve NAc, WT, R-SDS (sus)	3 3	group group	Two-tailed t-test	*0.0257	3.465	4	p=0.073
7F	Ifna16	mPFC, WT, naïve mPFC, WT, R-SDS (sus)	3 3	group group	Two-tailed t-test	*0.0212	3.679	4	p=0.7932
7F	Ccl20	NAc, WT, naïve NAc, WT, R-SDS (sus)	3 3	group group	Two-tailed t-test	*0.0356	3.117	4	p=0.8734
7F	Gm13271	NAc, WT, naïve NAc, WT, R-SDS (sus)	3 3	group group	Two-tailed t-test	*0.0118	4.389	4	p=0.4124
7F	Ifnb1	NAc, WT, naïve NAc, WT, R-SDS (sus)	3 3	group group	Two-tailed t-test	*0.0497	2.782	4	p=0.6924
7F	Lefty1	mPFC, WT, naïve mPFC, WT, R-SDS (sus)	3 3	group group	Two-tailed t-test	*0.0315	3.245	4	p=0.3135
7F	Cmtm4	mPFC, WT, naïve mPFC, WT, R-SDS (sus)	3 3	group group	Two-tailed t-test	**0.0064	5.227	4	p=0.4434
7H	Il1a	mPFC, WT, naïve mPFC, WT, R-SDS (sus)	3 3	group group	Two-tailed t-test	*0.0283	3.359	4	p=0.4046
7H	Il1a	NAc, WT, naïve NAc, WT, R-SDS (sus)	3 3	group group	Two-tailed t-test	0.1263	1.927	4	p=0.5531
7I	TNFa	mPFC, WT, naïve mPFC, WT, R-SDS (sus)	3 3	group group	Two-tailed t-test	*0.0319	3.234	4	p=0.3931
7I	TNFa	NAc, WT, naïve NAc, WT, R-SDS (sus)	3 3	group group	Two-tailed t-test	0.4000	0.9409	4	p=0.3969
7J	Il1b	mPFC, WT, naïve mPFC, WT, R-SDS (sus)	3 3	group group	Two-tailed t-test	0.1848	1.6	4	p=0.3402
7J	Ilb	NAc, WT, naïve NAc, WT, R-SDS (sus)	3 3	group group	Two-tailed t-test	*0.0203	3.731	4	p=0.69

Panel	Gene	Group	N value	Replicate	Statistical test	P value	t value	df (between)	F test to compare variances
7K	Il6	mPFC, WT, naïve	3	group	Two-tailed t-test	0.1692	1.675	4	p=0.7303
		mPFC, WT, R-SDS (sus)	3	group					

Panel	Gene	Group	N value	Replicate	Statistical test	P value	t value	df (between)	F test to compare variances
7K	Il6	NAc, WT, naïve	3	group	Two-tailed t-test	0.0606	2.592	4	p=0.5584
		NAc, WT, R-SDS (sus)	3	group					

Panel	Behavior	Group	N value	Replicate	Statistical test	ANOVA	P value	F value	Multiple comparison test	Comparison	P value	t value	df (between)
8B, Left	interaction	isotype, naïve	11	mouse	Two-way RM ANOVA	interaction	**0.0074	F (3, 40) = 4.602	Bonferroni	isotype, naïve, ICR(+) vs isotype, R-SDS, ICR(+)	***<0.0001	4.692	80
		isotype, R-SDS	11	mouse		group	**0.004	F (3, 40) = 5.182		isotype, R-SDS, ICR(-) vs isotype, R-SDS, ICR(+)	***0.0007	4.142	40
		anti-IL-1a+anti-TNFa, naïve	11	mouse		within subject effect (ICR(-), (+))	**0.0095	F (1, 40) = 7.417		isotype, R-SDS, ICR(+) vs anti-IL-1a+anti-TNFa, R-SDS, ICR(+)	*0.029	2.899	80
		anti-IL-1a+anti-TNFa, R-SDS	11	mouse		Subjects (matching)	0.5065	F (40, 40) = 0.9948					

Panel	Behavior	Group	N value	Replicate	Statistical test	ANOVA	P value	F value	Multiple comparison test	Comparison	P value	t value	df (between)
8B, Right	interaction	isotype, naïve	11	mouse	Two-way ANOVA	interaction	0.0926	F (1, 40) = 2.97	Bonferroni	isotype, naïve vs isotype, R-SDS	**0.0023	3.507	40
		isotype, R-SDS	11	mouse		antibody	0.5508	F (1, 40) = 0.3619		anti-IL-1a+anti-TNFa, naïve vs anti-IL-1a+anti-TNFa, R-SDS	0.5822	1.07	40
		anti-IL-1a+anti-TNFa, naïve	11	mouse		defeat	**0.0024	F (1, 40) = 10.47					
		anti-IL-1a+anti-TNFa, R-SDS	11	mouse									

Panel	Behavior	Group	N value	Replicate	Statistical test	ANOVA	P value	F value	Multiple comparison test	Comparison	P value	t value	df (between)
8C, Left	avoidance	isotype, naïve	11	mouse	Two-way RM ANOVA	interaction	**0.0059	F (3, 40) = 4.81	Bonferroni	isotype, naïve, ICR(+) vs isotype, R-SDS, ICR(+)	**0.0013	3.884	80
		isotype, R-SDS	11	mouse		group	0.1007	F (3, 40) = 2.22		isotype, R-SDS, ICR(-) vs isotype, R-SDS, ICR(+)	***0.0006	4.204	40
		anti-IL-1a+anti-TNFa, naïve	11	mouse		within subject effect (ICR(-), (+))	***0.0007	F (1, 40) = 13.45					
		anti-IL-1a+anti-TNFa, R-SDS	11	mouse		Subjects (matching)	0.3065	F (40, 40) = 1.175					

Panel	Behavior	Group	N value	Replicate	Statistical test	ANOVA	P value	F value	Multiple comparison test	Comparison	P value	t value	df (between)
8C, Right	avoidance	isotype, naïve	11	mouse	Two-way ANOVA	interaction	0.2384	F (1, 40) = 1.432	Bonferroni	isotype, naïve vs isotype, R-SDS	**0.0031	3.395	40
		isotype, R-SDS	11	mouse		antibody	0.952	F (1, 40) = 0.003668		anti-IL-1a+anti-TNFa, naïve vs anti-IL-1a+anti-TNFa, R-SDS	0.1928	1.703	40
		anti-IL-1a+anti-TNFa, naïve	11	mouse		defeat	***0.0009	F (1, 40) = 12.99					
		anti-IL-1a+anti-TNFa, R-SDS	11	mouse									

Panel	Behavior	Group	N value	Replicate	Statistical test	ANOVA	P value	F value	Multiple comparison test	Comparison	P value	t value	df (between)
8D, Left	interaction	isotype, R-SDS	11	mouse	Two-way RM ANOVA	interaction	0.2188	F (3, 40) = 1.541	Bonferroni	isotype, R-SDS, ICR(-) vs isotype, R-SDS, ICR(+)	***0.0005	4.218	40
		anti-IL-1a, R-SDS	12	mouse		group	**0.0038	F (3, 40) = 5.239		isotype, R-SDS, ICR(+) vs anti-IL-1a, R-SDS, ICR(+)	*0.0112	3.217	80
		anti-TNFa, R-SDS	11	mouse		within subject effect (ICR(-), (+))	***<0.0001	F (1, 40) = 23.31		isotype, R-SDS, ICR(+) vs anti-TNFa, R-SDS, ICR(+)	*0.0128	3.173	80
		anti-IL-1a+anti-TNFa, R-SDS	10	mouse		Subjects (matching)	0.2232	F (40, 40) = 1.275		isotype, R-SDS, ICR(+) vs anti-IL-1a+anti-TNFa, R-SDS, ICR(+)	***0.0008	4.009	80

Panel	Behavior	Group	N value	Replicate	Statistical test	P value	F value
8D, Right	interaction	isotype, R-SDS	11	mouse	One-way ANOVA	0.2188	F (3, 40) = 1.541
		anti-IL-1a, R-SDS	12	mouse			
		anti-TNFa, R-SDS	11	mouse			
		anti-IL-1a+anti-TNFa, R-SDS	10	mouse			

Panel	Behavior	Group	N value	Replicate	Statistical test	ANOVA	P value	F value	Multiple comparison test	Comparison	P value	t value	df (between)
8E, Left	avoidance	isotype, R-SDS	11	mouse	Two-way RM ANOVA	interaction	0.6827	F (3, 40) = 0.5026	Bonferroni	isotype, R-SDS, ICR(-) vs isotype, R-SDS, ICR(+)	**0.0042	3.533	40
		anti-IL-1a, R-SDS	12	mouse		group	0.3784	F (3, 40) = 1.056					
		anti-TNFa, R-SDS	11	mouse		within subject effect (ICR(-), (+))	***<0.0001	F (1, 40) = 25.82					
		anti-IL-1a+anti-TNFa, R-SDS	10	mouse		Subjects (matching)	0.2885	F (40, 40) = 1.194					

Panel	Behavior	Group	N value	Replicate	Statistical test	P value	F value
8E, Right	avoidance	isotype, R-SDS	11	mouse	One-way ANOVA	0.6827	F (3, 40) = 0.5026
		anti-IL-1a, R-SDS	12	mouse			
		anti-TNFa, R-SDS	11	mouse			
		anti-IL-1a+anti-TNFa, R-SDS	10	mouse			

Panel	Gene	Group	N value	Replicate	Statistical test	P value	t value	df (between)	F test to compare variances
S1A	S100a8	WT, naïve	5	mouse	Two-tailed t-test	***0.0002	6.172	9	p=0.1160
		WT, R-SDS (sus)	8	mouse					
Panel	Gene	Group	N value	Replicate	Statistical test	P value	t value	df (between)	F test to compare variances
S1A	S100a8	WT, naïve	5	mouse	Two-tailed t-test	**0.0011	5.879	6	p=0.4506
		WT, R-SDS (res)	3	mouse					
Panel	Gene	Group	N value	Replicate	Statistical test	P value	t value	df (between)	F test to compare variances
S1A	S100a9	WT, naïve	5	mouse	Two-tailed t-test	**0.0011	4.71	9	p=0.7523
		WT, R-SDS (sus)	8	mouse					
Panel	Gene	Group	N value	Replicate	Statistical test	P value	t value	df (between)	F test to compare variances
S1A	S100a9	WT, naïve	5	mouse	Two-tailed t-test	*0.0184	3.209	6	p=0.9342
		WT, R-SDS (res)	3	mouse					
Panel	Gene	Group	N value	Replicate	Statistical test	P value	t value	df (between)	F test to compare variances
S1A	Lcn2	WT, naïve	5	mouse	Two-tailed t-test	***<0.0001	8.94	9	p=0.0803
		WT, R-SDS (sus)	8	mouse					
Panel	Gene	Group	N value	Replicate	Statistical test	P value	t value	df (between)	F test to compare variances
S1A	Scgb3a1	WT, naïve	5	mouse	Two-tailed t-test with Welch's correction	**0.0023	5.014	6.15	p=0.0437
		WT, R-SDS (sus)	8	mouse					
Panel	Gene	Group	N value	Replicate	Statistical test	P value	t value	df (between)	F test to compare variances
S1A	Scgb3a1	WT, naïve	5	mouse	Two-tailed t-test	**0.0056	4.215	6	p=0.394
		WT, R-SDS (res)	3	mouse					
Panel	Gene	Group	N value	Replicate	Statistical test	P value	t value	df (between)	F test to compare variances
S1A	Lrg1	WT, naïve	5	mouse	Two-tailed t-test	***0.0002	5.959	9	p=0.4112
		WT, R-SDS (sus)	8	mouse					
Panel	Gene	Group	N value	Replicate	Statistical test	P value	t value	df (between)	F test to compare variances
S1A	Lrg1	WT, naïve	5	mouse	Two-tailed t-test	*0.0116	3.582	6	p=0.1639
		WT, R-SDS (res)	3	mouse					
Panel	Gene	Group	N value	Replicate	Statistical test	P value	t value	df (between)	F test to compare variances
S1A	Tmem52	WT, naïve	5	mouse	Two-tailed t-test	***<0.0001	6.85	9	p=0.8134
		WT, R-SDS (sus)	8	mouse					
Panel	Gene	Group	N value	Replicate	Statistical test	P value	t value	df (between)	F test to compare variances
S1A	Tmem52	WT, naïve	5	mouse	Two-tailed t-test	*0.0148	3.384	6	p=0.5351
		WT, R-SDS (res)	3	mouse					
Panel	Gene	Group	N value	Replicate	Statistical test	P value	t value	df (between)	F test to compare variances
S1A	Hbb-b1	WT, naïve	5	mouse	Two-tailed t-test	*0.0163	2.947	9	p=0.5361
		WT, R-SDS (sus)	8	mouse					
Panel	Gene	Group	N value	Replicate	Statistical test	P value	t value	df (between)	F test to compare variances
S1A	Slc44a5	WT, naïve	5	mouse	Two-tailed t-test	**0.0024	4.16	9	p=0.7418
		WT, R-SDS (sus)	8	mouse					
Panel	Gene	Group	N value	Replicate	Statistical test	P value	t value	df (between)	F test to compare variances
S1A	Slc44a5	WT, naïve	5	mouse	Two-tailed t-test	*0.0151	3.365	6	p=0.5467
		WT, R-SDS (res)	3	mouse					
Panel	Gene	Group	N value	Replicate	Statistical test	P value	t value	df (between)	F test to compare variances
S1A	8430408G22Rik	WT, naïve	5	mouse	Two-tailed t-test	*0.0118	3.147	9	p=0.6587
		WT, R-SDS (sus)	8	mouse					
Panel	Gene	Group	N value	Replicate	Statistical test	P value	t value	df (between)	F test to compare variances
S1A	Serpina3g	WT, naïve	5	mouse	Two-tailed t-test	**0.0012	4.638	9	p=0.3658
		WT, R-SDS (sus)	8	mouse					
Panel	Gene	Group	N value	Replicate	Statistical test	P value	t value	df (between)	F test to compare variances
S1A	Serpina3g	WT, naïve	5	mouse	Two-tailed t-test	*0.0198	3.151	6	p=0.3371
		WT, R-SDS (res)	3	mouse					
Panel	Gene	Group	N value	Replicate	Statistical test	P value	t value	df (between)	F test to compare variances
S1A	Lao1	WT, naïve	5	mouse	Two-tailed t-test	***0.0004	5.422	9	p=0.7523
		WT, R-SDS (sus)	8	mouse					
Panel	Gene	Group	N value	Replicate	Statistical test	P value	t value	df (between)	F test to compare variances
S1A	Lao1	WT, naïve	5	mouse	Two-tailed t-test	**0.0029	4.818	6	p=0.7507
		WT, R-SDS (res)	3	mouse					

Panel	Gene	Group	N value	Replicate	Statistical test	P value	t value	df (between)	F test to compare variances
S1A	Beta-s	WT, naïve WT, R-SDS (sus)	5 8	mouse mouse	Two-tailed t-test	*0.0289	2.597	9	p=0.416
Panel	Gene	Group	N value	Replicate	Statistical test	P value	t value	df (between)	F test to compare variances
S1A	Clec4d	WT, naïve WT, R-SDS (sus)	5 8	mouse mouse	Two-tailed t-test	**0.004	3.827	9	p=0.7575
Panel	Gene	Group	N value	Replicate	Statistical test	P value	t value	df (between)	F test to compare variances
S1A	Hba-a2	WT, naïve WT, R-SDS (sus)	5 8	mouse mouse	Two-tailed t-test	*0.0324	2.527	9	p=0.4174
Panel	Gene	Group	N value	Replicate	Statistical test	P value	t value	df (between)	F test to compare variances
S1A	Olfr1218	WT, naïve WT, R-SDS (sus)	5 8	mouse mouse	Two-tailed t-test	**0.0099	3.253	9	p=0.4817
Panel	Gene	Group	N value	Replicate	Statistical test	P value	t value	df (between)	F test to compare variances
S1A	Retnlg	WT, naïve WT, R-SDS (sus)	5 8	mouse mouse	Two-tailed t-test	**0.0065	3.525	9	p=0.422
Panel	Gene	Group	N value	Replicate	Statistical test	P value	t value	df (between)	F test to compare variances
S1A	Retnlg	WT, naïve WT, R-SDS (res)	5 3	mouse mouse	Two-tailed t-test	*0.0139	3.434	6	p>0.9999
Panel	Gene	Group	N value	Replicate	Statistical test	P value	t value	df (between)	F test to compare variances
S1A	Fmo2	WT, naïve WT, R-SDS (sus)	5 8	mouse mouse	Two-tailed t-test	***0.0008	4.984	9	p=0.6112
Panel	Gene	Group	N value	Replicate	Statistical test	P value	t value	df (between)	F test to compare variances
S1A	Fmo2	WT, naïve WT, R-SDS (res)	5 3	mouse mouse	Two-tailed t-test	*0.0224	3.055	6	p=0.1941
Panel	Gene	Group	N value	Replicate	Statistical test	P value	t value	df (between)	F test to compare variances
S1A	Lao1	WT, naïve WT, R-SDS (sus)	5 8	mouse mouse	Two-tailed t-test	***0.0003	5.615	9	p=0.5915
Panel	Gene	Group	N value	Replicate	Statistical test	P value	t value	df (between)	F test to compare variances
S1A	Lao1	WT, naïve WT, R-SDS (res)	5 3	mouse mouse	Two-tailed t-test	**0.0072	3.995	6	p=0.2931
Panel	Gene	Group	N value	Replicate	Statistical test	P value	t value	df (between)	F test to compare variances
S1A	Ch25h	WT, naïve WT, R-SDS (sus)	5 8	mouse mouse	Two-tailed t-test	*0.0463	2.309	9	p=0.726
Panel	Gene	Group	N value	Replicate	Statistical test	P value	t value	df (between)	F test to compare variances
S1A	Gm10683	WT, naïve WT, R-SDS (sus)	5 8	mouse mouse	Two-tailed t-test	***0.0008	4.921	9	p=0.0756
Panel	Gene	Group	N value	Replicate	Statistical test	P value	t value	df (between)	F test to compare variances
S1A	Gm10683	WT, naïve WT, R-SDS (res)	5 3	mouse mouse	Two-tailed t-test	*0.0133	3.468	6	p=0.1848

Panel	Gene	Group	N value	Replicate	Statistical test	P value	F value	Multiple comparison test	Comparison	P value	t value	df (between)
S1B	S100a8	WT, naïve WT, R-SDS (sus) WT, R-SDS (res)	5 6 3	mouse mouse mouse	One-way ANOVA	***0.0002	F (2, 11) = 21.01	Bonferroni	WT, naïve vs WT, R-SDS(sus) WT, naïve vs WT, R-SDS(res)	***0.0002 **0.0089	6.402 3.798	11 11
Panel	Gene	Group	N value	Replicate	Statistical test	P value	F value	Multiple comparison test	Comparison	P value	t value	df (between)
S1C	S100a9	WT, naïve WT, R-SDS (sus) WT, R-SDS (res)	5 6 3	mouse mouse mouse	One-way ANOVA	**0.0016	F (2, 11) = 12.23	Bonferroni	WT, naïve vs WT, R-SDS(sus) WT, naïve vs WT, R-SDS(res)	**0.0014 *0.0463	4.892 2.863	11 11

Panel	Behavior	Group	N value	Replicate	Statistical test	ANOVA	P value	F value	Multiple comparison test	Comparison	P value	t value	df (between)
S1D, Left	interaction	WT, naïve WT, R-SDS	5 9	mouse mouse	Two-way RM ANOVA	Interaction defeat within subject effect (ICR(-), (+)) Subjects (matching)	0.0533 0.1073 0.5009 0.3122	F (1, 12) = 4.592 F (1, 12) = 3.03 F (1, 12) = 0.4816 F (12, 12) = 1.335	Bonferroni	WT, naïve, ICR(+) vs WT, R-SDS, ICR(+)	*0.024	0.0861	24
Panel	Behavior	Group	N value	Replicate	Statistical test	P value	t value	df (between)	F test to compare variances				
S1D, Right	interaction	WT, naïve WT, R-SDS	5 9	mouse mouse	Two-tailed t-test with Welch's correction	*0.019	2.795	10	p=0.0259				
Panel	Behavior	Group	N value	Replicate	Statistical test	ANOVA	P value	F value	Multiple comparison test	Comparison	P value	t value	df (between)
S1E, Left	avoidance	WT, naïve WT, R-SDS	5 9	mouse mouse	Two-way RM ANOVA	Interaction defeat within subject effect (ICR(-), (+)) Subjects (matching)	*0.0435 *0.0441 0.1485 0.214	F (1, 12) = 5.094 F (1, 12) = 5.056 F (1, 12) = 2.384 F (12, 12) = 1.599	Bonferroni	WT, naïve, ICR(+) vs WT, R-SDS, ICR(+)	**0.0084	3.164	24
Panel	Behavior	Group	N value	Replicate	Statistical test	P value	t value	df (between)	F test to compare variances				
S1E, Right	avoidance	WT, naïve WT, R-SDS	5 9	mouse mouse	Two-tailed t-test with Welch's correction	*0.0147	3.046	8.546	p=0.0018				

Panel	Gene	Group	N value	Replicate	Statistical test	P value	t value	df (between)
S1F	CD11b	EGFP(-)	6	mouse	Two-tailed t-test	***<0.0001	20.47	10
		EGFP(+)	6	mouse				

Panel	Gene	Group	N value	Replicate	Statistical test	ANOVA	P value	F value	Multiple comparison test	Comparison	P value	t value	df (between)
S1G	TLR2	EGFP(-), naïve	4	mouse	Two-way ANOVA	Interaction	0.1101	F (1, 12) = 2.977	Bonferroni	EGFP(-), naïve vs EGFP(+), naïve	**0.0022	4.258	12
		EGFP(-), R-SDS	4	mouse		genotype	***<0.0001	F (1, 12) = 60.01		EGFP(-), R-SDS vs EGFP(+), R-SDS	***<0.0001	6.698	12
		EGFP(+), naïve	4	mouse		defear	0.4632	F (1, 12) = 0.5742					
		EGFP(+), R-SDS	4	mouse									

Panel	Gene	Group	N value	Replicate	Statistical test	ANOVA	P value	F value	Multiple comparison test	Comparison	P value	t value	df (between)
S1H	TLR4	EGFP(-), naïve	4	mouse	Two-way ANOVA	Interaction	0.7131	F (1, 12) = 0.1418	Bonferroni	EGFP(-), naïve vs EGFP(+), naïve	*0.0427	2.646	12
		EGFP(-), R-SDS	4	mouse		genotype	**0.0014	F (1, 12) = 16.96		EGFP(-), R-SDS vs EGFP(+), R-SDS	*0.0159	3.178	12
		EGFP(+), naïve	4	mouse		defeat	0.5552	F (1, 12) = 0.3684					
		EGFP(+), R-SDS	4	mouse									

Panel	Gene	Group	N value	Replicate	Statistical test	ANOVA	P value	F value	Multiple comparison test	Comparison	P value	t value	df (between)
S1I	IL1RI	EGFP(-), naïve	5	mouse	Two-way ANOVA	Interaction	*0.0499	F (1, 14) = 4.603	Bonferroni	EGFP(-), naïve vs EGFP(+), naïve	0.821	0.8484	14
		EGFP(-), R-SDS	4	mouse		genotype	**0.0048	F (1, 14) = 11.19		EGFP(-), R-SDS vs EGFP(+), R-SDS	0.0033	3.883	14
		EGFP(+), naïve	4	mouse		defeat	*0.0477	F (1, 14) = 4.71					
		EGFP(+), R-SDS	5	mouse									

Panel	Behavior	Group	N value	Replicate	Statistical test	ANOVA	P value	F value	Multiple comparison test	Comparison	P value	t value	df (between)
S1J	interaction	WT	8	mouse	Two-way RM ANOVA	Interaction	0.5215	F (2, 21) = 0.6716	Bonferroni	WT, day0 vs WT, day10	*0.0276	2.869	21
		TLR2KO	8	mouse		defeat	***0.0005	F (1, 21) = 16.99		TLR4KO, day0 vs TLR4KO, day10	*0.0296	2.837	21
		TLR4KO	8	mouse		genotype	0.6169	F (2, 21) = 0.4944					
						Subjects (matching)	0.0748	F (21, 21) = 1.9					

Panel	Behavior	Group	N value	Replicate	Statistical test	ANOVA	P value	F value	Multiple comparison test	Comparison	P value	t value	df (between)
S1K	avoidance	WT	8	mouse	Two-way RM ANOVA	Interaction	0.6455	F (2, 21) = 0.447	Bonferroni	WT, day0 vs WT, day10	*0.0292	2.843	21
		TLR2KO	8	mouse		genotype	0.8113	F (2, 21) = 0.2113		TLR4KO, day0 vs TLR4KO, day10	*0.0311	2.815	21
		TLR4KO	8	mouse		defeat	***0.0004	F (1, 21) = 17.9					
						Subjects (matching)	0.2306	F (21, 21) = 1.386					

Panel	Behavior	Group	N value	Replicate	Statistical test	ANOVA	P value	F value	Multiple comparison test	Comparison	P value	t value	df (between)
S1L, Left	interaction	IL-1RIKO, naïve	11	mouse	Two-way RM ANOVA	Interaction	*0.0127	F (1, 21) = 7.414	Bonferroni	IL-1RIKO, naïve, ICR(+) vs IL-1RIKO, R-SDS, ICR(+)	*0.0175	2.75	42
		IL-1RIKO, R-SDS	12	mouse		defeat	0.1503	F (1, 21) = 2.229					
						within subject effect (ICR(-), (+))	0.8101	F (1, 21) = 0.05923					
						Subjects (matching)	*0.0336	F (21, 21) = 2.269					

Panel	Behavior	Group	N value	Replicate	Statistical test	P value	t value	df (between)	F test to compare variances
S1L, Right	interaction	IL-1RIKO, naïve	11	mouse	Two-tailed t-test with Welch's correction	*0.0135	2.818	14.27	p=0.0044
		IL-1RIKO, R-SDS	12	mouse					

Panel	Behavior	Group	N value	Replicate	Statistical test	ANOVA	P value	F value	Multiple comparison test	Comparison	P value	t value	df (between)
S1M, Left	avoidance	IL-1RIKO, naïve	11	mouse	Two-way RM ANOVA	Interaction	*0.0221	F (1, 21) = 6.111	Bonferroni	IL-1RIKO, naïve, ICR(+) vs IL-1RIKO, R-SDS, ICR(+)	*0.0191	2.715	42
		IL-1RIKO, R-SDS	12	mouse		defeat	0.1345	F (1, 21) = 2.424		IL-1RIKO, R-SDS, ICR(-) vs IL-1RIKO, R-SDS, ICR(+)	*0.0295	2.657	21
						within subject effect (ICR(-), (+))	0.2424	F (1, 21) = 1.447					
						Subjects (matching)	0.0789	F (21, 21) = 1.875					

Panel	Behavior	Group	N value	Replicate	Statistical test	P value	t value	df (between)	F test to compare variances
S1M, Right	avoidance	IL-1RIKO, naïve	11	mouse	Two-tailed t-test with Welch's correction	*0.0237	2.572	12.6	p=0.0002
		IL-1RIKO, R-SDS	12	mouse					

Panel	Behavior	Group	N value	Replicate	Statistical test	P value	t value	df (between)	F test to compare variances
S1N	elevated plus maze	IL-1RIKO, naïve	11	mouse	Two-tailed t-test with Welch's correction	0.9613	0.04939	14.62	p=0.0381
		IL-1RIKO, R-SDS	12	mouse					

Panel	IHC	Group	N value	Replicate	Statistical test	P value	F value
S2B	mPFC, CD68	TLR2KO. naïve	5	mouse	One-way ANOVA	0.0818	F (4, 14) = 2.597
		TLR2KO, R-SDS (sus)	5	mouse			
		TLR2KO, R-SDS (res)	3	mouse			
		TLR-DKO. naïve	3	mouse			
		TLR-DKO, R-SDS	3	mouse			

Panel	IHC	Group	N value	Replicate	Statistical test	P value	F value
S2C	mPFC, Iba-1	TLR2KO. naïve	5	mouse	One-way ANOVA	0.1567	F (4, 14) = 1.957
		TLR2KO, R-SDS (sus)	5	mouse			
		TLR2KO, R-SDS (res)	3	mouse			
		TLR-DKO. naïve	3	mouse			
		TLR-DKO, R-SDS	3	mouse			

Panel	IHC	Group	N value	Replicate	Statistical test	P value	F value	Multiple comparison test	Comparison	P value	t value	df (between)
S2E	mPFC, CD68	TLR4KO. naïve	8	mouse	One-way ANOVA	***0.0005	F (4, 19) = 8.21	Bonferroni	TLR4KO, naive vs TLR4KO, R-SDS(sus)	**0.0044	4.238	19
		TLR4KO, R-SDS (sus)	3	mouse					TLR4KO, R-SDS(sus) vs TLR4KO, R-SDS(res)	***0.0003	5.457	19
		TLR4KO, R-SDS (res)	4	mouse								
		TLR-DKO. naïve	5	mouse								
		TLR-DKO, R-SDS	5	mouse								

Panel	IHC	Group	N value	Replicate	Statistical test	P value	F value
S2F	mPFC, Iba-1	TLR4KO. naïve	8	mouse	One-way ANOVA	0.1274	F (4, 20) = 2.039
		TLR4KO, R-SDS (sus)	3	mouse			
		TLR4KO, R-SDS (res)	4	mouse			
		TLR-DKO. naïve	5	mouse			
		TLR-DKO, R-SDS	5	mouse			

Panel	IHC	Group	N value	Replicate	Statistical test	ANOVA	P value	F value
S2H	mPFC, CD68	isotype, naïve	4	mouse	Two-way ANOVA	Interaction	0.486	F (2, 24) = 0.7438
		isotype, 1.5h	5	mouse		antibody	0.0966	F (1, 24) = 2.991
		isotype, 4h	6	mouse		time	0.1827	F (2, 24) = 1.826
		anti-IL-1a anti-TNFa, naïve	4	mouse				
		anti-IL-1a anti-TNFa, 1.5h	5	mouse				
		anti-IL-1a anti-TNFa, 4h	6	mouse				

Panel	IHC	Group	N value	Replicate	Statistical test	ANOVA	P value	F value
S2J	NAc, CD68	isotype, naïve	4	mouse	Two-way ANOVA	Interaction	0.2898	F (2, 24) = 1.305
		isotype, 1.5h	5	mouse		antibody	0.4742	F (1, 24) = 0.5287
		isotype, 4h	6	mouse		time	0.7175	F (2, 24) = 0.3366
		anti-IL-1a anti-TNFa, naïve	4	mouse				
		anti-IL-1a anti-TNFa, 1.5h	5	mouse				
		anti-IL-1a anti-TNFa, 4h	6	mouse				

Panel	IHC	Group	N value	Replicate	Statistical test	ANOVA	P value	F value
S3C	NAc, CD68	WT. naïve	8	mouse	Two-way ANOVA	Interaction	0.5158	F (4, 42) = 0.8266
		WT, S-SDS, 1.5h	7	mouse		genotype	0.3388	F (1, 42) = 0.9363
		WT, S-SDS, 4h	3	mouse		time	0.2851	F (4, 42) = 1.301
		WT, R-SDS (sus), 1.5h	6	mouse				
		WT, R-SDS (sus), 4h	3	mouse				
		TLR-DKO. naïve	7	mouse				
		TLR-DKO, S-SDS, 1.5h	6	mouse				
		TLR-DKO, S-SDS, 4h	3	mouse				
		TLR-DKO, R-SDS, 1.5h	5	mouse				
		TLR-DKO, R-SDS, 4h	4	mouse				

Panel	IHC	Group	N value	Replicate	Statistical test	ANOVA	P value	F value
S3E	NAc, Iba-1	WT. naïve	11	mouse	Two-way ANOVA	Interaction	0.7466	F (4, 55) = 0.485
		WT, S-SDS, 1.5h	8	mouse		genotype	0.8164	F (1, 55) = 0.05442
		WT, S-SDS, 4h	3	mouse		time	**0.0029	F (4, 55) = 4.592
		WT, R-SDS (sus), 1.5h	7	mouse				
		WT, R-SDS (sus), 4h	3	mouse				
		TLR-DKO. naïve	11	mouse				
		TLR-DKO, S-SDS, 1.5h	7	mouse				
		TLR-DKO, S-SDS, 4h	3	mouse				
		TLR-DKO, R-SDS, 1.5h	8	mouse				
		TLR-DKO, R-SDS, 4h	4	mouse				

Panel	IHC	Group	N value	Replicate	Statistical test	P value	F value
S3F	NAc, CD68	WT, naïve	5	mouse	One-way ANOVA	0.7017	F (4, 22) = 0.549
		WT, 1.5h	5	mouse			
		WT, 4h	6	mouse			
		TLR-DKO, 1.5h	5	mouse			
		TLR-DKO, 4h	6	mouse			

Panel	IHC	Group	N value	Replicate	Statistical test	P value	F value
S3G	NAc, Iba-1	WT, naïve	5	mouse	One-way ANOVA	0.4471	F (4, 22) = 0.9635
		WT, 1.5h	5	mouse			
		WT, 4h	6	mouse			
		TLR-DKO, 1.5h	5	mouse			
		TLR-DKO, 4h	6	mouse			

Panel	IHC	Group	N value	Replicate	Statistical test	P value	F value	Multiple comparison test	Comparison	P value	t value	df (between)
S4C	mPFC, c-Fos	TLR2KO. naïve	7	mouse	One-way ANOVA	***0.0003	F (4, 23) = 8.252	Bonferroni	TLR2KO, naive vs TLR2KO, R-SDS(res)	*0.0129	3.665	23
		TLR2KO, R-SDS (sus)	6	mouse					TLR-DKO, naive vs TLR-DKO, R-SDS	**0.0027	4.302	23
		TLR2KO, R-SDS (res)	4	mouse								
		TLR-DKO. naïve	5	mouse								
		TLR-DKO, R-SDS	6	mouse								

Panel	IHC	Group	N value	Replicate	Statistical test	P value	F value	Multiple comparison test	Comparison	P value	t value	df (between)
S4D	mPFC, c-Fos	TLR4KO. naïve	9	mouse	One-way ANOVA	***<0.0001	F (4, 22) = 15.12	Bonferroni	TLR4KO, naive vs TLR4KO, R-SDS(res)	***<0.0001	7.222	22
		TLR4KO, R-SDS (sus)	3	mouse					TLR-DKO, naive vs TLR-DKO, R-SDS	#0.0931	2.85	22
		TLR4KO, R-SDS (res)	4	mouse					TLR4KO, R-SDS(sus) vs TLR4KO, R-SDS(res)	**0.0035	4.222	22
		TLR-DKO. naïve	5	mouse								
		TLR-DKO, R-SDS	6	mouse								

Panel	IHC	Group	N value	Replicate	Statistical test	P value	F value
S5C	CFSE	WT microglia, TLR-DKO, naïve	3	mouse	One-way ANOVA	0.7629	0.2781
		WT microglia, TLR-DKO, 10x defeat	5	mouse			
		TLR-DKO microglia, TLR-DKO, 10x defeat	5	mouse			

Panel	Behavior	Group	N value	Replicate	Statistical test	ANOVA	P value	F value	Multiple comparison test	Comparison	P value	t value	df (between)
S5D, Left	interaction	WT, naïve	6	mouse	Two-way RM ANOVA	Interaction	**0.0037	F (1, 15) = 11.81	Bonferroni	(-), WT, naïve, ICR(+) vs (-), WT, 4x defeat, ICR(+)	***0.0003	4.29	30
		WT, 4x defeat	11	mouse		defeat	*0.0158	F (1, 15) = 7.404		(-), WT, 4x defeat, ICR(-) vs (-), WT, 4x defeat, ICR(+)	**0.0018	4.13	15
						within subject effect (ICR(-), (+))	0.162	F (1, 15) = 2.164					
						Subjects (matching)	0.2432	F (15, 15) = 1.443					

Panel	Behavior	Group	N value	Replicate	Statistical test	P value	t value	df (between)	F test to compare variances
S5D, Right	interaction	(-), WT, naïve	11	mouse	Two-tailed t-test with Welch's correction	***0.0007	4.353	14	p=0.0441
		(-), WT, 4x defeat	12	mouse					

Panel	Behavior	Group	N value	Replicate	Statistical test	ANOVA	P value	F value	Multiple comparison test	Comparison	P value	t value	df (between)
S5E, Left		(-), TLR-DKO, 4x defeat	10	mouse	Two-way RM ANOVA	Interaction	**0.0022	F (4, 40) = 5.057	Bonferroni	(-), TLR DKO, 4x defeat, ICR(+) vs WT microlia, TLR-DKO, defeat, ICR(+)	*0.0173	3.243	80
		WT microglia, TLR-DKO, naïve	9	mouse		group	0.1584	F (4, 40) = 1.749		WT microlia, TLR-DKO, naïve, ICR(+) vs WT microlia, TLR-DKO, 4x defeat, ICR(+)	**0.0023	3.859	80
	interaction	WT microglia, TLR-DKO, 4x defeat	16	mouse		within subject effect (ICR(-), (+))	***0.0002	F (1, 40) = 17.5					
		TLR-DKO microglia, TLR-DKO, naïve	3	mouse		Subjects (matching)	*0.0125	F (40, 40) = 2.055					
		TLR-DKO microglia, TLR-DKO, 4x defeat	9	mouse									

Panel	Behavior	Group	N value	Replicate	Statistical test	P value	F value	Multiple comparison test	Comparison	P value	t value	df (between)
S5E, Right		(-), TLR-DKO, 4x defeat	10	mouse	One-way ANOVA	**0.0022	F (4, 40) = 5.057	Bonferroni	(-), TLR-DKO, 4x defeat vs WT microglia, TLR-DKO, 4x defeat	*0.0175	3.355	40
		WT microglia, TLR-DKO, naïve	9	mouse					WT microglia, TLR-DKO, naive vs WT microglia, TLR-DKO, 4x defeat	**0.0094	3.574	40
	interaction	WT microglia, TLR-DKO, 4x defeat	16	mouse					WT microglia, TLR-DKO, 4x defeat vs TLR-DKO microglia, TLR-DKO, 4x defeat	*0.0413	3.042	40
		TLR-DKO microglia, TLR-DKO, naïve	3	mouse								
		TLR-DKO microglia, TLR-DKO, 4x defeat	9	mouse								

Panel	Behavior	Group	N value	Replicate	Statistical test	ANOVA	P value	F value	Multiple comparison test	Comparison	P value	t value	df (between)
S5F, Left	avoidance	(-), WT, naïve	6	mouse	Two-way RM ANOVA	Interaction	*0.0143	F (1, 15) = 7.678	Bonferroni	(-), WT, naïve, ICR(+) vs (-), WT, 4x defeat, ICR(+)	**0.0026	3.549	30
		(-), WT, 4x defeat	11	mouse		defeat	*0.0377	F (1, 15) = 5.196		(-), WT, 4x defeat, ICR(-) vs (-), WT, 4x defeat, ICR(+)	**0.0041	3.725	15
						within subject effect (ICR(-), (+))	0.1186	F (1, 15) = 2.741					
						Subjects (matching)	0.3521	F (15, 15) = 1.221					

Panel	Behavior	Group	N value	Replicate	Statistical test	P value	t value	df (between)	F test to compare variances
S5F, Right	avoidance	(-), WT, naïve	6	mouse	Two-tailed t-test with Welch's correction	**0.0032	3.685	11.79	0.0045
		(-), WT, 4x defeat	11	mouse					

Panel	Behavior	Group	N value	Replicate	Statistical test	ANOVA	P value	F value	Multiple comparison test	Comparison	P value	t value	df (between)
S5G, Left		(-), TLR-DKO, 4x defeat	10	mouse	Two-way RM ANOVA	Interaction	*0.0255	F (4, 40) = 3.111	Bonferroni	(-), TLR DKO, 4x defeat, ICR(+) vs WT microlia, TLR-DKO, defeat, ICR(+)	*0.0311	3.049	80
		WT microglia, TLR-DKO, naïve	9	mouse		group	0.2291	F (4, 40) = 1.471		WT microlia, TLR-DKO, naïve, ICR(+) vs WT microlia, TLR-DKO, 4x defeat, ICR(+)	**0.0074	3.509	80
	avoidance	WT microglia, TLR-DKO, 4x defeat	16	mouse		within subject effect (ICR(-), (+))	0.2738	F (1, 40) = 1.231					
		TLR-DKO microglia, TLR-DKO, naïve	3	mouse		Subjects (matching)	0.1532	F (40, 40) = 1.386					
		TLR-DKO microglia, TLR-DKO, 4x defeat	9	mouse									

Panel	Behavior	Group	N value	Replicate	Statistical test	P value	F value	Multiple comparison test	Comparison	P value	t value	df (between)
S5G, Right		(-), TLR-DKO, 4x defeat	10	mouse	One-way ANOVA	*0.0255	F (4, 40) = 3.111	Bonferroni	WT microglia, TLR-DKO, naive vs WT microglia, TLR-DKO, 4x defeat	#0.0575	2.918	40
		WT microglia, TLR-DKO, naïve	9	mouse								
	avoidance	WT microglia, TLR-DKO, 4x defeat	16	mouse								
		TLR-DKO microglia, TLR-DKO, naïve	3	mouse								
		TLR-DKO microglia, TLR-DKO, 4x defeat	9	mouse								

Panel	Behavior	Group	N value	Replicate	Statistical test	ANOVA	P value	F value	Multiple comparison test	Comparison	P value	t value	df (between)
S5H, Left	interaction	(-), WT, naïve	6	mouse	Two-way RM ANOVA	Interaction	*0.0371	F (1, 15) = 5.233	Bonferroni	(-), WT, naïve, ICR(+) vs (-), WT, 10x defeat, ICR(+)	*0.019	2.771	30
		(-), WT, 10x defeat	11	mouse		defeat	0.1066	F (1, 15) = 2.947		(-), WT, 10x defeat, ICR(-) vs (-), WT, 10x defeat, ICR(+)	*0.0194	2.96	15
						within subject effect (ICR(-), (+))	0.2377	F (1, 15) = 1.513					
						Subjects (matching)	0.2033	F (15, 15) = 1.549					

Panel	Behavior	Group	N value	Replicate	Statistical test	P value	t value	df (between)	F test to compare variances
S5H, Right	interaction	(-), WT, naïve	6	mouse	Two-tailed t-test with Welch's correction	***0.0007	4.353	14	p=0.0441
		(-), WT, 10x defeat	11	mouse					

Panel	Behavior	Group	N value	Replicate	Statistical test	ANOVA	P value	F value
S5I, Left		(-), TLR-DKO, 10x defeat	10	mouse	Two-way RM ANOVA	Interaction	0.2944	F (4, 37) = 1.283
		WT microglia, TLR-DKO, naïve	9	mouse		group	0.2845	F (4, 37) = 1.309
	interaction	WT microglia, TLR-DKO, 10x defeat	16	mouse		within subject effect (ICR(-), (+))	***<0.0001	F (1, 37) = 19
		TLR-DKO microglia, TLR-DKO, naïve	3	mouse		Subjects (matching)	0.4034	F (37, 37) = 1.084
		TLR-DKO microglia, TLR-DKO, 10x defeat	9	mouse				

Panel	Behavior	Group	N value	Replicate	Statistical test	P value	F value
S5I, Right		(-), TLR-DKO, 10x defeat	10	mouse	One-way ANOVA	0.2944	F (4, 37) = 1.283
		WT microglia, TLR-DKO, naïve	9	mouse			
	interaction	WT microglia, TLR-DKO, 10x defeat	16	mouse			
		TLR-DKO microglia, TLR-DKO, naïve	3	mouse			
		TLR-DKO microglia, TLR-DKO, 10x defeat	9	mouse			

Panel	Behavior	Group	N value	Replicate	Statistical test	ANOVA	P value	F value	Multiple comparison test	Comparison	P value	t value	df (between)
S5J, Left	avoidance	(-), WT, naïve	6	mouse	Two-way RM ANOVA	Interaction	0.0585	F (1, 15) = 4.192	Bonferroni	(-), WT, naïve, ICR(+) vs (-), WT, 10x defeat, ICR(+)	*0.0303	2.577	30
		(-), WT, 10x defeat	11	mouse		group	0.1249	F (1, 15) = 2.642		(-), WT, 10x defeat, ICR(-) vs (-), WT, 10x defeat, ICR(+)	*0.0165	3.042	15
						within subject effect (ICR(-), (+))	0.1379	F (1, 15) = 2.456					
						Subjects (matching)	0.3373	F (15, 15) = 1.247					

Panel	Behavior	Group	N value	Replicate	Statistical test	P value	t value	df (between)	F test to compare variances
S5J, Right	avoidance	(-), WT, naïve	6	mouse	Two-tailed t-test with Welch's correction	*0.0193	2.679	12.63	p=0.0125
		(-), WT, 10x defeat	11	mouse					

Panel	Behavior	Group	N value	Replicate	Statistical test	ANOVA	P value	F value
S5K, Left		(-), TLR-DKO, 10x defeat	10	mouse	Two-way RM ANOVA	Interaction	0.4923	F (4, 37) = 0.8679
		WT microglia, TLR-DKO, naïve	9	mouse		group	0.7346	F (4, 37) = 0.5017
	avoidance	WT microglia, TLR-DKO, 10x defeat	16	mouse		within subject effect (ICR(-), (+))	0.2108	F (1, 37) = 1.622
		TLR-DKO microglia, TLR-DKO, naïve	3	mouse		Subjects (matching)	0.7008	F (37, 37) = 0.8399
		TLR-DKO microglia, TLR-DKO, 10x defeat	9	mouse				

Panel	Behavior	Group	N value	Replicate	Statistical test	P value	F value
S5K, Right		(-), TLR-DKO, 10x defeat	10	mouse	One-way ANOVA	0.4574	F (4, 37) = 0.9296
		WT microglia, TLR-DKO, naïve	9	mouse			
	avoidance	WT microglia, TLR-DKO, 10x defeat	16	mouse			
		TLR-DKO microglia, TLR-DKO, naïve	3	mouse			
		TLR-DKO microglia, TLR-DKO, 10x defeat	9	mouse			

Panel	Gene	Group	N value	Replicate	Statistical test	P value	F value	Multiple comparison test	Comparison	P value	t value	df (between)
S6A		control miR	9	well	One-way ANOVA	***<0.0001	F (2, 21) = 102.1	Bonferroni	control miR vs TLR2 miR	***<0.0001	13.78	21
	TLR2	TLR2 miR	8	well					TLR2 miR vs TLR4 miR	***<0.0001	10.11	21
		TLR4 miR	7	well								

Panel	Gene	Group	N value	Replicate	Statistical test	P value	F value	Multiple comparison test	Comparison	P value	t value	df (between)
S6A		control miR	9	well	One-way ANOVA	***<0.0001	F (2, 20) = 47.69	Bonferroni	control miR vs TLR4 miR	***<0.0001	8.257	20
	TLR4	TLR2 miR	8	well					TLR2 miR vs TLR4 miR	***<0.0001	8.815	20
		TLR4 miR	7	well								

Panel	Gene	Group	N value	Replicate	Statistical test	P value	t value	df (between)	F test to compare variances
S6B		TLR2, control miR	9	well	Two-tailed t-test	***<0.0001	5.56	17	p=0.2874
	TLR2	TLR2, TLR2/4 miR	10	well					

Panel	Gene	Group	N value	Replicate	Statistical test	P value	t value	df (between)	F test to compare variances
S6B		TLR4, control miR	10	well	Two-tailed t-test with Welch's correction	***0.0001	5.973	9.953	p=0.0003
	TLR4	TLR4, TLR2/4 miR	9	well					

Panel	Gene	Group	N value	Replicate	Statistical test	P value	t value	df (between)	F test to compare variances
S6G		control miR	4	well	Two-tailed t-test	***0.0008	7.233	5	p=0.3123
	TLR2	TLR2 miR	3	well					

Panel	Gene	Group	N value	Replicate	Statistical test	P value	t value	df (between)	F test to compare variances
S6G		control miR	4	well	Two-tailed t-test	0.2356	1.318	6	p=0.6554
	TLR2mt7	TLR2 miR	4	well					

Panel	Gene	Group	N value	Replicate	Statistical test	P value	t value	df (between)	F test to compare variances
S6H		control miR	3	well	Two-tailed t-test	***<0.0001	0.9556	5	p=0.1325
	TLR4	TLR4 miR	4	well					

Panel	Gene	Group	N value	Replicate	Statistical test	P value	t value	df (between)	F test to compare variances
S6H		control miR	3	well	Two-tailed t-test	0.3934	0.9556	4	p=0.1992
	TLR4mt8	TLR4 miR	3	well					

Panel	IHC	Group	N value	Replicate	Statistical test	P value	F value	Multiple comparison test	Comparison	P value	t value	df (between)
S7B, Left		Control, naïve	5	mouse	One-way ANOVA	*0.0253	F (2, 12) = 5.073	Bonferroni	Control, naïve vs Control, R-SDS(sus)	*0.0387	2.918	12
	PSD-95	Control, R-SDS(sus)	6	mouse								
		Control, R-SDS(res)	4	mouse								

Panel	IHC	Group	N value	Replicate	Statistical test	P value	t value	df (between)	F test to compare variances
S7B, Right		TLR2/4KD, naïve	4	mouse	Two-tailed t-test	0.8353	0.2148	8	p=0.2664
	PSD-95	TLR2/4KD, R-SDS	6	mouse					

Panel	IHC	Group	N value	Replicate	Statistical test	P value	F value
S7C, Left		Control, naïve	5	mouse	One-way ANOVA	0.2211	F (2, 12) = 1.716
	PSD-95	Control, R-SDS(sus)	6	mouse			
		Control, R-SDS(res)	4	mouse			

Panel	IHC	Group	N value	Replicate	Statistical test	P value	t value	df (between)	F test to compare variances
S7C, Right		TLR2/4KD, naïve	4	mouse	Two-tailed t-test	0.4858	0.7307	8	p=0.5614
	PSD-95	TLR2/4KD, R-SDS	6	mouse					